Universität Zürich
Institut für Hirnforschung
Direktor: Prof. Dr. phil. Dr. med. h.c. M. E. Schwab

Universität Freiburg, Schweiz
Departement für Medizin
Institut für Physiologie
Direktor: Prof. Dr. med. J.-P. Montani

Arbeit unter Leitung von
Prof. Dr. phil. E. M. Rouiller und Dr. phil. G. Loquet

Neural Adaptation in the Auditory Nerve and the Anteroventral Cochlear Nucleus of the Rat in Response to Repetitive Acoustic Stimuli

INAUGURAL-DISSERTATION
zur Erlangung der Doktorwürde der Medizinischen Fakultät
der Universität Zürich

vorgelegt von
Kaspar Ueli Meyer
von Zürich

Genehmigt auf Antrag von Prof. Dr. phil. Dr. med. h.c. M. E. Schwab
Zürich 2005

Several people have contributed significantly to the smooth progression of my dissertation. Most of all, I am indebted to the following two:

Professor Eric M. Rouiller, PhD

I am extremely grateful to you for supervising my thesis. Although I could not be present at the institute as much as I would have liked to, you always gave me the impression of being accepted as a member of our group and of having your support. I especially appreciated your permanent availability (the proofreading during your summer holiday, for example) and your staying calm when I thought it had all been for nothing. I enjoyed working with you not only from an academic but also from a personal point of view.

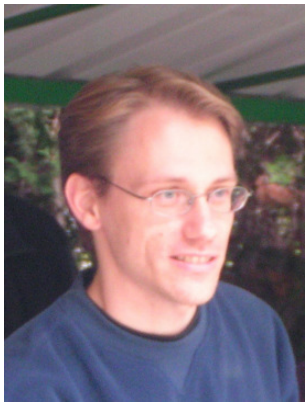

Gérard Loquet, PhD

I would like to express to you my profound gratitude for the great amount of time you have devoted to supporting me throughout this project. Thank you for teaching me practical skills, showing me how to write scientifically (or trying to do so, at least), for helping me out in the many battles I fought with my computer, for sometimes insisting in your perfectionism. All of these and many other things added up to make me conceive an idea of the "spirit of science". Thank you for transmitting it to me.

In addition to those preceding, many other people have supported me in one way or another:

***Professor Martin E. Schwab, PhD, MD h.c.**: Thank you very much for agreeing to represent this dissertation at the Faculty of Medicine of the University of Zürich.*

***Josef Corpataux and Bernard Morandi:** Thank you for taking care of our animals and, Sepi, for the funny moments we sometimes had when you stopped by.*

***Françoise Tinguely**: Thanks a lot for taking care of the histological procedures. I have always appreciated your reliability and your hearty geniality.*

***Véronique Moret**: I am very grateful to you for all the scanning and the handling of the graphs. You have been a great help.*

*Finally, I'm indebted to **Bernard Aebischer, André Gaillard, and Laurent Monney** for the technical support during the experiment, and to a number of other people (**Murielle Rouiller**, **Caroline Durif**, **Anne-Valérie Jacomme, PhD**, **Christine Roulin**, **Alexandre Babalian, PhD**, **Thierry Wannier, PhD**, **Eric Schmidlin, PhD**, **Alexander Wyss**, **Professor Jean-Pierre Montani, MD**, **and David Michel**) – not for direct contributions to this project but for their friendliness and cordiality.*

In the course of the experiment which is the subject of this thesis, and of others in which I participated, about fifteen rats were sacrificed, several of them by myself.

Animal experiments contribute to our biomedical knowledge and improve our understanding of many diseases. As is clear from the first paragraph, I am in favor of animal models. Nonetheless, the question about the legitimacy of using other species in order to improve our own quality of life cannot easily be answered, and even if one agrees with my personal opinion, legitimacy should not be taken for a "free ticket" allowing us to use animals in whichever way we please.

First of all, I think that, in each and every case, we have the responsibility to consider meticulously the usefulness of an experiment, and that, doing so, we have to be forceful enough to discard an investigation if we feel it does not fulfill the standards we have set. When conducting an experiment, we should be doing so because we believe that we will ultimately help humanity, and not because we aim at publishing an article in an international journal.

Second, I believe that we have to try our hardest in order to design experiments which imply minimal stress and pain on the animals we use. Even if it may sometimes seem easier not to do so, we must always remember that we are not working with things but with beings, and that, even though they are not human, we owe them our utmost respect.

I TABLE OF CONTENTS

I TABLE OF CONTENTS 5

II ABSTRACT 10

III ABBREVIATIONS AND UNITS 13

1 Abbreviations 14

2 Units 15

IV INTRODUCTION 16

1 Introduction to the Auditory System 17

1.1 Sound 17

1.2 Anatomy 18

1.2.1 External Ear 18

1.2.2 Middle Ear 18

1.2.3 Inner Ear 18

1.2.4 Auditory Pathways 20

1.3 Physiology 22

1.3.1 External Ear and Middle Ear 22

1.3.2 Inner Ear 23

1.3.3 Auditory Nerve 24

1.3.4 Cochlear Nucleus 28

1.3.5 Auditory Relays in the Brainstem, Mesencephalon, Thalamus, and Cortex 30

2 Adaptation in the Peripheral Auditory System 31

2.1 What Is Adaptation? 31

2.1.1 Adaptation, Habituation, and Fatigue 31

2.1.2 Adaptation in Various Human Sensory Receptors 32

2.2 Adaptation in the Auditory Nerve 33

2.2.1 Introduction 33

2.2.2 Adaptation in Response to Single Tone Bursts 34

2.2.3 Adaptation in Response to Trains of Tone Bursts or Clicks 36

2.2.4 Masking Studies 38

2.3 Adaptation in the Cochlear Nucleus 41

2.3.1 Introduction 41

2.3.2 Adaptation in Response to Single Tone Bursts 42

2.3.3 Adaptation in Response to Trains of Tone Bursts or Clicks 42

2.3.4 Recovery from Adaptation 43

V RESEARCH AIMS 45

1 Outline of the Present Study 46

2 Aims of the Present Study 46
2.1 Justification of the Recording Method 46
2.2 Study of Adaptation 46
2.3 Histology 47
3 Signification of Results 47

VI MATERIALS AND METHODS 48

1 Animals 49
2 Experimental Procedures 49
2.1 Animal Preparation 49
2.2 Acoustic Stimulation 50
2.2.1 Tone Bursts 51
2.2.2 Clicks 51
2.2.3 Repetitive Acoustic Stimulation 52
2.3 Histology 52

VII RESULTS 55

1 Auditory Near-Field Evoked Potentials in Response to Tone Bursts 56
2 Auditory Near-Field Evoked Potentials in Response to Clicks 56
3 Auditory Near-Field Evoked Potentials in Response to Repetitive Clicks 58
3.1 N_1-P_1 Component of the Auditory Near-Field Evoked Potential 58
3.1.1 General Time Course 58
3.1.2 Effects of Stimulus Repetition Rate 60
3.1.3 Effects of Stimulus Intensity 61
3.2 P_1-N_2 Component of the Auditory Near-Field Evoked Potential 67
3.2.1 General Time Course 67
3.2.2 Effects of Stimulus Repetition Rate 68
3.2.3 Effects of Stimulus Intensity 69
3.3 Comparison of the N_1-P_1 and P_1-N_2 Components of the Auditory Near-Field Evoked Potential 73
3.3.1 Effects of Stimulus Repetition Rate 73
3.3.2 Effects of Stimulus Intensity 76
4 Histology 77

VIII DISCUSSION 78

1 Preface 79

2 Origin of the Recorded Activity 79

2.1 Position of the Recording Electrode 79

2.2 Latencies of the N_1 and the N_2 Peaks of the Auditory Near-Field Evoked Potential 79

3 Comparison of Adaptation Patterns of the N_1-P_1 and P_1-N_2 Components of the Auditory Near-Field Evoked Potential 82

3.1 General Time Courses 82

3.2 Steady-State Amplitude 83

4 Comparison to Prior Results 85

4.1 Adaptation Time Course 86

4.2 Effects of Stimulus Repetition Rate on Adaptation 86

4.3 Effects of Stimulus Intensity on Adaptation 87

5 The Nature of Adaptation 87

5.1 Models of Adaptation 88

5.1.1 Is Adaptation Additive or Multiplicative? 88
5.1.2 Neurotransmitter Kinetics 92
5.1.3 Post-Synaptic Receptor Kinetics 94

5.2 Possible Sites of Adaptation 95

5.2.1 Middle Ear Muscles and Cochlear Mechanics 95
5.2.2 Hair Cells 96
5.2.3 Influence of the Olivo-Cochlear Bundle on Hair Cells 97
5.2.4 Hair Cell-Nerve Fiber Synapse 98
5.2.5 Auditory Nerve 98
5.2.6 Signal Transmission from Primary to Secondary Auditory Neurons 98

5.3 Implication of Auditory-Nerve Refractoriness in Adaptation 99

5.3.1 A Model of Refractoriness 99
5.3.2 Absolute and Relative Refractory Periods 100
5.3.3 Raw Output of the Model of Refractoriness 101
5.3.4 Refractoriness Applied to the Adapted Output of the Hair Cell-Nerve Fiber Synapse 103
5.3.5 Refractoriness at the Basis of Discrepancies between the Adaptation Patterns of the N_1-P_1 and P_1-N_2 Components of the Auditory Near-Field Evoked Potential ? 106
5.3.6 Summary 108

IX CONCLUSION 110

1 Results of the Present Study 111

2 Adaptation Patterns in the Auditory Nerve and the Cochlear Nucleus 111

3 Adaptation Patterns in Response to Acoustic and Electric Stimulation **112**

X REFERENCES **115**

XI ADDENDUM **126**

- Loquet G, Meyer K, Rouiller EM. Effects of Intensity of Repetitive Acoustic Stimuli on Neural Adaptation in the Ventral Cochlear Nucleus of the Rat. Exp Brain Res 2003; 153 : 436-442.

XII CURRICULUM VITAE **134**

II ABSTRACT

Adaptation is a common feature of sensory receptor organs. In psychophysics, it describes the fact that the perceived intensity of a stimulus is greatest at its onset and then declines. In the auditory system, using electrophysiological techniques, adaptive processes can be observed even in response to tones as short as a few milliseconds. The adaptive processes can be demonstrated, for instance, in terms of a time-dependent decrease of the receptor potential of a cochlear hair cell in response to a constant stimulus, or in form of the reduced firing rate of a primary auditory neuron innervated by such a cell. Unfortunately, cochlear implants designed to help profoundly deaf patients still do not reproduce these adaptation properties. This loss of information may contribute to the low level of speech intelligibility commonly reported by patients using these devices in noisy conditions.

The present study was designed to complete a previous report on auditory adaptation in response to repetitive acoustic stimulation carried out by Loquet and Rouiller (2002). In contrast to their report, in which adaptation had been studied in response to trains of repetitive acoustic clicks presented at various repetition rates but at only one fixed intensity, the present investigation aimed at an assessment of the effects of both of these stimulus parameters on adaptation. For this purpose, auditory near-field evoked potentials (ANEPs) were recorded from electrodes chronically implanted in the ventral cochlear nucleus of unanaesthetized Long-Evans rats. Stimuli consisted of trains of repetitive clicks presented at five different intensities (5, 10, 30, 50, and 70 dB SPL) and at six different repetition rates (100, 200, 400, 600, 800, and 1'000 pulses per second). An individual response potential was observed to each click of a train, the waveform consisting of two negative (N_1 and N_2) and an interposed positive (P_1) peak. It was hypothesized that N_1 and N_2 represent the activity of fibers of the auditory nerve and neurons in the cochlear nucleus, respectively. Whereas Loquet and Rouiller (2002) had focused on the first one of these two negative deflections, the present study aimed at quantifying the behavior of both peaks by assessing both the N_1-P_1 and the P_1-N_2 voltage differences in the responses recorded throughout the stimulus trains.

For both components of the ANEP, response amplitudes were highest at train onset. They then diminished rapidly during the first few milliseconds of stimulation (rapid adaptation) and more progressively thereafter (short-term adaptation), to finally reach a quasi-steady state. For the N_1-P_1 component, mathematical approximation showed that in most cases both adaptive amplitude decreases followed exponential time courses. The overall adaptation process could thus be modeled by a two-time-constant exponential decay superposed to a steady state. No mathematical fitting procedure was carried out for the behavior of the P_1-N_2 component, but its adaptation time courses were very similar to those of the N_1-P_1 component. As stimulus intensity and / or repetition rate were increased, adaptation occurred faster and was more pronounced (lower steady-state amplitudes). These effects were qualitatively and, except for minor discrepancies, quantitatively similar for both ANEP components.

At highest stimulus intensities and repetition rates, adaptation time courses were sometimes observed which did not follow the two-time-constant exponential decay described above. Instead, those response traces displayed an extremely pronounced rapid adaptation with response amplitudes immediately following stimulus train onset being clearly too low for the above described fitting

procedure. This finding could be explained in terms of refractoriness of auditory-nerve fibers. The results produced by a mathematical model incorporating these refractory properties suggest that they may indeed by implicated in the adaptation process and might have to be considered when trying to improve the stimulus paradigms of cochlear implants.

Our results fit in well among the existing literature on neural adaptation in the auditory periphery and also confirm the predictions of some mathematical models by means of which other investigators tried to mimic the functioning of the peripheral auditory relays. It seems reasonable to assume that by implementing the present quantification of the adaptation properties of the peripheral auditory system on coding strategies of cochlear implants, speech intelligibility of implant users could be improved. Furthermore, by quantifying adaptation on the level of the ventral cochlear nucleus, too, the present report produces valuable information also for auditory implants which do not stimulate the dendrites of primary auditory neurons but directly the brain stem at the level of the cochlear nucleus.

III ABBREVIATIONS & UNITS

1 Abbreviations

Below, the abbreviations used in this thesis are listed in alphabetical order (acronyms starting with a Greek letter or a numeral are stated last). All abbreviations are also given within the text, immediately after the first mention of the word they stand for, and bracketed by parentheses. In some cases, there is more than one abbreviation for a certain term, due to the fact that the acronyms used in the present paper do not always coincide with those employed in the graphs of other reports we refer to.

A	Amplitude of the auditory near-field evoked potential	IC	inferior colliculus
ABR	auditory brainstem response	IHC	inner hair cell
AN	auditory nerve	K	time constant of a one-stage adaptation process
an	auditory nerve	K_{ST}	short-term-adaptation time constant
ANEP	auditory near-field evoked potential	K_1	rapid-adaptation time constant
AP	action potential	K_2	short-term-adaptation time constant
ARP	absolute refractory period	LL	lateral lemniscus
AVCN	anteroventral cochlear nucleus	LSON	lateral superior olivary nucleus
BM	basilar membrane	MGB	medial geniculate body
CAP	compound action potential	MNTB	medial nucleus of the trapezoid body
CF	characteristic frequency	MSON	medial superior olivary nucleus
CN	cochlear nucleus	N_1	first negative peak of the auditory near-field evoked potential
CNIC	central nucleus of the inferior colliculus	N_2	second negative peak of the auditory near-field evoked potential
DCN	dorsal cochlear nucleus	OHC	outer hair cell
EAM	external auditory meatus	P_1	first positive peak of the auditory near-field evoked potential
ENIC	external nucleus of the inferior colliculus	PNIC	pericentral nucleus of the inferior colliculus
EP	evoked potential	pps	pulses per second
EPSP	excitatory post-synaptic potential	PSTH	peri- / post-stimulus time histogram

PVCN	posteroventral cochlear nucleus	SR	spontaneous firing rate
RRP	relative refractory period	T	time
SA	spontaneous activity	t	time
SD	standard deviation	VCN	ventral cochlear nucleus
SG	spiral ganglion	y_1	y-intercept of the rapid adaptation component
SOC	superior olivary complex	y_2	y-intercept of the short-term adaptation component
SPL	sound pressure level		

2 Units

Below, the unit abbreviations used in the following text are listed in alphabetical order. Most of them correspond to the SI (Système international). However, the following pages contain figures taken from textbooks and other reports, which, in some cases, did not stick to the abbreviations of the SI. Therefore, there may be more than one acronym for a given unit.

A	ampère	Pa	pascal
B	bel	s	second
g	gram	sec	second
h	hour	V	volt
Hz	hertz	W	watt
m	meter	Ω	ohm
M	molar (moles per liter)	℃	degree centigrade
min	minute		

In combination with the above units the following prefixes were used:

c	centi (10^{-2})	M	mega (10^{6})
d	deci (10^{-1})	k	kilo (10^{3})
m	milli (10^{-3})	µ	micro (10^{-6})
p	pico (10^{-12})		

IV INTRODUCTION

1 Introduction to the Auditory System

1.1 Sound

Sound is a longitudinal wave that can pass through any material medium (solids, liquids, and gases). In the following, we will concentrate on sound waves in air, because this is what we are usually exposed to. Air is a gas consisting of different kinds of atoms and molecules. If an external vibratory source is applied to these particles, they will start an oscillating movement relatively to their original position. Thus periodically coming closer together and shifting farther apart, they will produce condensations and rarefactions in the medium (Fig. 4.1). These oscillatory movements do not remain restricted to their original site but will be conveyed to adjacent particles, and the wave will thus propagate.

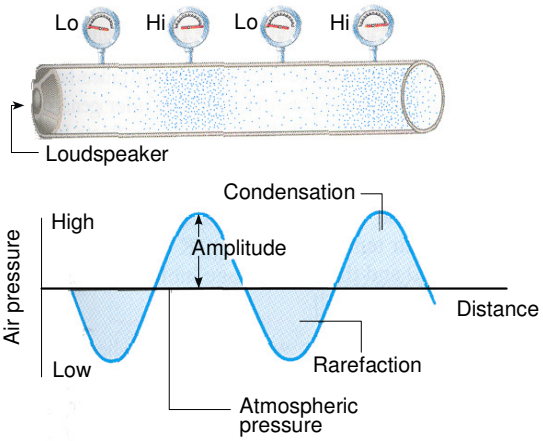

Figure 4.1 A sound wave represented as a series of periodic condensations and rarefactions of air. Modified from Cutnell and Johnson, 1997.

A sound wave is usually described by two main parameters: its frequency and its intensity. Frequency is the rate at which the air particles oscillate, more precisely the number of complete cycles of condensations and rarefactions that occur in one second, expressed in hertz (Hz). A pure tone is an example of a sound that has just a single frequency, as opposed to complex sounds which consist of several waves having various frequencies. The intensity (I) of a sound wave is defined as the amount of energy delivered during a certain time to a certain surface standing at a right angle to the direction of propagation. In acoustics, however, one usually does not refer to the absolute value of intensity but to the resulting ratio when comparing it to a certain reference level (I_{ref}). The unit used is the decibel (dB) and the ratio is usually expressed logarithmically since, in humans, there is a factor of about 10^{12} between the lowest audible sound and the threshold of pain; therefore

$$dB = 10 \cdot \log_{10} \frac{I}{I_{ref}} .$$

Because the intensity of a wave is proportional to the square of its pressure amplitude (p), the preceding equation can also be expressed as follows:

$$dB = 10 \cdot \log_{10} \frac{p^2}{p_{ref}^2} = 20 \cdot \log_{10} \frac{p}{p_{ref}} ,$$

where p_{ref} again is an arbitrary reference value. In hearing experiments I_{ref} and p_{ref} are usually assigned the specific values of 10^{-12} W / m^2 (I_0) and $2 \cdot 10^{-5}$ Pa (p_0), respectively, both of which are close to the lowest sounds the normal human ear is able to perceive at a frequency of 1'000 Hz. When comparing a wave's intensity to these reference values, the resulting dB value is said to express its sound pressure level (SPL):

$$\text{dB SPL} = 10 \cdot \log_{10} \frac{I}{I_0} = 20 \cdot \log_{10} \frac{p}{p_0} .$$

The auditory research field most often uses the last part of the preceding equation.

1.2 Anatomy

This section provides an overview of the mammalian auditory system. It mainly describes the anatomical structures as they are found in humans but also includes observations obtained from cats and rodents.

1.2.1 External Ear

The external ear comprises the auricle, or pinna, a single piece of cartilage attached to the side of the head, and the external auditory meatus (EAM; Fig. 4.2). The EAM is an air-filled canal whose lateral, cartilaginous part is continuous with the auricle and whose medial two-thirds, in humans, are formed by the temporal bone. The EAM is separated from the middle ear by the tympanic membrane.

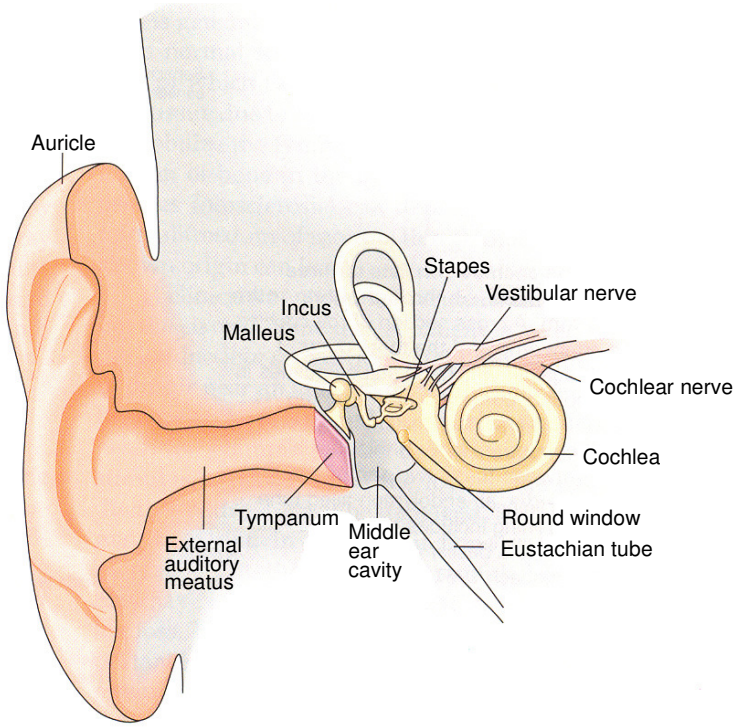

Figure 4.2 Structure of the human ear. Taken from Hudspeth, 2000.

1.2.2 Middle Ear

The middle ear comprises the tympanic membrane, or tympanum, the tympanic cavity containing the ossicles (middle ear bones), and the Eustachian tube (Fig. 4.2).

The tympanic membrane separates the EAM from the tympanic cavity and is in contact with the malleus, the first one of the three ossicles. The ossicular chain, completed by the incus and the stapes, traverses the air-filled tympanic cavity and ends at the oval window. Two of the ossicles are contacted by a muscle: the tensor tympani muscle is connected to the malleus and innervated by the trigeminal nerve, the stapedius muscle is fixed to the stapes and innervated by the facial nerve. The Eustachian tube runs from the anterior middle-ear wall to the lateral wall of the nasopharynx.

1.2.3 Inner Ear

The inner ear is separated from the middle ear by the oval window and lies in the petrous part of the temporal bone. It can be divided into a vestibular and an acoustic part.

The vestibular part of the inner ear shares the bony and the membranous labyrinths with the acoustic part and is responsible for our sense of equilibrium. It consists of the utricule, the saccule, and the three semicircular canals.

The cochlea, the acoustic part of the inner ear, is a bony structure that resembles the shell of a common snail. Inside, the cochlear duct runs from the base to the top, winding itself spirally around an osseous central pillar called modiolus. The number of turns is about 2 ¾ in humans and 2 ¼ in the rat (West, 1985). The inside of the canal is further divided by an osseous lamella into two cavities, the scala vestibuli and the scala tympani (Fig. 4.3.A). Between these two, running along the outside of the cochlear canal, there is a third duct called scala media. It is separated from the scala vestibuli by Reissner's membrane and from the scala tympani by the basilar membrane (BM). The BM is narrow at the base of the cochlea and becomes wider towards the apex. The scala media contains endolymph whereas the two adjacent cavities are filled with perilymph.

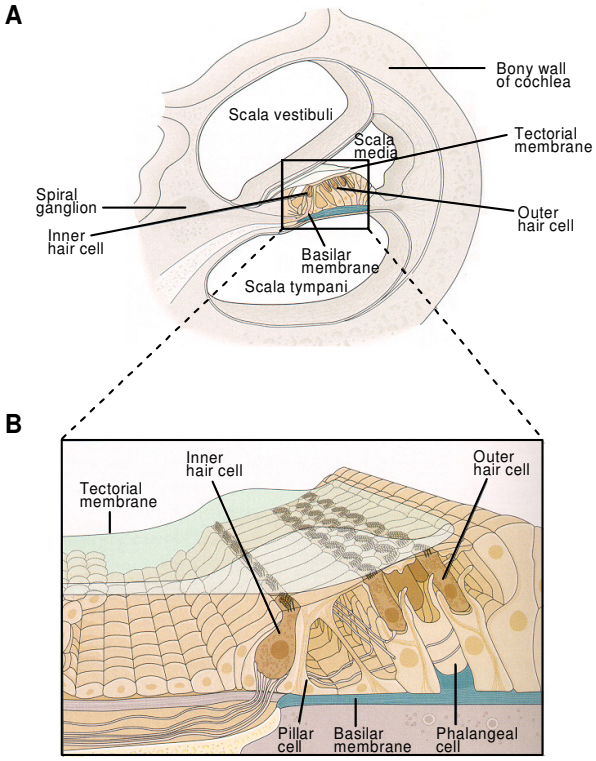

Figure 4.3 (A) Cross-sectional view of the cochlear duct. (B) Cellular architecture of the organ of Corti. Taken from Hudspeth, 2000.

Above the basilar membrane, a complex arrangement of receptor cells and various accessory cells forms the organ of Corti, the actual sensory organ of hearing (Fig. 4.3.B). The most central structures of this organ are the internal and external pillar cells which enclose a triangular space called tunnel of Corti. Medially to the pillar cells there is a single row of inner hair cells (IHCs) and laterally to them there are three rows of outer hair cells (OHCs). The number of IHCs and OHCs in humans is about 2'800 to 4'000 and 11'200 to 16'000, respectively (Bredberg, 1968). In the rat, there are about 960 IHCs and 3'470 OHCs (Keithley and Feldman, 1982). The hair cells owe their name to tufts of microscopic, hair-like structures which are situated on top of them and referred to as stereocilia (Fig. 4.4). The organ of Corti is covered by the tectorial membrane, a gelatinous plate fixed to an epithelial ridge situated just medially of the receptor organ. The stereocilia of the OHCs are firmly attached to this

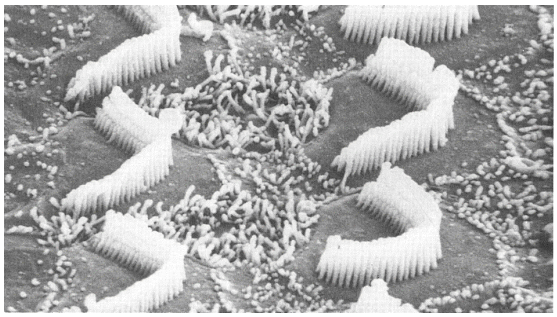

Figure 4.4 Scanning electron micrograph of the organ of Corti after removal of the tectorial membrane. Two rows of OHCs are visible with the typical, V-shaped arrangement of stereocilia. Taken from Hudspeth, 2000.

membrane's undersurface. Synapses located at the basal part of the hair cells establish contact with the dendrites of primary auditory neurons.

1.2.4 Auditory Pathways

Auditory Nerve

The ensemble of primary auditory neurons makes up the auditory nerve (AN) and forms the afferent innervation of the cochlea. The cell bodies of these neurons (about 30'000 in humans, 50'000 in the cat) constitute the spiral ganglion (SG) which is located inside the modiolus. Two kinds of cells can be distinguished among this population (Spoendlin, 1972, 1974, 1979; Kiang et al., 1982; Ryugo et al., 1991). Type I cells, making up about 95% of spiral ganglion neurons, innervate the IHCs. They are big, bipolar and myelinated. Type II cells, on the other hand, representing the remaining 5%, are smaller, pseudo-unipolar, unmyelinated, and contact the OHCs (Fig. 4.5).

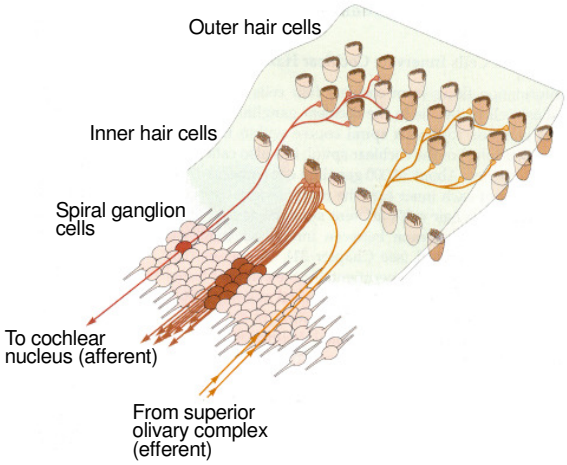

Figure 4.5 Innervation of the organ of Corti. Taken from Hudspeth, 2000.

The dendrites of type I cells are usually not ramified and therefore contact a single IHC. Each IHC, however, shares synapses with about 20 afferent nerve fibers (data from the cat; Spoendlin, 1972). Type II neurons have ramified dendrites which contact about 10 OHCs (Spoendlin, 1972). An OHC is innervated by 6 to 10 type II neurons (Webster, 1992).

Cochlear Nucleus

All AN fibers terminate in the cochlear nucleus (CN) where they form synapses with secondary auditory neurons (Fekete et al., 1984; Rouiller et al., 1986; Liberman 1991, 1993). In humans, the CN is situated at the medullo-pontine junction, medially to the inferior cerebellar peduncle. Three subdivisions of the nucleus have been identified based on innervation patterns and the location of different populations of neurons (Fig. 4.6; Osen, 1969). Shortly after entering the nucleus, the AN fibers of both types (I and II) bifurcate into an anterior ascending branch and a posterior descending branch (Lorente de No, 1933). The area innervated by the ascending branches corresponds to the anteroventral cochlear nucleus (AVCN) and contains three principal types of cells, namely spherical and globular bushy cells, and multipolar (or stellate) cells. Descending AN branches innervate the

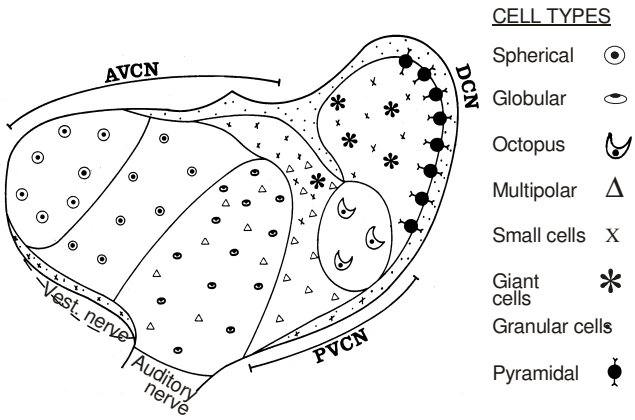

Figure 4.6 Schematic pseudolateral view of the CN of the cat indicating its principal subdivisions as well as its main neuronal populations. Modified from Rouiller, 1997.

posteroventral cochlear nucleus (PVCN), which mainly contains two cell types (multipolar and octopus cells), and the dorsal cochlear nucleus (DCN) which comprises pyramidal, giant, granular, and small granule cells. The DCN and the PVCN are separated from the AVCN by the point of entry of the AN, termed nerve root region. The AVCN, the PVCN, and the nerve root region together form the ventral cochlear nucleus (VCN). When comparing the volume of the main CN divisions, the AVCN is found to be the largest, followed in decreasing order by the DCN, the nerve root region and the PVCN.

Superior Olivary Complex, Lateral Lemniscus, and Inferior Colliculus

Ascending projections from the CN mainly run to the superior olivary complex (SOC) which consists of three main nuclei (lateral superior olivary nucleus (LSON), medial superior olivary nucleus (MSON), and medial nucleus of the trapezoid body (MNTB)) and several periolivary nuclei, all of which are located in the ventral part of the brainstem (Fig. 4.7). The SOC receives input from both the ipsi- and the contralateral ventral cochlear nuclei via the ventral and the intermediate acoustical striae and is therefore the first stage in the auditory pathway where information from both ears converges.

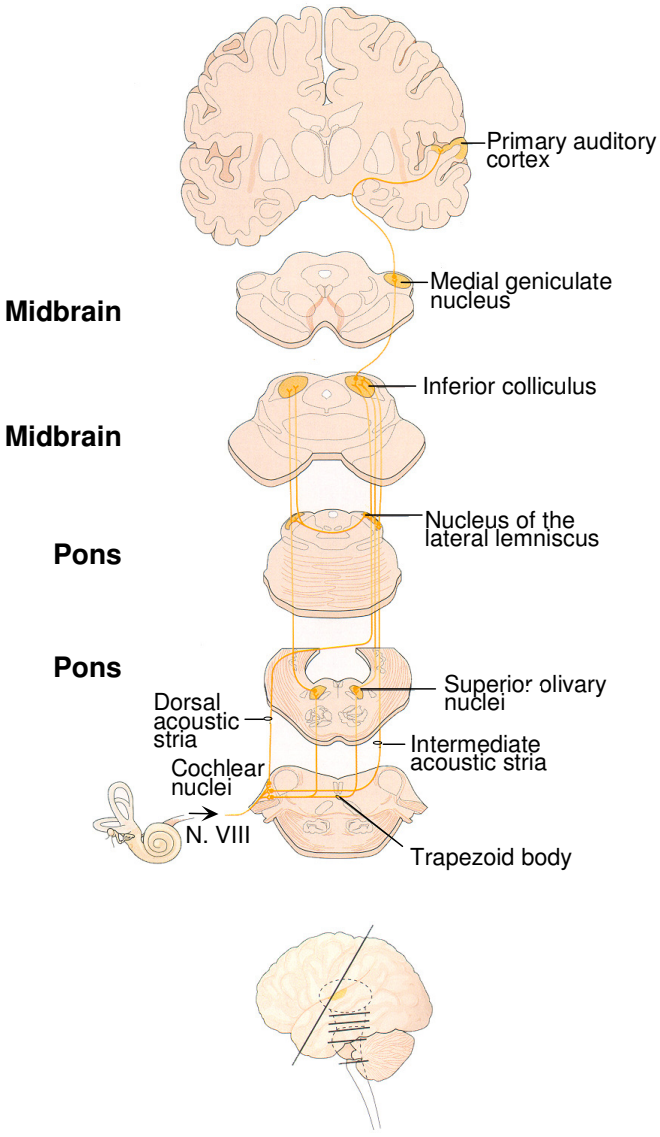

Figure 4.7 Schematic view of the central auditory pathways extending from the CN to the auditory cortex. Taken from Hudspeth, 2000.

Some CN fibers also project directly to higher structures in the auditory pathway (Fig. 4.7). On their way to the mesencephalon, the axons from the CN and the SOC travel in the lateral lemniscus (LL). Within this fiber bundle, there is a narrow condensation of cell bodies making up the nucleus of the LL. The LL receives bilateral information from the cochlear nuclei and the nuclei of the SOC, and its projections go to the contralateral analogue and to the inferior colliculus (IC) on both sides.

The IC is the main auditory structure of the mesencephalon and classically divided into three distinct nuclei: the central nucleus (CNIC), displaying a lamellar organization, the pericentral nucleus (PNIC), and the external nucleus (ENIC). The IC is a quasi-mandatory relay station of the auditory

pathway and receives afferences from the cochlear nuclei (mainly via the dorsal acoustic stria), the SOC, and the LL. It represents the principal source of ascending inputs to the auditory thalamus.

Thalamus and Cerebral Cortex

The ascending auditory pathways from the IC via the thalamus to the auditory cortex have been subdivided into three parallel systems, namely the tonotopic, the non-tonotopic, and the multimodal system (for a review e.g. de Ribaupierre, 1997). Each one of these three has its origin in a distinct nucleus of the IC (the CNIC, the PNIC, and the ENIC, respectively), makes a stopover in a specific part of the auditory thalamus, and finally connects to a well-circumscribed area of the auditory cortex. All three of these systems are reciprocal, meaning that there are also descending projections from the auditory cortex back to the thalamus and then to the IC. The most important relay station in the thalamus is the medial geniculate body (MGB). The auditory areas of the human cerebral cortex are located on the transverse gyrus of Heschl (Brodman's areas 41 and 42).

1.3 Physiology

1.3.1 External Ear and Middle Ear

The external ear and the middle ear are collectively referred to as the conductive system of the hearing organ because it is their main function to transmit a stimulus from the environmental air to the inner ear. Basically, incoming sound waves are conducted along the EAM to the tympanic membrane and will cause the latter to vibrate. Subsequently, the ossicular chain will carry these movements across the tympanic cavity to the membrane sealing the oval window (Fig. 4.8).

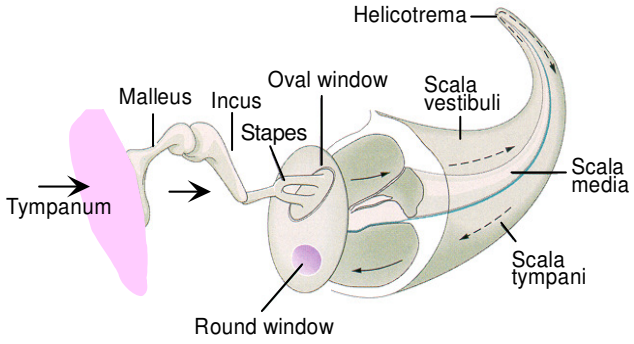

Figure 4.8 Schematic view of the transmission of a signal along the conductive system of the ear. Taken from Hudspeth, 2000.

However, the conductive system does not just transmit incoming sounds but also modifies them. First, the EAM has an intrinsic resonant frequency and will amplify tones of the corresponding spectral range more than others. Second, sounds of all frequencies will be amplified while passing through the middle ear, due, on the one hand, to the surface ratio between the tympanic membrane and the oval window and, on the other hand, to a lever action of the ossicles. Moreover, there is an acoustic reflex at the level of the middle ear ossicles, which, by means of contraction of the tensor tympani and stapedius muscles, can cause the ossicular chain to stiffen. This reflex occurs in response to high-intensity sound stimulation (above 80 to 90 dB SPL, especially at low frequencies) and likely plays a protective role for the cochlea in case of prolonged acoustic overstimulation.

1.3.2 Inner Ear

The movements of the membrane sealing the oval window will be forwarded to the BM by the fluids contained in the scala vestibuli. Inward and outward motions of the stapes will cause the BM to move down and up, respectively (Fig. 4.9). As a result, a special kind of wave pattern develops which runs along the BM from the base to the apex and is therefore referred to as traveling wave (Fig. 4.10; von Békésy, 1960). As this wave moves along, its amplitude increases gradually, reaches a peak at a certain point, and diminishes quickly thereafter. Due to its varying width, there is a gradient of stiffness along the BM. This has as a consequence that a high-frequency sound will produce a traveling wave with a peak in the stiffer part of the BM, close to the base of the cochlea. A tone of lower frequency, on the other hand, produces a peak in the more apical, flaccid part of the membrane (Fig. 4.11). This mechanical frequency selectivity is called place coding mechanism. Because the basilar and the tectorial membranes pivot about different lines of insertion, any joint up-and-down motion of the two will result in a slight shear displacement between them (Fig. 4.12). The hair bundles of both the IHCs and the OHCs will be affected by this movement: those of the OHCs because they are directly inserted into the tectorial membrane, those of the IHCs probably because of fluid movements in the cleft between the two membranes. Subsequently, it is the hair cells' mission to convert the mechanical energy delivered to them into neural signals. A close-up look at their hair bundles reveals the presence of filamentous connections between the individual cilia. These connections are called tip-links and are attached to so-called transduction channels situated in the cell membrane of the cilia. Deflection of the hair bundles (after the cascade of events described above) will increase the tension in the tip links, open the transduction channels and permit the inflow of positively charged substances (mainly potassium ions). The subsequent depolarization of the cell membrane, termed receptor potential, entails calcium influx in the basal part of the hair cell, and the increased intracellular calcium concentration will ultimately result in neurotransmitter (glutamate) release into the synaptic cleft.

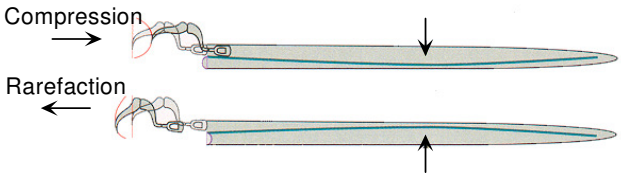

Figure 4.9 Schematic view of the BM movements in response to sound. Taken form Hudspeth, 2000.

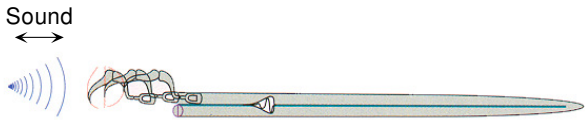

Figure 4.10 Schematic representation of the traveling wave generated by a sound stimulus. Taken from Hudspeth, 2000.

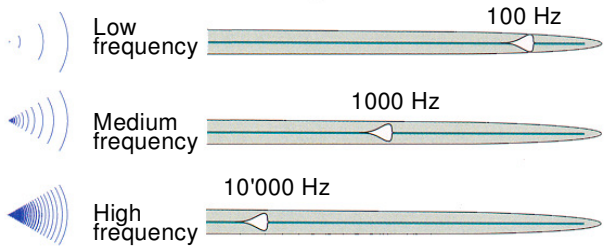

Figure 4.11 Place coding mechanism of the cochlea. Taken from Hudspeth, 2000.

It is likely that the greatest part of information about an incoming sound is forwarded to the brain by IHCs, whereas the role of OHCs in stimulus coding seems to be minor. However, the latter cells are thought to have another important role in the hearing process: in addition to the passive properties of the BM described above (place coding mechanism), they also seem to contribute to the frequency

selectivity of the ear. When an OHC is electrically stimulated in vitro, it responds by changing its length (Zenner et al., 1985). It is thought that the receptor potential exhibited by OHCs located close to the point of maximum amplitude of the traveling wave could therefore result in rhythmic contractions of those cells in phase with the oscillations of the BM. The latter movements would thus be amplified in a specific but very small area. Consequently, only a low number of IHCs would be activated by a pure tone, resulting in an increased frequency discrimination by the ear. It seems, however, that this "cochlear amplifier" (Davis, 1983) works considerably less well at the apex of the cochlea; in that region, the frequency of a sound is more likely to be coded by a neural mechanism called phase-locking (see below).

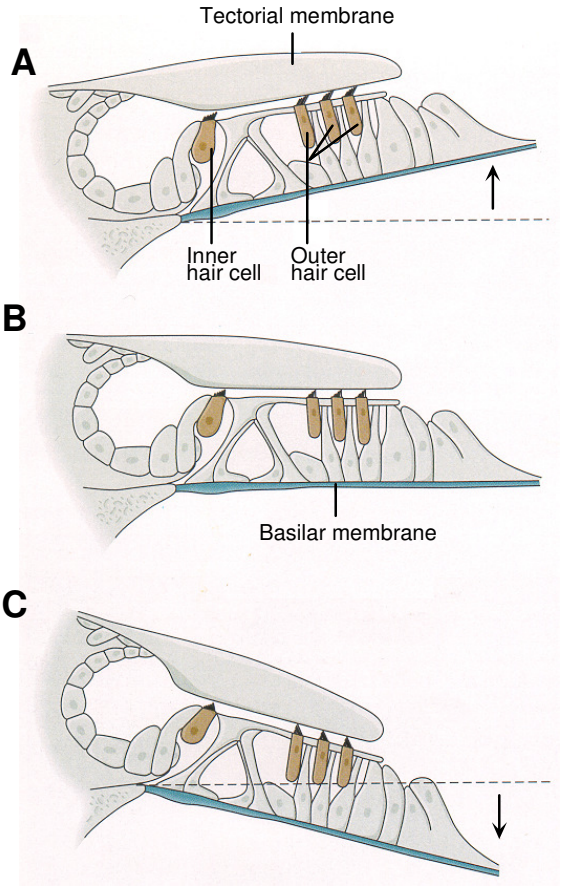

Figure 4.12 Schematic representation of the relative motion between the basilar and the tectorial membranes. The resulting shear movement is detected by the stereocilia of the hair cells. Taken from Hudspeth, 2000.

1.3.3 Auditory Nerve

The innervation patterns of the neurons of the SG have already been described in the anatomy section on the AN. 90 to 95 % of SG cells (type I neurons) contact IHCs and the remaining 5 to 10 % (type II neurons) connect to OHCs. Until now, hardly any information has been obtained as to the firing patterns of type II SG cells; consequently, the following discussion exclusively concerns SG neurons of type I.

Spontaneous Activity, Threshold, and Dynamic Range

Neurotransmitter molecules liberated by hair cells in response to a tonal stimulus will diffuse across the synaptic cleft and bind to receptors located on the cell membrane of the dendrites of SG neurons. This entails a change in the membrane potential of the AN fiber, referred to as excitatory post-synaptic potential (EPSP). This depolarization will, as soon as it has reached a certain threshold value, trigger action potentials (APs) which are then conducted along the AN nerve fiber.

Even in the absence of a stimulus, AN fibers fire spikes spontaneously. Based on the rate of this spontaneous activity (SA), they can be divided into three groups (high SA (> 18 spikes / s), medium SA (0.5 to 18 spikes / s), and low SA (< 0.5 spikes / s)). It is interesting to note that SA and threshold values of a SG cell are usually correlated: neurons displaying high SA typically have low thresholds, whereas medium- and low-SA units have intermediate and high thresholds (Fig. 4.13; for a review, see e.g. Rouiller, 1997). When responding to stimuli above threshold, the relation between the SPL of the stimulus and the firing rate of an individual neuron is approximately linear within certain boundaries,

referred to as the unit's dynamic range (Hudspeth, 2000). Neurons presenting lowest thresholds are generally the first ones to saturate and also present a smaller dynamic range than the fibers with higher thresholds. Furthermore, threshold levels correlate with three classes of rate-intensity functions: saturating (low thresholds), sloping-saturation (intermediate thresholds), and straight (highest thresholds; Winter et al., 1990). It should be noted that the thresholds of SG neurons contacting a single IHC may vary considerably (Liberman, 1982); the output of the IHC is thus directed into various parallel channels of different dynamic ranges, thereby increasing the overall dynamic range that can be used by that particular IHC.

It should be mentioned that the above correlations between SA, threshold, and dynamic range were observed both in the cat (Rhode and Smith, 1985) and in the guinea pig (Müller and Robertson, 1991), but not in the Mongolian gerbil (Westerman and Smith, 1984).

Tuning Curve and Characteristic Frequency

Because of the place coding mechanism, an IHC is, depending on its position along the BM, most sensitive to tones of a specific frequency. Since an AN fiber only receives input from a single IHC, this frequency selectivity is passed on: the nerve fiber has a so-called characteristic frequency (CF) at which its response threshold is minimal. The unit will also respond to off-CF stimuli, but only at higher intensities. These properties are typically represented by the threshold tuning curve of the fiber (Fig. 4.13). Units of low SA are usually quite sharply tuned to their CF: when moving stimulus frequency off CF, the intensity needed to evoke a response becomes higher very quickly (their threshold tuning curves are thus characterized by a sharp peak). This behavior is also present but less pronounced in high-SA units (Rhode and Smith, 1985).

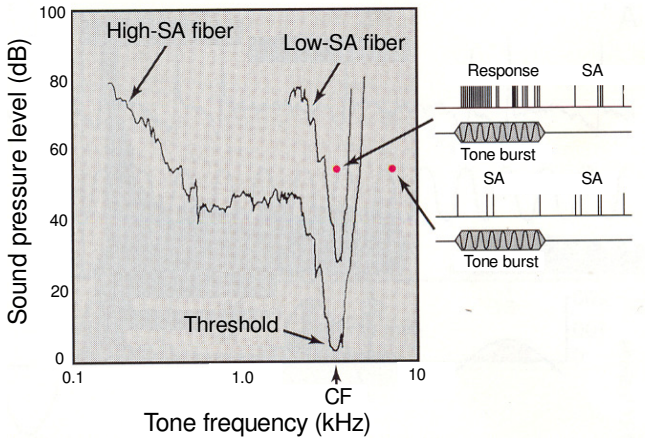

Fig. 4.13 Tuning curves of both a high- and a low-SA AN fiber. The high-SA fiber's threshold is around 3 dB SPL, its CF about 3 kHz (logarithmic x-axis). Note the correlation between the fibers' SA and their thresholds (as mentioned further above in the text). Taken from Brown, 1999.

Thus, when the ear is stimulated by a pure tone of a certain frequency, some AN fibers will display a more marked response than others: stimulus frequency is coded within the pattern of activity among the fibers of the AN. A second mechanism by which information about stimulus frequency can be transmitted is so-called phase-locking. This term means that, in response to low frequency tones, the APs of AN fibers are not randomly distributed but time-locked to the phase of the tonal stimulus (Fig. 4.14.A). In other words, the intervals separating consecutive AP's are equal to the period or integral multiples of the period of the stimulating tone, as shown by the inter-spike-interval histogram (Fig. 4.14.B). Phase-locking is also demonstrated by the period histogram (Fig. 4.14.C) where it can be observed that APs preferentially occur during a specific part of the period of the stimulating tone. Although the absolute refractory period (ARP) of an AN fiber (around 0.85 ms (e.g. Mulheran, 1999))

sets a theoretical limit to its firing rate, phase-locking can be observed up to stimulus frequencies of 4 to 5 kHz; even if an individual fiber will no longer be capable of responding to every cycle of a tone, it will keep on firing at a specific point within the stimulus cycle.

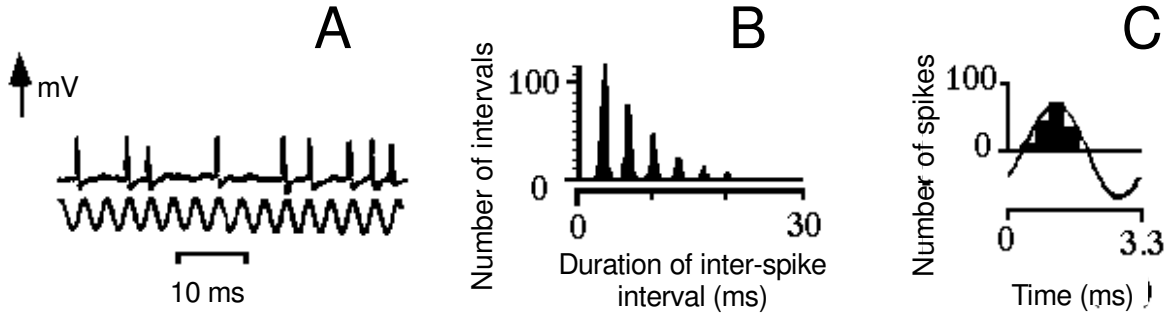

Fig. 4.14 Phase-locking demonstrated in three different ways. A: schematic representation of a pure tone (lower panel) and the recording of the firing pattern of an AN fiber in response to it. B: distribution of the inter-spike intervals recorded from an AN-fiber population in response to a sinusoidal stimulus as a function of interval duration (inter-spike-interval histogram). C: number of spike discharges recorded from an AN fiber as a function of periodicity of the underlying stimulus (period histogram). Taken from Rouiller, 1997.

Up to now there is no conclusive information as to which one of the two frequency-coding mechanisms is used by the auditory system. It seems, though, that the place coding mechanism is of special importance when interpreting high-frequency stimuli, since in those cases, phase-locking can no longer be observed. For low frequencies, it is likely that a combination of both mechanisms is used. Phase-locking may be crucial especially for high-intensity stimuli, when the mechanical tuning exerted by the OHCs is not efficient anymore, and, therefore, the place code can no longer be used.

Response Pattern Evoked by Tone Bursts

The activity of single AN fibers is usually represented in peri- or post-stimulus time histograms (PSTHs). For this purpose, the time segment of interest (situated during or after the stimulus, respectively) is subdivided into many individual, small time intervals, referred to as bins. The number of APs (fired by the nerve fiber(s) at issue) falling within each one of the bins is then determined and represented in form of columns (see Fig. 4.16).

A tone burst is defined as the presentation of a pure tone during a given interval of time. The sound wave making up this pure tone does not reach its maximum amplitude immediately but during a certain rise time. Likewise, the offset of the burst is not instantaneous but occurs during a so-called fall time (see also Fig. 6.4).

In the absence of sounds, AN fibers exhibit SA, as discussed before. During SA, the intervals between individual APs obey a Poisson's distribution (Fig. 4.15). In response to a pure tone burst (duration 50 ms, for instance), the spike rate of an AN fiber will abruptly increase at stimulus onset and then progressively decline to a plateau over a few tens of

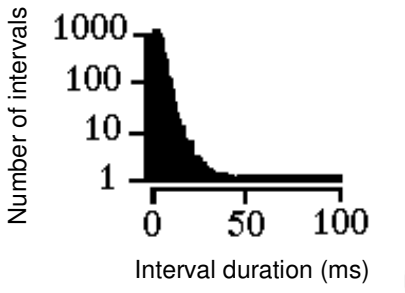

Fig. 4.15 Distribution of the inter-spike intervals recorded from a population of AN fibers as a function of their duration in the absence of a stimulus. Taken from Rouiller, 1997.

milliseconds (Fig. 4.16). This decrease of discharge rate to a steady-state level corresponds to the phenomenon of adaptation. Once the stimulus ceases, spike rate quickly returns to SA level. In some cells, there may be a short drop below this mark, corresponding to a brief inhibition at stimulus offset (Fig. 4.16). Neglecting this episodic offset inhibition, in summary, all AN fibers display a comparable response pattern to a tone burst, consisting of an excitatory response lasting throughout the duration of the stimulus, with an adaptation of discharge rate shortly after stimulus onset.

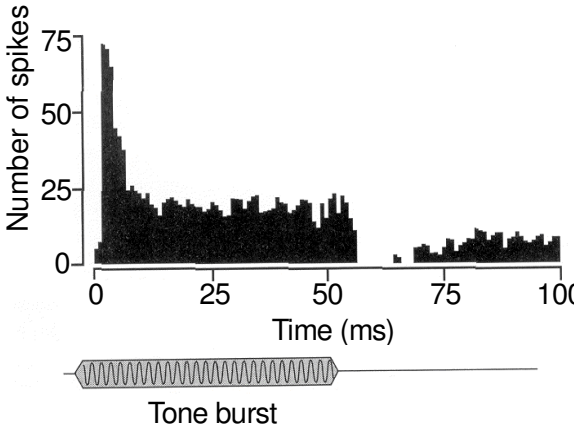

Fig. 4.16 PSTH obtained from an AN fiber in response to the tone burst indicated in the lower part of the figure. Taken from Brown, 1999.

Response Pattern Evoked by Clicks

As opposed to a tone burst, a click stimulus is not based on a continuous sound wave but on a single condensation or rarefaction of the air induced by a single movement of the sound source (see also Fig. 6.5).

In response to a single click stimulus, the PSTHs of AN fibers with CFs up to 3 or 4 kHz usually display multiple peaks (Fig. 4.17; e.g. Kiang et al., 1965a; Evans, 1975). When analyzing the interval between these peaks for a given fiber, it turns out that its duration is inversely proportional to the unit's CF (Kiang,1965; Kiang et al., 1965a; Fig. 4.18). AN fibers with CFs above 4 kHz, on the other hand, usually display only a single peak in their PSTH for a click stimulus. Fig. 4.17 also demonstrates that, in response to a click, the latency of the first PSTH peak is an inverse function of CF. The latency of units with a CF above 2 to 3 kHz is between 1.3 and 1.8 ms, whereas for fibers with lower CFs, latency values can be as high as 4 to 5 ms (Kiang et al., 1965a). This finding may be explained in terms of the traveling wave along the BM: it takes it longer to reach the apex of the cochlea where the low-CF fibers are located.

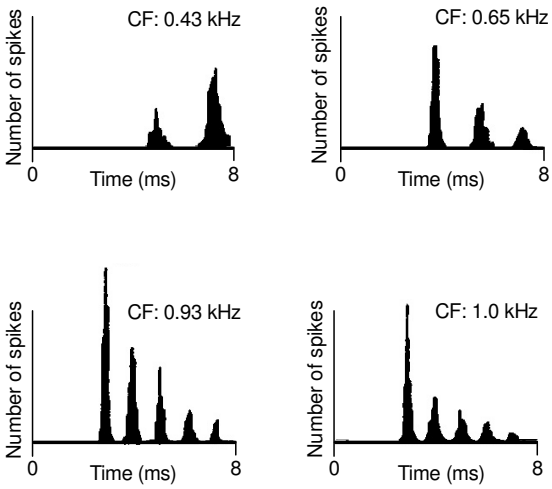

Fig. 4.17 Typical PSTHs recorded from AN fibers with different CFs in response to a single click stimulus. Modified from Kiang et al., 1965a.

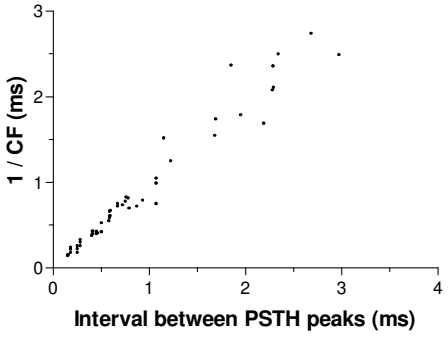

Fig. 4.18 Relationship between the CF of a unit and the inter-peak interval in the unit's PSTH in response to a click stimulus. Modified from Kiang et al., 1965a.

In response to trains of repetitive clicks, the AN displays time-locked activity at rates up to 3'000 pulses per second (pps; Peake et al., 1962a; Kiang et al., 1965a). This suggests that the AN can very accurately code the temporal features of a stimulus paradigm, a valuable property, for instance, for the coding of rapid amplitude modulations as they occur in spoken language.

Efferent Fibers

In addition to the type I and II afferent fibers discussed above, the eight cranial nerve contains the so-called olivocochlear bundle whose medial and lateral components have their origins in distinct parts of the SOC. The olivocochlear bundle seems to modulate both sensitivity and frequency selectivity of the hair cells (Brown and Nuttall, 1984) and could therefore be of importance for the detection of sounds in the presence of loud background noise (Winslow and Sachs, 1988).

1.3.4 Cochlear Nucleus

Response Types

The neurons located in the CN exhibit a wide variety of different response types to a simple tone burst (for a review see e.g. Kiang et al., 1965b; Evans, 1975; Rouiller, 1997). Situated mainly in the AVCN, there is a cell population whose response to the presentation of a tone burst is comparable to that of AN fibers. These units are therefore called "primary-like" (Fig. 4.19). Other neurons, also situated in the AVCN and referred to as "primary-like with notch", exhibit a comparable response envelope except for a brief pause immediately following the first peak. This pause can be attributed to the refractory period of these neurons (1 to 2 ms) following the precisely time-locked response to the onset of the stimulus.

Another response type is displayed by the so-called "chopper" units. The envelope of their PSTH is very much comparable to that of primary-like units, however, the sequence of their action potentials is divided into several individual peaks separated by intervals with fewer spikes. It should be noted that the duration of the intervals between the peaks is not correlated with the

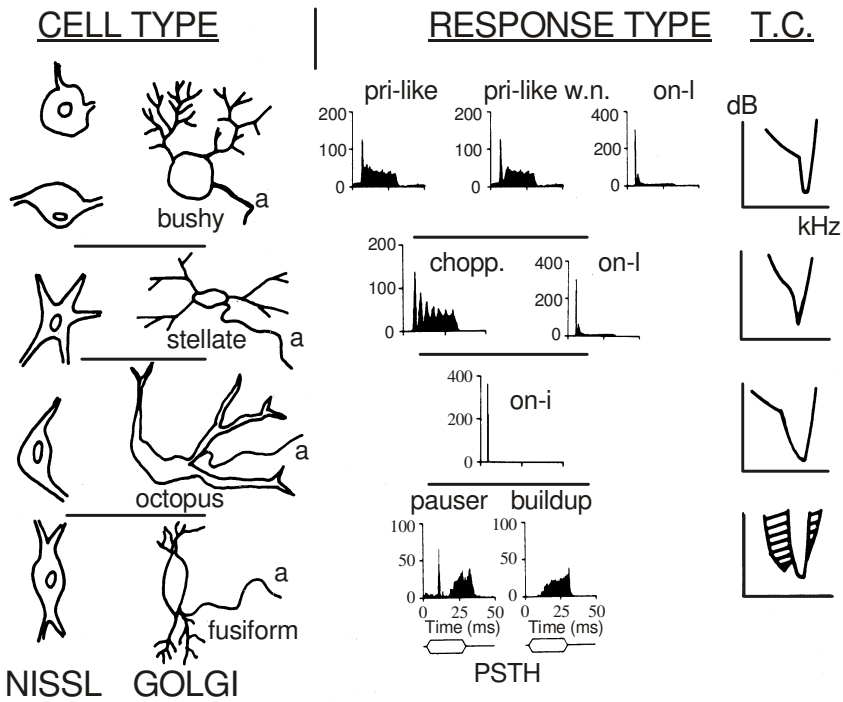

Fig. 4.19 Correlation between anatomical (appearance in Nissl and Golgi stainings) and electrophysiological (single-unit response types (represented by PSTHs) and tuning curves) properties of neurons in the CN. a: axon; chopp.: chopper units; pri-like: primary-like units; pri-like w.n.: primary-like with notch units; T.C.: tuning curve. Modified from Rouiller, 1997.

frequency of the presented stimulus (e.g. Kiang, 1965), indicating that such responses are distinct from phase-locking.

The so-called “on” units are characterized by a high discharge rate at the very beginning of a tone burst which then quickly decreases. In “on-type i” units, the firing rate after the initial peak is practically zero, whereas “on-type l” units maintain a low discharge rate during the rest of the stimulus.

Clearly different unit types are observed in the DCN with discharge patterns exhibiting inhibitory influences. Activity of “pauser” units is suppressed after an initial excitatory peak and recovers during the second half of the stimulus. “Build-up” units present a progressive increase in firing rate towards the end of the stimulus. Finally, “inhibitory” units display a suppression of activity throughout the whole tone burst.

From the above paragraphs, it is evident that the response types observed in the CN are not randomly distributed but can often be associated with one or several of its anatomical divisions. The same holds true, as discussed further above, for the various morphological cell types of the CN. These two facts allow for conclusions as to the correspondence between a given response type and a certain category of neurons. There is evidence that primary-like, primary-like with notch, chopper, and on-type i units are correlated to spherical, globular, stellate, and octopus cells, respectively (Fig. 4.19; for a review see Rouiller, 1997). Pauser and build-up units are likely to correspond to fusiform cells in the DCN. This scheme of correlation has been largely confirmed by a number of studies in which a neuroanatomical marker was injected directly into neurons previously classified physiologically (Rhode et al., 1983a, 1983b; Rouiller and Ryugo, 1984; Smith and Rhode, 1985, 1987, 1989; Smith et al., 1991, 1993; Feng et al., 1994; Ostapoff et al., 1994; Hancock and Voigt, 2002a, 2002b). This more direct approach further suggests that on-type l responses could be obtained from bushy cells (globular cells most likely), stellate cells, or giant cells. For the latter cell type, chopper responses have also been observed.

Intensity Functions

Whereas units from the VCN (mainly primary-like, primary-like with notch, and chopper units) display monotonic rate functions resembling those of AN fibers, non-monotonic rate curves are found for many units in the DCN (mainly pauser and build-up units; Evans, 1975; Rhode and Smith, 1986).

Phase-Locking

Phase-locking can be observed up to frequencies around 3 to 4 kHz in primary-like and primary-like with notch units. In chopper and on-type i units, phase-locking is limited to frequencies of 1 kHz or below. In pauser and build-up units, there is no synchronization of responses at all, except, at times, for very low frequencies.

The ability of CN units to code temporal features of a presented stimulus has also been assessed by observing their responses to sinusoidally amplitude-modulated sounds (tones or noise). As mentioned above, amplitude modulation is an important feature of complex sounds such as speech. On, chopper, primary-like, and primary-like with notch units displayed strong synchronization of their discharges with the phase of amplitude modulation. In the discharge patterns of on and chopper units,

in particular, amplitude modulations were sometimes even better represented than in AN fibers (Frisina et al., 1990).

Tuning Curves

In the same way as AN fibers, the neurons in the CN are frequency-selective. The tuning curves of primary-like, primary-like with notch, chopper, and on-type I units are quite similar to those observed in AN fibers, whereas the frequency selectivity of units with on-type i responses decreases more quickly as stimulus intensity is increased. Pauser and build-up units, besides being excited by frequencies close to their CF, are inhibited by tones falling in adjacent, higher- and lower-frequency ranges, referred to as inhibitory side bands (Fig. 4.19).

Tonotopy

AN fibers with high CFs tend to end in more dorsal and medial regions of the CN than those with low CFs. Despite the complex cytoarchitecture of the CN, this tonotopic arrangement holds in all three of its divisions (Fig. 4.20).

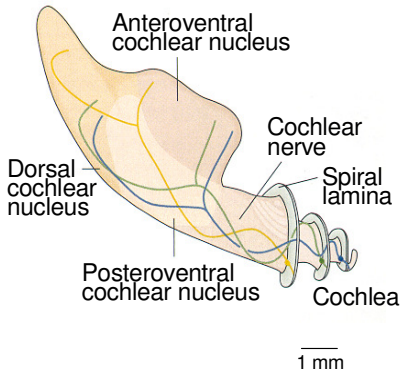

Fig. 4.20 Schematic representation of the tonotopic projection of AN fibers into the CN. Taken from Hudspeth, 2000.

Response Pattern Evoked by Clicks

In response to a click stimulus, low-CF primary-like units of the CN display the same multiple peaks in their PSTHs as AN fibers (Kiang et al., 1965b). Analogously, the inter-peak interval is inversely proportional to the unit's CF. Primary-like units with a CF above 4 kHz, however, as well as chopper and on units, show a single peak in their PSTH in response to a click. The behavior of pauser and build-up units is intermediate to that of the cell types just discussed: neither do they exhibit multiple peaks nor is there a single, well-defined maximum of discharges; their spikes are concentrated temporally, but not as highly as, for example, in chopper units. The latencies of CN units are about 1 ms longer than those of AN fibers and thus range from 2 to 5 ms (cat; Evans, 1975). In the AVCN, in particular, Kiang et al. (1965b) observed latencies between 2.1 and 3.3 ms.

1.3.5 Auditory Relays in the Brainstem, Mesencephalon, Thalamus, and Cortex

Parallel Channels

On their way from the CN to the cerebral cortex, auditory signals run from one relay to the next in an ascending direction. The auditory pathway can thus be said to be serially organized. However, not all fibers use the same relay stations. This is apparent, for instance, at the level of the ventral, intermediate, and dorsal acoustical striae, or when considering the three fiber tract systems leading from the IC to the MGB and the cortex. Thus, in addition to a serial organization, the auditory system processes information by means of several parallel channels.

Interaural Interactions

The SOC is the first relay in the auditory pathway which receives extensive innervation originating from both ears. An important psychophysical achievement based on interaural interactions is the localization of a sound source with respect to the horizontal axis. This task can be accomplished by evaluating differences in either time (MSON) or intensity (LSON) between the signals coming from the two ears. Such interaural time and intensity cues are also processed in the IC. At the level of the thalamus and the auditory cortex, the cells receiving binaural inputs make up about nine tenths of the whole population. In the auditory cortex, summation columns (excited by stimuli from either ear) can be distinguished from suppression columns (excited by signals coming from one ear, inhibited by inputs from the other).

Tonotopy and Frequency Selectivity

Like the CN, the SOC is tonotopically organized over large parts of its area. As for the higher-up auditory relays, there are some which also exhibit a tonotopic arrangement (e.g. the LL, CNIC, parts of the MGB, certain cortical areas) and some that do not or to a lesser degree (e.g. PNIC, ENIC, parts of the MGB, the reticular nucleus of the thalamus, certain cortical areas). Generally, structures containing sharply tuned units are also organized tonotopically.

Response Types and Phase-Locking

Many of the response types described in relation with the CN can be encountered again along the various relays of the auditory pathway. There are, for example, responses resembling primary-like (MSON), primary-like with notch (MSON, MNTB), and chopper (LSON) units of the CN. Higher up, there are ever more neurons responding to the onset of stimulation (e.g. LL, CNIC, and certain cortical areas). Inhibitory responses also become more frequent as one advances along the auditory pathway.

Phase-locking not only exists in the AN and the CN but also in higher auditory relays (SOC, LL, CNIC, MGB). However, in these higher auditory relays, it is restricted to relatively low frequencies (e.g. 1 kHz in the thalamus) and found less frequently because of its limitation to the few units exhibiting sustained responses.

2 Adaptation in the Peripheral Auditory System

2.1 What Is Adaptation?

2.1.1 Adaptation, Habituation, and Fatigue

Adaptation is a common feature of sensory receptors. From a psychophysical point of view, the term means that the way one perceives a prolonged stimulus of time-constant properties changes as the stimulus carries on. The effects of adaptation may manifest themselves in a variety of different ways, depending on the sensory modality concerned. Also, various physiological mechanisms can be at the basis of the ultimate psychophysical manifestation of adaptation. In the sequence of events in a sensory organ, these mechanisms may be located at the very level of the receptor cell (e.g. IHCs,

cones and rods of the retina), before it (e.g. pupillary contraction), or after it (adaptation in the neural pathways).

The key feature to distinguish adaptation from fatigue is the fact that during adaptation, the sensitivity of a sensory receptor is not changed. Thus, even though in a fully adapted state, a sensory organ will be able to react to a sudden change in stimulus intensity. On the other hand, if a receptor undergoes fatigue, this means that it becomes "worn down", that in some way, its reserves are used up. Therefore, the receptor will no longer be able to react to a change in stimulus intensity in the way it usually would. Auditory fatigue usually occurs when the ear is exposed to a very loud environment over a long time.

The third term that has to be defined in this context is habituation. In order to conceive an idea of this concept, one may think of the people living in the northern suburbs of Zürich as, for the time being, the south approach to Unique Airport seems to be the inescapable consequence of our lacking willingness to accept prior, better, solutions to the problem of incoming air traffic. As planes will constantly fly over their roofs at an altitude of only little more than 100 m during their final approach, habituation might come in handy since, from a psychophysical point of view, it means that one becomes less conscious of a repetitive stimulus. On a physiological basis, quite similarly, habituation refers to a change in response due to stimulus repetition (e.g. Givois and Pollack, 2000), however, without the loss of the ability to respond to an increase in stimulus intensity (e.g. Coro et al., 1998). In summary: when a series of identical stimuli is presented to the ear, habituation refers to differences between the consecutive individual responses whereas adaptation is what occurs within each one of them.

Why is it, considering the above definitions, that this paper is considered to be about adaptation and not about habituation? We feel that the notion of "repetitive tones" inasmuch as it is referred to in the concept of habituation is not fulfilled by our stimulus paradigm. The stimuli used in this investigation are repetitive clicks presented at pulse rates between 100 and 1'000 pps, actually resembling the presentation of pure, continuous tones of the same frequency range. Therefore, basing ourselves on the above definition of adaptation, we think that this is the most adequate description of the phenomena described in the present study.

2.1.2 Adaptation in Various Human Sensory Receptors

To further illustrate the phenomenon of adaptation, some examples shall be considered.

Visual Adaptation

When walking from outdoors inside your house on a sunny day, it will be hard to see for a few moments, but eventually, things will lighten up: the eye has adapted to the change in illumination. The sensitivity of the cells in the human eye depends on the amounts of photopigments within them. Small changes in the concentrations of rhodopsin can cause enormous variations of the receptor cells' sensitivity (as much as 500'000-fold). Being in bright light for a while, most of the rhodopsin is reduced to opsins and retinal, and much of the retinal is degraded to vitamin A. The concentration of photopigments is thus reduced and the eye becomes less sensitive. On the other hand, when being in

the dark for a long time, retinal and opsins are converted back into light-sensitive pigments, and, moreover, vitamin A is turned back into retinal. The eye's sensitivity will therefore increase again. In addition to these mechanisms, changes in pupillary size can cause variations in the amount of light entering the eye in the first place. Finally, the neurons in the successive stages of the visual pathways also contribute to the overall adaptation; their adaptive component is very rapid, but only fewfold.

Thermal and Mechanoreceptive Adaptation

When entering the bathtub, the temperature of the water may first feel quite hot and then gradually becomes more comfortable. In our skin there are cold and warmth receptors. When a warmth receptor is subject to an abrupt rise in temperature, its discharge rate will rapidly increase and then adapt during the next few seconds and, more slowly, over the next half an hour or more. Inversely, when subject to a sudden decrease in temperature, the same receptor will practically abolish its SA and then, as it adapts, pick back up part of it progressively.

Also underneath the skin, besides the thermal receptors, mechanoreceptors also have well established adaptive properties. In Meissner's and Pacinian corpuscules adaptation is rapid, whereas Merkel's disk receptors as well as Ruffini endings adapt more slowly.

2.2 Adaptation in the Auditory Nerve

2.2.1 Introduction

Literature on adaptation as it occurs in the AN is abundant. Studies on the subject usually fall into one out of three categories. A first approach consists of describing the neural response to simple stimuli, such as tone bursts, their length varying from about 20 to 500 ms (e.g. Peake et al., 1962a; Kiang, 1965; Westerman and Smith, 1984; Chimento and Schreiner, 1990, 1991). To assess long-term and very long-term adaptation, tone durations of several seconds or even minutes can be used (Javel, 1996). A second way to study adaptation is to investigate how the AN responds to series – "trains" – of short stimuli, such as tone bursts or clicks. Whereas train length may vary considerably (from a few milliseconds to several minutes), the individual stimuli are usually between 50 and 100 µs in duration. Third, there are different kinds of masking studies in which a test tone follows, or is superimposed to, an adapting tone (e.g. Smith and Zwislocki, 1975; Smith, 1977, 1979; Smith and Brachman, 1982; Chimento and Schreiner, 1990, 1991, 1992).

Another aspect in which adaptation studies diverge is the type of activity recorded. There are two common categories: single-unit and whole-nerve studies. In the former, the investigator is interested in the activity of single neurons of the AN (e.g. Kiang, 1965; Smith and Zwislocki, 1975; Smith, 1977, 1979; Smith and Brachman, 1982; Westerman and Smith, 1984; Chimento and Schreiner, 1991). The responses recorded from a fiber are usually presented in terms of PSTHs. In whole-nerve studies, on the other hand, the interest lies in the ensemble of all AN fibers. The electrodes used are larger than those applied in single-unit studies and usually placed near the round window (e.g. Peake et al., 1962a) or in the AN (e.g. Chimento and Schreiner, 1990, 1992). The summed activity of nerve fibers thus recorded is referred to as compound action potential (CAP).

2.2.2 Adaptation in Response to Single Tone Bursts

A schematic PSTH of the response of an AN fiber to a simple tone burst is shown in Fig. 4.21. A great number of efforts have been made during the past years to describe the basic time course of this response behavior, and to find out how it is affected by changes in stimulus parameters. In the following, the most important results about each one of the stages of the adaptation process shall be reviewed.

From early on, it was clear that in response to single tone bursts, the response of the AN was most pronounced at stimulus onset and then decreased, as the stimulus carried on, finally to reach a plateau level (Kiang, 1965; Peake et al., 1962a). Subsequently, this time course of response had to be quantified. The decay in firing rate after the initial peak was reported to be exponential in time by the great majority of authors, with time constants varying among species (Table 4.1). These short-term-adaptation time constants did not depend on stimulus intensity (with the only exception of the recordings carried out by Chimento and Schreiner (1990) in the cat). Additionally, the ratio between the

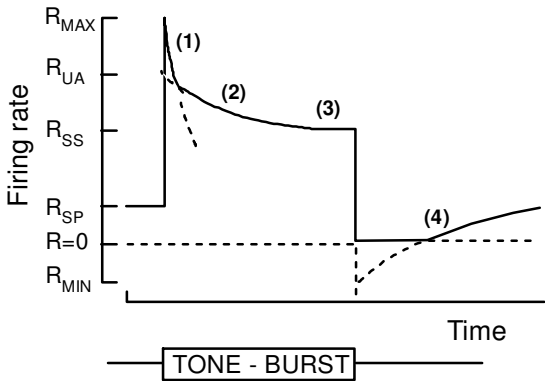

Fig. 4.21 Schematic representation of the different stages of adaptation. (1) Rapid adaptation; (2) short-term adaptation; (3) steady state; (4) recovery to SA. R: firing rate; R_{MAX}: maximum firing rate; R_{MIN}: minimum firing rate; R_{SS}: firing rate during steady state; R_{SP}: spontaneous firing rate; R_{UA}: y-intercept of short-term adaptation. Taken from Harris and Dallos, 1979.

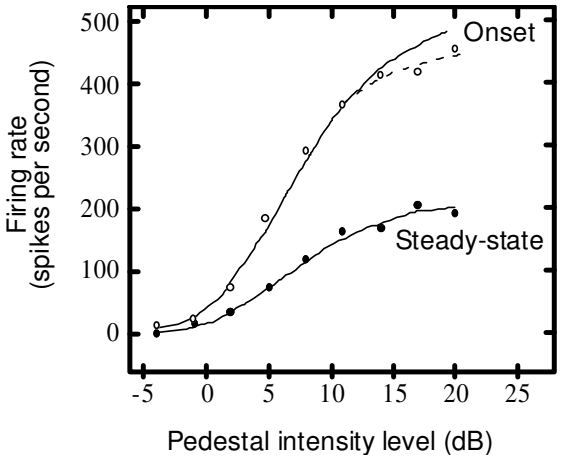

Fig. 4.22 Onset and steady-state firing rate of an AN fiber as a function of stimulus intensity. The two functions are proportional to each other except for a slight deviation at high stimulus intensities which could be due to the upper bound of the unit's dynamic range. Modified from Smith and Zwislocki, 1975.

Species	K_{ST} (ms)	Study	Recording Method
Chinchilla	15	Harris and Dallos (1979)	Single unit
Guinea pig	40	Smith and Zwislocki (1975)	Single unit
Mongolian gerbil	40	Smith (1977)	Single unit
	60	Westerman and Smith (1984)	Single unit
Cat	74 – 116 *	Chimento and Schreiner (1990)	Whole nerve
	94	Chimento and Schreiner (1991)	Single unit

Tableau 4.1 Short-term adaptation time constants of various species as found by different authors. * Chimento and Schreiner (1990) observed the short-term time constant to be intensity-dependent. K_{ST}: short-term-adaptation time constant.

discharge rate at stimulus onset and that during steady state did not depend on the intensity of the stimulus, either; in other words: steady-state discharge rate was a linear function of initial firing rate (Fig. 4.22). Short-term adaptation was therefore taken to be intensity-independent (Smith and Zwislocki, 1975; Smith, 1979; Westerman and Smith, 1984).

Subsequently, attention focused on the existence of another, faster component of adaptation that seemed to be of importance only during the first few milliseconds of response. Rapid adaptation, too, was reported to be exponential in time (e.g. Smith and Zwislocki, 1975, Chimento and Schreiner, 1991). Several reports found the time constant in single fibers to be between 1 and 10 ms (Smith and Zwislocki, 1975; Smith and Brachman, 1982; Westerman and Smith, 1984; Rhode and Smith, 1985; Chimento and Schreiner, 1991). This is in agreement with Yates et al. (1985), although, at low intensities, the latter authors found time constants as high as 15 to 25 ms. Whole-nerve recordings yielded comparable values, e.g. 5.2 ms in the cat (Chimento and Schreiner, 1990).

The time constant of rapid adaptation, in contrast to that of its short-term counterpart, depended on intensity: it decreased as stimulus level was increased (Westerman and Smith, 1984; Yates et al. 1985). Moreover, high-CF units tended to have smaller rapid time constants than low-CF units (Westerman and Smith, 1984; Rhode and Smith, 1985). This is in contrast, however, to the data of Chimento and Schreiner (1990, 1991), who found their rapid time constant to depend neither on stimulus intensity nor on the CF of the responding unit. Possible causes for this discrepancy could be differences between species or analysis methods. Furthermore, intensity and CF dependency could be related, at least when recording CAPs: at higher stimulus intensities, the peak of the traveling wave along the BM is not as well defined as at low intensities, it becomes wider, which means that additional nerve fibers will be stimulated, in particular fibers located more basally than the actual peak (this is apparent from the threshold tuning curve of a typical AN fiber, see Fig. 4.13). If these newly recruited fibers (with higher CFs) actually displayed faster adaptation, an increase in stimulus intensity could indeed lower the adaptation time constant of CAP recordings.

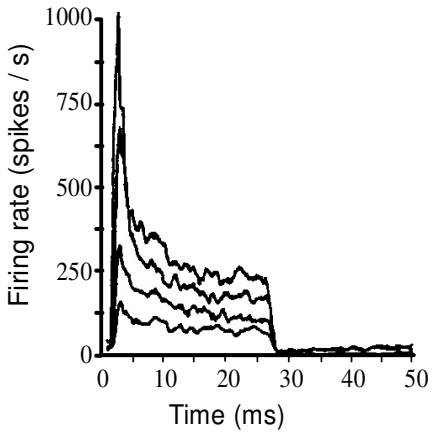

Fig. 4.23 PSTH of a high-CF, high-SA fiber in response to 25-ms tone bursts presented at 66, 69, 76, and 85 dB SPL. (Modified from Müller and Robertson, 1991)

Not only the time constant but also the amplitude of the rapid adaptation component was reported to depend on various stimulus parameters (Smith and Brachman, 1982; Westerman and Smith, 1984; Rhode and Smith, 1985;Yates et al., 1985). For example, at increasing intensities, the initial drop of activity as displayed by the PSTH became more pronounced, firing rates at stimulus onset sometimes reaching values five to eight times as high as those observed during steady state (Rhode and Smith, 1985;Yates et al., 1985; Müller and Robertson, 1991; Fig. 4.23). However, this only seemed to be true for high-SA fibers, whereas in units with low SA, it was observed that the initial peak could actually become less pronounced when increasing intensity (Müller and Robertson, 1991). SA not only influenced intensity-dependency of the onset-to-steady-state

ratio but also the ratio itself: Rhode and Smith (1985) observed the quotient to be an increasing function of both SA and CF, its values ranging from 1.0 for SA = 0 to over 8 for high SA and CFs near 10 kHz.

When combining the rapid and the short-term components, the whole adaptation process could thus be described by a mathematical model consisting of two superposed exponential decays which ultimately led to a plateau (Fig. 4.21; Harris and Dallos, 1979; Westerman and Smith, 1984; Chimento and Schreiner, 1990, 1991). The beginning of the steady-state phase was observed after 50 ms in the cat (Kiang, 1965) and after 80 ms in the chinchilla (Harris and Dallos, 1979). Of course, there is no exact definition of how constant a firing rate or a CAP amplitude has to be in order to be considered steady, and there were other reports indicating that in the guinea pig and the Mongolian gerbil firing rate had become quasi-steady after 150 ms (Smith and Zwislocki, 1975; Smith, 1979), but was still not truly constant after 300 ms (Westerman and Smith, 1984).

Other, yet slower adaptation components have also been observed. In response to a continuous, long tone burst, the discharge rate of AN fibers kept on decreasing for as long as 13 minutes (Kiang et al., 1965a). A thorough investigation of long-term and very-long-term adaptation was conducted by Javel (1996) in cats. Both processes followed exponential time courses, and their time constants were 3.64 s and 45.22 s, respectively. The long-term component's magnitude increased with intensity and decreased with SA.

At the end of a tonal stimulus, the firing rate of an AN fiber may transiently fall to below spontaneous discharge rate but then recovers, following again an exponential time course, to the original spontaneous activity (Fig. 4.21). Time constants for this process have been reported for various species: 37 ms in the chinchilla (Harris and Dallos, 1979), 95 ms in the Mongolian gerbil (Harris and Dallos, 1979), and between 20 ms (Yates et al., 1985) and 95 ms (Harris and Dallos, 1979) in the guinea pig. Interestingly, if one discards the value obtained by Yates et al. (1985), these time constants are in constant ratio (about 2.5 : 1) to those presented in Table 4.1 for short-term adaptation, independently of species.

2.2.3 Adaptation in Response to Trains of Tone Bursts or Clicks

When stimulating the AN with trains of repetitive clicks or noise bursts, Peake et al. (1962a) noted the amplitudes of the CAPs to the individual pulses to be high at first and then to decrease gradually, very much as it has been described above for continuous tones. The amplitude decline occurred faster at high repetition rates (Fig. 4.24). It could be observed most clearly during the first few milliseconds of the train but continued throughout as much as 10 minutes before

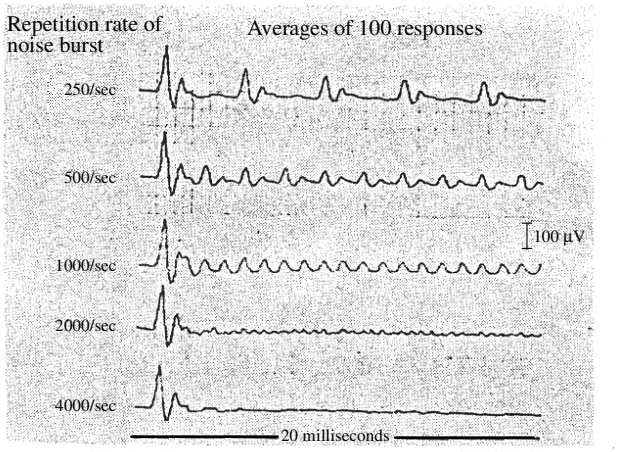

Fig. 4.24 Averaged neural responses to trains of noise bursts (train duration: 20 ms; burst duration: 100 µs) at several burst rates. Recordings from an electrode placed near the round window. Taken from Peake et al., 1962a.

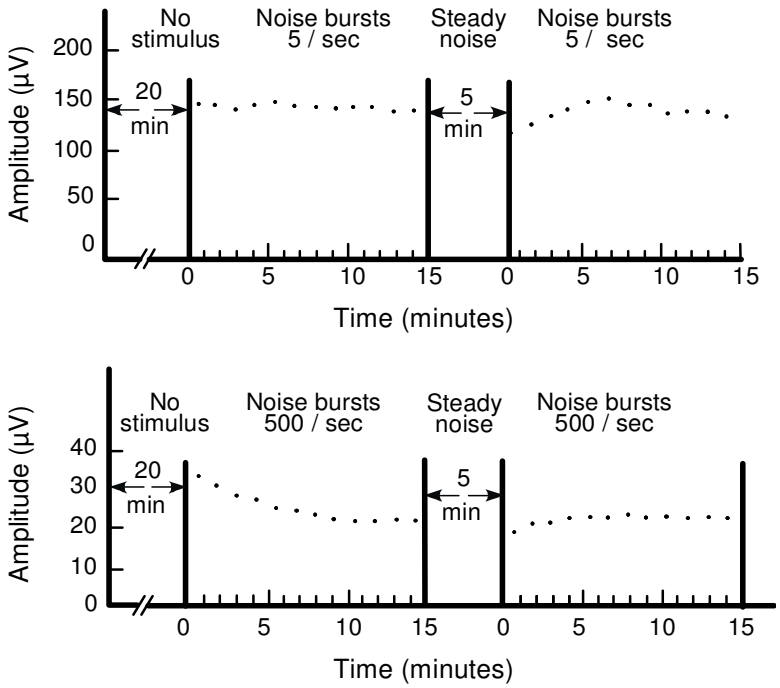

Fig. 4.25 Averaged neural responses to 15-minute trains of repetitive tone bursts (100 µs) presented at two different repetition rates. Taken from Peake et al., 1962a.

leveling out (Fig. 4.25; note the accordance with the data of Kiang et al. (1965a) obtained by using continuous tones). The response amplitude during the steady state depended, above all, on repetition rate (Figs. 4.25 and 4.26) but also on the duration and the intensity of the individual stimuli (Peake et al., 1962b; Fig. 4.26). In this respect, it is interesting to note that stimulus duration and repetition rate could be unified in the concept of the inter-stimulus silent interval, which comprises the time elapsed between the offset of a stimulus and the onset of the next one. Silent interval turned out

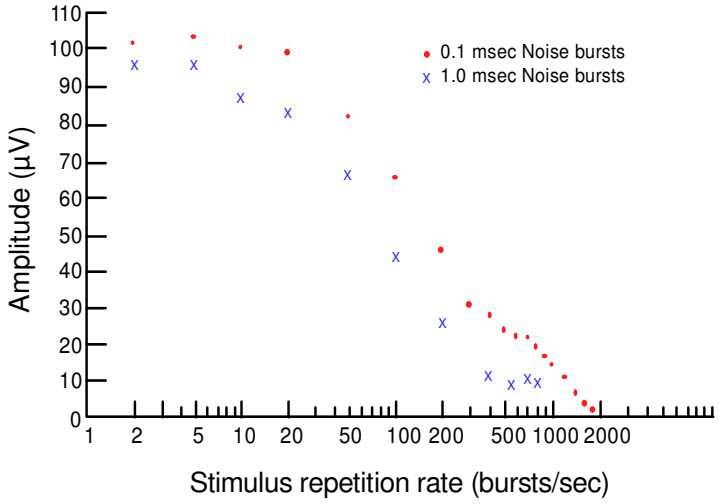

Fig. 4.26 Amplitude of the average steady-state response plotted as a function of stimulus rate for two different burst lengths. (Modified from Peake et al., 1962b).

to be the most important determinant of response amplitude during the steady state (Huang and Buchwald, 1980). In other words, even when stimulus duration and repetition rate were widely varied, the steady-state level remained approximately constant as long as the silent interval between stimuli was not changed.

2.2.4 Masking Studies

Among masking studies, on the one hand, there are the classical forward-masking investigations in which an adapting tone (masker) is followed by a test tone (probe; Fig. 4.27; e.g. Smith, 1977, 1979; Harris and Dallos, 1979; Chimento and Schreiner, 1990, 1991, 1992). This paradigm can be particularly useful to investigate the time course of recovery from adaptation (which takes place between the masker and the probe), and the way in which this recovery is affected by changes in duration and intensity of the adapting tone. On the other hand, there has been a variety of studies which did not use a probe after but during the adapting tone (Fig. 4.28; e.g. Smith and Zwislocki, 1975; Smith and Brachman, 1982). The adapting stimulus is then usually referred to as pedestal, and the probe can be regarded as an increment of intensity superimposed to it (intensity decrements have been used as well). Again, there is an interest in how the various parameters of the pedestal affect the response to the probe.

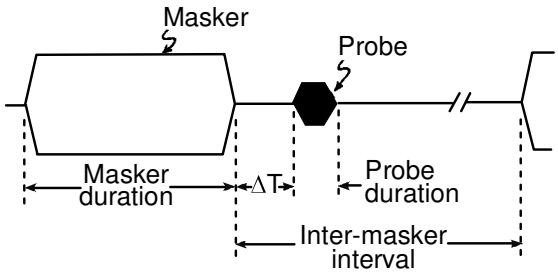

Fig. 4.27 Schematic representation of the standard forward-masking paradigm. ΔT: masker-probe interval. Modified from Harris and Dallos, 1979.

Forward Masking

In the classical forward-masking paradigm applied to AN fibers, the response to a probe is decreased when the stimulus is preceded by a masker (e.g. Smith, 1977, 1979; Chimento and Schreiner, 1990). Alterations of the parameters of the masker such as its intensity, duration, or frequency will influence the decrement in the response to the probe (Smith, 1977, 1979; Harris and Dallos, 1979). However, it was shown that the amount of forward masking could be more closely related to the firing rate evoked by the masking stimulus than to its parameters themselves. Thus, two masking tones of different intensities and frequencies could produce approximately the same decrement in probe response as long as the firing rates they evoked were about equal to one another. As elegantly put by Harris and Dallos (1979): iso-rate contours are also iso-forward-masking contours. This even held for broadband noise.

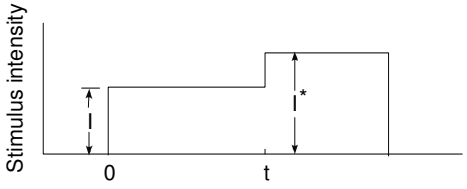

Fig. 4.28 Schematic representation of a pedestal stimulus with a superimposed intensity increment. I: pedestal intensity; I*: total intensity after presentation of intensity increment. Taken from Smith and Zwislocki, 1975.

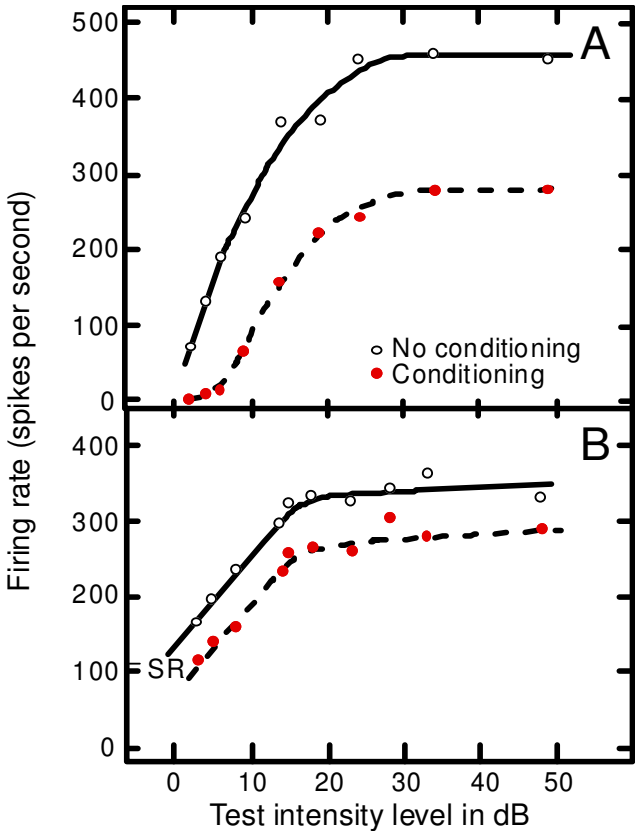

Fig. 4.29 Rate-intensity functions for a probe tone in the presence and absence of a preceding masking tone in two different AN fibers. SR: spontaneous rate. Modified from Smith, 1979.

Likewise, the decrease in response amplitude to the probe did not depend on the masker's absolute duration but on the amount of decay in firing rate occurring during the response to it (Smith, 1977). This relationship was found to be approximately linear with discrepancies at short and long masker durations (Harris and Dallos, 1979).

The intensity of the probe, on the other hand, did not influence the response decrement, i.e. at any intensity, the adapted and unadapted responses differed by the same additive constant (Fig. 4.29; Smith, 1977, 1979). In a more general way, it could be said that the onset amplitude of the response to a probe was exclusively determined by features of the masker (Harris and Dallos, 1979; Chimento and Schreiner, 1992).

This last statement does not refer to the time interval between the probe and the masker tones, which, evidently, is an important determinant of probe tone amplitude since the adapted AN fibers recover during this period. The shape of the recovery process seems to be exponential for all species. However, inter-species differences were found for the number of time constants invoked and for the values of these constants and their intensity dependence (Chimento and Schreiner, 1990, 1991). In the cat, one- or two-time-constant processes were observed. When two time constants could be applied, their mean values were 22 ms (single unit) / 16 ms (whole nerve) for the rapid and 184 ms (single unit) / 125 ms (whole nerve) for the short-term component. If recovery was better fit by a one-stage equation, the time constant was 95 ms in single units (Chimento and Schreiner, 1990, 1991) and 50 to 120 ms for the CAP (Abbas, 1984). All these values were independent of masker intensity and, in single-unit studies, of CF. Recovery in the Mongolian gerbil was observed to consist of a single exponential process with a time constant of 115 ms. In the chinchilla, Harris and Dallos (1979) could fit the observed recovery curve with one exponential component at low masker levels, the time constant ranging from 32 to 74 ms as intensity increased from 10 to 60 dB above unit threshold. At higher masker intensities, a second, slower exponential process had to be introduced (with a time constant in the range of 160 ms). Moreover, also in the chinchilla, high-SA fibers were observed to recover more quickly than low-SA fibers (Relkin and Doucet, 1991; Relkin et al., 1995). Even three recovery stages were witnessed in CAP recordings from guinea pigs (Eggermont, 1985). CAP amplitude stayed constant during the first millisecond after

masker offset, then increased with a time constant of 4 to 5 ms during the next 16 ms, and finally went through a third recovery stage with a time constant of 50 to 60 ms to be complete after 250 ms or more. In humans, recovery took about four times as long (Eggermont, 1985). When recovering from long-term adaptation, the recovery time constant depended on the masker's duration; it ranged from 1 to 10 s in response to a one-minute masker and could become as high as 400 s in response to a 15-minute masker at high intensity (Abbas, 1984).

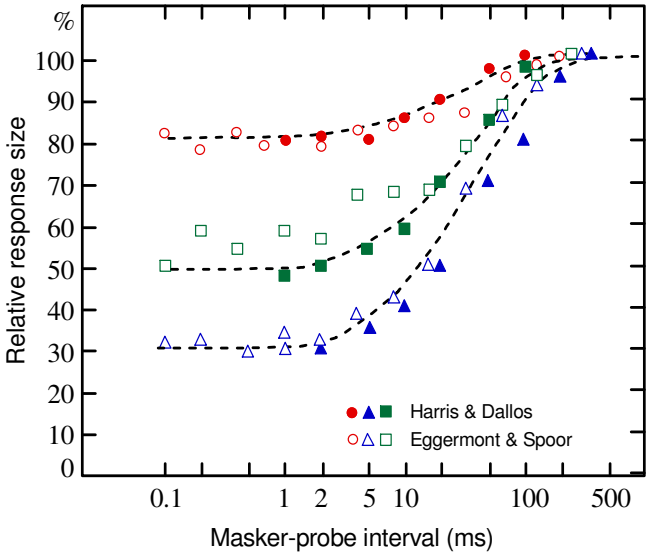

Fig. 4.30 Comparison of recovery from adaptation for both single-unit responses and CAPs as assessed by forward masking. Shown are selected data from Harris and Dallos (1979) and from Eggermont and Spoor (1973). Data were obtained at three different masker-probe ratios. The actual ratios are not the same, however, for ratios inducing a comparable amount of adaptation shortly after masker offset, recovery time courses are similar. The data points represent relative response amplitudes with respect to the response to the unmasked probe. Taken from Eggermont, 1985.

It should be noted that comparison of single-unit data (Harris and Dallos, 1979) to results obtained by recording CAPs (Eggermont and Spoor, 1973) suggests that the former may well be at the basis of the observations about the latter (Fig. 4.30; Eggermont, 1985). This hypothesis found more support in the results of Relkin et al. (1995) who, in chinchillas, found a two-stage CAP recovery time course whose time constants were similar to those found for low- and high-SA fibers, respectively, in a previous single-unit study (Relkin and Doucet, 1991).

Another interesting comparison can be made between the post-stimulus suppression of SA on the one hand and the decreased response amplitude to a probe following a masker on the other hand. The absolute value of the response decrement to the probe in forward masking is usually greater than that of the drop in SA following a simple tone. However, this discrepancy could be accounted for by the fact that SA itself is often quite low, and firing rate simply cannot drop below (Smith, 1977; Harris and Dallos, 1979). In the chinchilla, when normalizing the amplitudes of the two processes, their time courses match each other very well (both having time constants of about 37 ms; Fig. 4.31; Harris and Dallos, 1979). Also, the reduction in both probe response amplitude and SA depends on the intensity of the foregoing tone.

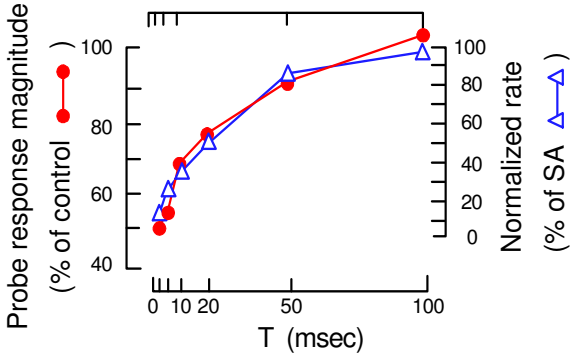

Fig. 4.31 Comparison of the recovery of probe amplitude in forward masking with post-stimulus recovery of SA. Note that when adjusting the respective y-axes of the two processes, their time courses are approximately similar. Taken from Harris and Dallos, 1979.

Chimento and Schreiner (1991, 1992), as opposed to other forward-masking investigators, used long probe tones (290 ms) to investigate the form of the response when the recovery process from the masker and adaptation to the probe itself occurred simultaneously. As silent interval was increased from 0 to 400 ms, the response envelope progressed systematically from a recovery to an adaptation function (Fig. 4.32). Practically all traces could be fit either by an ascending or by a descending two-time-constant exponential-decay equation. Recordings from single units and from the whole AN yielded similar results.

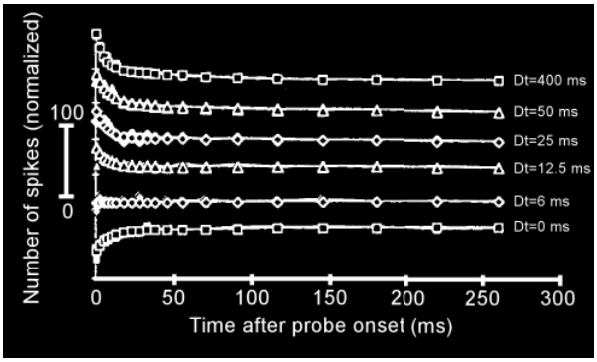

Fig. 4.32 Time course of responses to 290-ms probes following a masker after varying silent intervals (indicated to the right of the traces). Data were derived from 19 AN fibers and then averaged. All traces, except for the one obtained at a silent interval of 6 ms, could be fit by an equation involving two exponential processes. Dt: silent interval between masker and probe tones. Taken from Chimento and Schreiner, 1991.

Intensity Increments and Decrements Superimposed to Tone Pedestals

When using a stimulus paradigm such as the one in Fig. 4.28, response to the probe was observed to be reduced in the presence of a pedestal, sometimes to the point where the total firing rate to the superposed masker and probe tones was smaller than to the probe alone (Smith, 1979). A key finding of such pedestal / increment studies was that the increase in firing rate in response to an intensity increment did not depend on the onset time of the increment. In other words, even if the firing rate during the pedestal had diminished to steady-state level, an increment in stimulus intensity provoked the same sudden increase in firing rate as it did when presented just after, or even at, the onset of the pedestal tone (Smith and Zwislocki, 1975; Smith, 1979). The same observation was made for intensity decrements, too. These findings turned out to be of importance when trying to model adaptation mathematically; they shall be reconsidered in section VIII.5.1.1.

2.3 Adaptation in the Cochlear Nucleus

2.3.1 Introduction

Literature on adaptation in the CN is less abundant than that for the AN. As in the AN, activity of neurons in the CN can be recorded in different ways. The changing features among the different techniques are the size as well as the site of implantation of the electrodes, and therefore also the type of activity recorded. As opposed to single-unit studies (e.g. Møller, 1969), auditory near-field evoked potentials (ANEPs; e.g. Loquet and Rouiller, 2002) permit to monitor the activity of a group of cells, without, however, considering the whole nucleus. Additionally, there are more global recordings, such as CN evoked potentials (EPs; e.g. Huang, 1981) or the standard auditory evoked brain stem response (ABR) derived from surface electrodes (e.g. Shaw, 1990).

2.3.2 Adaptation in Response to Tone Bursts

Kiang (1965) found that in response to both short and long tone bursts (100 and 1000 ms, respectively), some CN units displayed response behavior well comparable to that of the primary auditory neurons, whereas others responded radically differently. He attributed these differences to the varying anatomical location of the recorded units within the CN. Meanwhile, it is clear that the unit types of the CN display a wide variety of different response patterns to simple tone bursts (see above Fig. 4.19; e.g. Kiang et al., 1965b; Evans, 1975; Rouiller, 1997), indicating that their adaptive properties are much less uniform than those of AN fibers. Whereas some CN units (primary-like, primary-like with notch, and chopper) exhibit adaptive properties quite comparable to those of the AN, others (on, pauser, and build-up) display totally different behavior. In the Mongolian gerbil, the firing rate of primary-like units has been observed to follow an exponential adaptation time course with a time constant of about 40 ms (Smith, 1977), a value similar to results obtained from the AN.

2.3.3 Adaptation in Response to Trains of Tone Bursts or Clicks

Several studies suggest that CN neurons respond strongly at the beginning of a train of repetitive clicks or tone bursts and then adapt as the train carries on (Møller, 1969; Huang, 1981; Loquet and Rouiller, 2002). In a single-unit study, Møller (1969) distinguished between “sustained” and “transient”

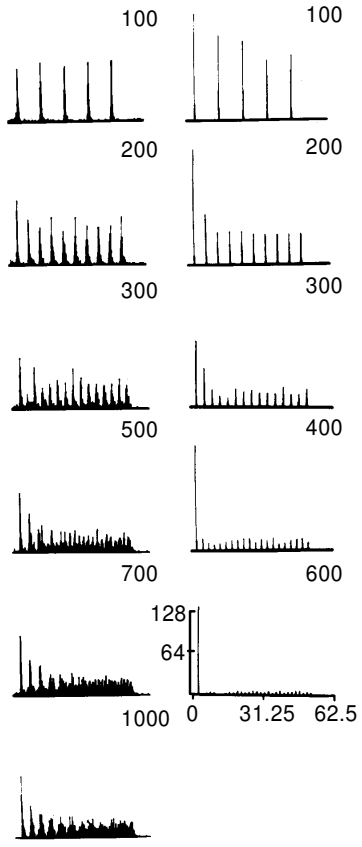

Fig. 4.33 PSTHs of two CN units recorded in response to 50-ms trains of repetitive clicks at various repetition rates (indicated in the upper right-hand corner of each graph). Panels on the left are derived from a “sustained” unit, those on the right from a “transient” unit. Modified from Møller, 1969.

units, referring to their behavior in response to continuous sound ("transient" units are likely to correspond to what has been called on units herein, and "sustained" responses probably represent either primary-like, primary-like with notch, or chopper units). When stimulated with repetitive clicks at a low rate, both transient and sustained units responded reliably to all individual stimuli; as repetition rate was increased, however, their firing rates started to adapt. At high repetition rates, as illustrated in Fig. 4.33, the behavior of both cell types resembled their response to continuous sound: in sustained units, the firing rate adapted after an initial peak but did not drop below a certain limit, whereas transient units only responded at the very onset of the train.

A similar decrease of response activity was observed in the cat (Huang, 1981) and in the rat (Loquet and Rouiller, 2002), based on evoked and near-field evoked potentials, respectively. Quantification of results suggested an adaptation time course consisting of two superposed, exponentially decaying components and a plateau (Loquet and Rouiller, 2002). Both adaptation stages proved to be rate-dependent: the rapid time constant decreased from 6.7 ms at 100 pps to 0.41 ms at 1'000 pps, and the short-term component's range went from 41.1 ms at 100 pps to 3.36 ms at 1'000 pps. Likewise, the amplitude of the average steady state response decreased as stimulus repetition rate was increased. As in the AN, it was observed that the inter-stimulus time interval was an important determinant of the plateau amplitude (Huang and Buchwald, 1980): stimulus paradigms using widely different tone burst durations and repetition rates yielded similar results as long as silent interval was held constant. No amplitude decrements were observed when this interval was greater than 100 ms.

2.3.4 Recovery from Adaptation

There is no unanimous data as to the time course of recovery of the neurons in the CN. On the one hand, Huang (1981) observed amplitude recovery of CN EP to follow an exponential time course. On the other hand, single-unit studies using a forward-masking paradigm suggested that most primary-like, primary-like with notch, and chopper units followed a linear-in-log-time recovery pattern (Fig. 4.34; Boettcher et al., 1990; Shore, 1995). While some of the on, pauser, and build-up units displayed comparable recovery time courses, others behaved quite differently, presenting no adaptation at all, U-shaped or exponential-in-log-time patterns. Full recovery lasted between 275 and 525 ms (Boettcher et al., 1990).

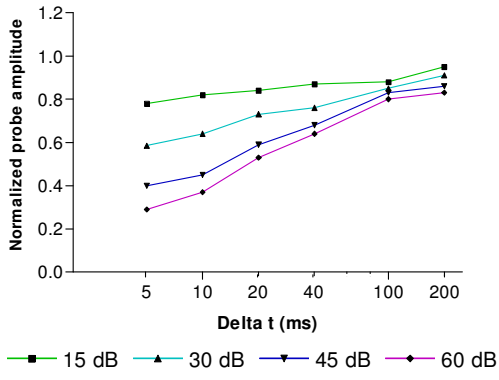

Fig. 4.34 Mean recovery functions of a total of 36 primary-like units as assessed by forward masking. Delta t denotes the masker-probe interval. Modified from Boettcher et al., 1990.

Furthermore, in forward-masking paradigms, response to the probe depended, as in the AN, on the intensity of the masking tone (Fig. 4.34; Boettcher et al., 1990; Shore, 1995). The decrement in probe tone

response seemed to be directly related to the intensity of the masker. This is in contrast to data derived from the AN, where the decrement was most closely related to the firing rate evoked by the masking tone. The amplitude of the response to the probe tone not only depended on the masker's intensity but also on its duration (Shore, 1995). The last two findings go hand in hand with the transient decrease of SA at the end of a simple acoustic stimulus: recovery time to the original SA was witnessed to increase as a function of both the masker's duration and level (Starr, 1965; Boettcher et al., 1990). Additionally, in both guinea pigs and chinchillas, CN units with high SA displayed less masking and faster recovery time courses than low-SA units (Boettcher et al., 1990; Shore, 1995), analogously to what has been said above about AN recovery.

V RESEARCH AIMS

1 Outline of the Present Study

Our investigation aimed at an electrophysiological assessment of the adaptation properties of the peripheral relays in the mammalian auditory system in response to repetitive acoustic stimulation. We recorded ANEPs from electrodes implanted in the AVCN of adult Long-Evans rats. The electrodes were implanted chronically, allowing for repeated recording sessions over large periods of time. The animals were awake during the experiments, permitting us to preclude eventual effects of anesthesia on the recorded potentials.

2 Aims of the Present Study

2.1 Justification of the Recording Method

The suitability of our recording technique had to be verified. This objective was approached in several ways. First, we determined stimulus intensity thresholds for the detection of the ANEP in response to single tone bursts presented at various stimulus frequencies. The threshold curves thus established could be compared to those obtained in prior studies (see section VII.1). Second, the amplitude of both negative components of the ANEP (N_1-P_1 and P_1-N_2, see Fig. 6.5) were assessed in response to click stimuli presented at various intensities in order to verify if our method yielded realistic amplitude-intensity curves. The data obtained is presented in section VII.2. Third, latency measurements were carried out for both ANEP components (see also section VII.2). Besides further justifying our recording technique, the latency values proved useful when trying to establish correlations between the individual components of the ANEP and the neural populations possibly at their basis. A detailed discussion of the latter topic is given in section VIII.2.

2.2 Study of Adaptation

The present study was designed to complete a previous investigation on auditory adaptation conducted by Loquet and Rouiller (2002). In contrast to their report, in which adaptation had been studied in response to trains of repetitive acoustic clicks presented at various repetition rates but at only one fixed intensity, both of these stimulus parameters were varied in the present investigation. Moreover, whereas the mentioned report had focused on the N_1-P_1 component of the ANEP, the present study aimed at an assessment of the adaptive behavior of both negative ANEP deflections. For this purpose, the amplitudes of both peaks as they were obtained in response to the consecutive clicks in a train were measured and then graphically displayed. For the N_1-P_1 component, the response traces thus established could be well fit by an equation consisting of two superposed exponential decays and a steady state (section VII.3.1.1). This mathematical description of adaptation allowed for an accurate determination of the time constants of the two exponential processes as a function of both stimulus intensity and repetition rate (results presented in sections VII.3.1.2 and VII.3.1.3 and discussed in sections VIII.4.2 and VIII.4.3, respectively). Furthermore, the amount of adaptation was quantified for both ANEP components in terms of the ratio between the average

response amplitude obtained during the steady state and that evoked by the first click of a train. The susceptibility of this quotient to stimulus intensity and repetition rate is described in sections VII.3.1.2 and VII.3.1.3 for the N_1-P_1 component and in sections VII.3.2.2 and VII.3.2.3 for the P_1-N_2 component. Additionally, a detailed comparison of the behavior of the two ANEP components is given in section VII.3.3 and discussed in section VIII.3.

In addition to the purely phenomenological approach to the adaptive behavior of the auditory periphery described in the preceding paragraph, it was also an aim of the present study to come up with possible physiological explanations for the data found. The methodology of this assessment of the nature of adaptation was two-fold: in section VIII.5.1 a few mathematical models of auditory adaptation shall be outlined, whereas in section VIII.5.2, possible sites of the adaptive processes along the auditory pathway shall be discussed. Finally, section VIII.5.3 is designed to investigate the extent to which the theoretical predictions emerging from these two approaches are met by our empirical results.

2.3 Histology

The brains of the animals used in the study were processed histologically in order to verify the position of the recording electrode within the AVCN. The photomicrographs taken are displayed in section VII.4.

3 Signification of Results

As mentioned before, amplitude modulation is an important characteristic of complex sounds such as speech. A series of repetitive clicks presented at a high stimulus rate can be considered an extreme form of an amplitude-modulated signal. The goal of the present study was an accurate description of adaptation as it occurs in the peripheral mammalian auditory system in response to this kind of stimulation. Knowledge of the adaptive properties of neurons in the AN and the CN in response to such acoustic stimuli will allow for a comparison with the response behavior of the same units in reply to analogous electric stimulation (i.e. a stimulus paradigm consisting of repetitive electric pulses). The significance of this comparison lies in the important clinical application of the electric stimulation paradigm in terms of certain speech-coding strategies of auditory implants stimulating either the AN (intra-cochlearly) or directly the CN. In order to optimize these speech-coding strategies (i.e. in order to ever better reproduce electrically the events in the auditory system in response to natural, acoustic signals) a thorough knowledge of the adaptive behavior of the auditory periphery in response to both acoustic and electric stimulation is essential. Only by comparing these two will we be able to determine which adaptive components of sound processing we skip by stimulating directly the dendrites of the AN or the neurons of the CN, and must therefore compensate by adapting the electrical stimulus paradigm.

VI MATERIALS & METHODS

1 Animals

Male adult Long-Evans rats (Janvier Laboratories, France), weighing approximately 300 g, were housed in individual cages (425 x 266 x 150 mm) from the beginning of the experiments. Food pellets (Kliba-Mühlen, Basel, Switzerland, ref.: 343) and tap water were available ad libitum. The temperature in the animal room was maintained at 20 ± 1 °C and light was on from 07.00 until 19.00 h. Experimental procedures were approved by the Swiss veterinary authorities and performed in accordance with "Principles of Laboratory Animal Care" (NIH publication No. 86-23, revised 1985) and the 1964 Declaration of Helsinki for animal care.

2 Experimental Procedures

2.1 Animal Preparation

Six rats were implanted with a chronic electrode in the left AVCN in order to record ANEPs. Before surgery, the animals were treated with atropine sulfate (0.05 mg / kg, subcutaneous) to minimize respiratory distress and a non-steroidal anti-inflammatory drug (Carprofen, 4 mg / kg, intramuscular) to reduce inflammation and pain. Then, they were deeply anaesthetized with pentobarbital (Vetanarcol®, 40 mg / kg, intraperitoneal). The animals were placed in a stereotaxic apparatus (Muromachi Instruments, Japan, Model 1404) equipped with special ear bars to prevent damages to the tympanic membrane. One custom-made perforated ear bar was used for acoustic stimulation. A midline incision

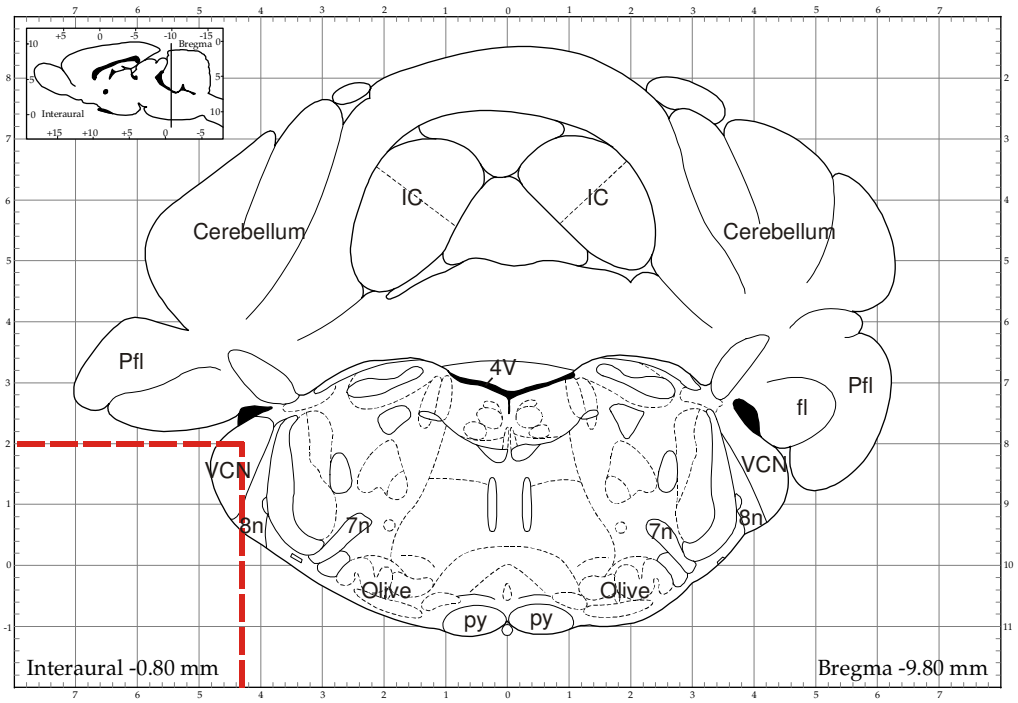

Figure 6.1 Coronal section of a rat's brain at the level of the VCN. The location of the chronic recording electrode is indicated by the dotted red lines. 4V: fourth ventricle; 7n: facial nerve; 8n: auditory nerve; fl: flocculus; IC: inferior colliculus; Pfl: paraflocculus; py: pyramidal tract. Modified from Paxinos and Watson, 1998.

was made on the scalp and the skull reference point bregma was exposed. From this landmark, based on Paxinos and Watson's atlas (Paxinos and Watson, 1998), stereotaxic coordinates of the left VCN were accurately determined (9.80 mm caudal, 4.30 mm lateral, 8.00 mm ventral). A tungsten microelectrode (2 to 4 MΩ impedance) covered with Teflon (except at the tip) was implanted in the left VCN to record ANEPs, and a ground microelectrode was placed on the dura mater in the nasal region (adapted from Henderson et al., 1973). The optimal position of the recording electrode was assessed by observing the waveform of the ANEP while advancing it into the CN (mean electrode position 7.99 ± 0.35 mm ventral to bregma). Then, the two electrodes were soldered to a socket and fixed to the skull using dental cement. The animals were allowed to recover for one week before recording.

2.2 Acoustic Stimulation

Testing was performed in an audiometric room (Model AC-1 Chamber, IAC, Germany) on awake rats placed in a restraining device (Fig. 6.2) that ensured a constant distance (10 cm) between the speaker (JBL® 2405) and the left pinna. Acoustic signals were synthesized digitally using SigGen32 software (Tucker-Davis Technologies (TDT) System II) and, after digital / analogue conversion (DA1 in the schematic representation of the equipment, Fig. 6.3), fed into a programmable attenuator (PA5) before delivery to the speaker. Calibration of the system was carried out with a

Fig. 6.2 Picture of a Long-Evans rat placed in the restraining device during a recording session.

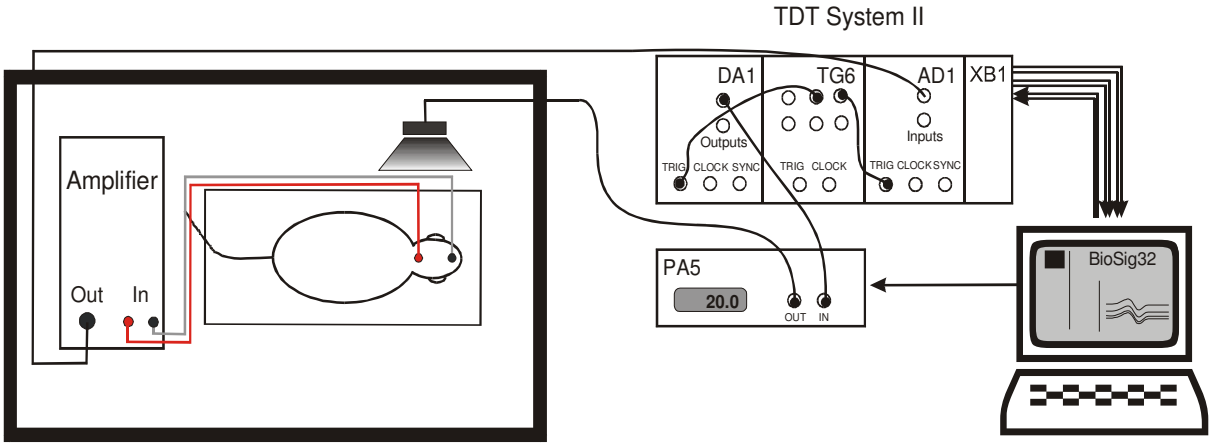

Figure 6.3 Block diagram of the equipment used to measure and store auditory evoked responses. AD1: analogue / digital converter; DA1: digital / analogue converter; PA5: programmable attenuator; TG6: timing generator; XB1: BUS module.

sound level meter (B&K, 2231) by measuring the SPL emitted by the speaker when driven by a pure tone signal at 9 V peak level. The calibration microphone (B&K, 4155 prepolarized free-field ½ inch) was positioned at the location which, during the experiments, was occupied by the central point of the animal's head. The ANEPs were amplified (10^3), bandpass-filtered between 30 Hz and 5 kHz, and fed into an analogue / digital converter (AD1 in Fig. 6.3). The data acquisition software BioSig32 was used to automate ANEP averaging and to store data for off-line analysis. During the experiments, the ambient noise level within the audiometric room did not exceed 69 dB SPL when considering the overall spectra linear level and 38 dB SPL when considering the frequencies above 1 kHz.

2.2.1 Tone bursts

Audiometric test stimuli were tone bursts of 3 ms duration (0.5 ms rise / fall time) shaped by cosine-squared functions, presented 250 times, alternately in phase, and repeated at a rate of 10 per second. For each burst the analysis window lasted 10 ms. ANEP thresholds were determined for 11 tone frequencies ranging from 1 to 30 kHz by varying the stimulation intensity in 5-dB SPL increments. The amplitude of the N_1-P_1 component of the ANEP was measured as the voltage difference between the first negative (N_1) and the positive (P_1) peak (Fig. 6.4). A trough-to-peak amplitude of 10 µV was considered threshold in our experiment.

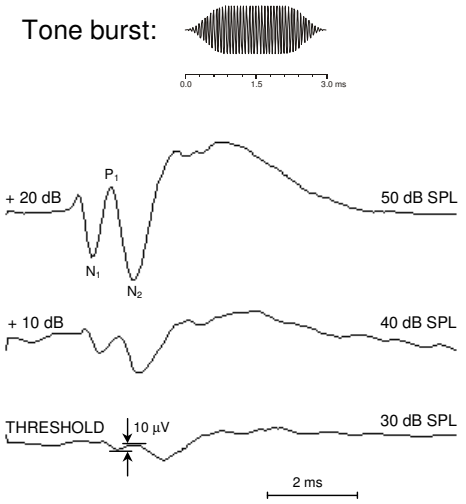

Fig. 6.4 Typical ANEP traces elicited by 16-kHz tone bursts (Rat 6). Stimulus intensity in dB SPL is indicated to the upper right of each response curve. Negative polarity is downward.

2.2.2 Clicks

In order to establish intensity functions, single rectangular-pulse condensation clicks (duration 100 µs) were presented at intensities ranging from 0 to 70 dB SPL (5-dB-SPL steps). 250 stimuli were presented at each intensity at a rate of 10 per second. For each stimulus the analysis window lasted 10 ms. Again, the amplitude of the N_1-P_1 component of the ANEP was measured as the voltage difference between the N_1 and P_1 peaks (Fig. 6.5).

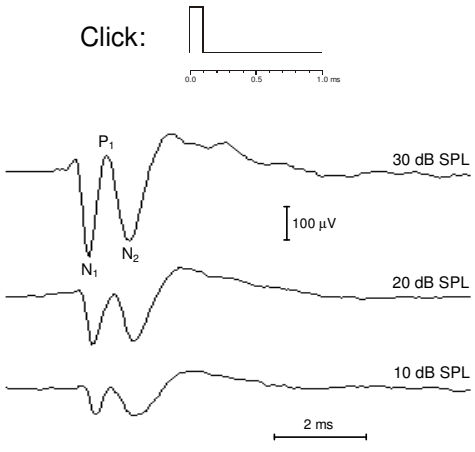

Fig. 6.5 Typical ANEP traces elicited by clicks (Rat 6). Stimulus intensity is given to the upper right of each response curve. Negative polarity is downward.

2.2.3 Repetitive Acoustic Stimulation

Acoustic stimulation consisted of repetitive rectangular-pulse condensation clicks (duration 100 µs) delivered in trains of a constant duration of 250 ms, followed by a 250-ms silent period before the next train (50% duty cycle). Six different intra-train pulse rates (100, 200, 400, 600, 800, and 1'000 pps) and five intensities (5, 10, 30, 50, and 70 dB SPL) were tested. A train of given parameters was presented 50 times, and the response traces were then averaged. The analysis window stretched over the whole 250-ms train length. The amplitudes of both the N_1-P_1 and the P_1-N_2 components of the ANEPs were measured as the voltage difference between the respective negative peak and P_1. At repetition rates higher than 400 pps, responses to individual clicks started to overlap so that the amplitude of a certain response was influenced by the preceding one (Fig. 6.6). In order to circumvent this contamination, a subtraction method was used (Wilson et al., 1997; Loquet and Rouiller, 2002). This method consisted in recording separately response traces to trains of n clicks and to trains of (n+1) clicks (50 presentations of each), averaging them, and then subtracting the former from the latter, thus only exposing the response to click (n+1) (Fig. 6.7). However, this technique would, especially at high repetition rates, require a very large number of trains to isolate the ANEP to every click. Therefore, in order to avoid overstimulation of the AN during recording sessions, ANEPs were collected for all consecutive clicks during the initial 20 ms, then for one click every 10 ms during the next 60 ms, and for only three individual clicks during the remaining 170 ms of the train. The N_1-P_1 and P_1-N_2 amplitudes thus obtained were measured, normalized relatively to the highest response in the train (which was usually the first one) and then plotted as a function of the position of the evoking click in the train (see Fig. 7.4.B).

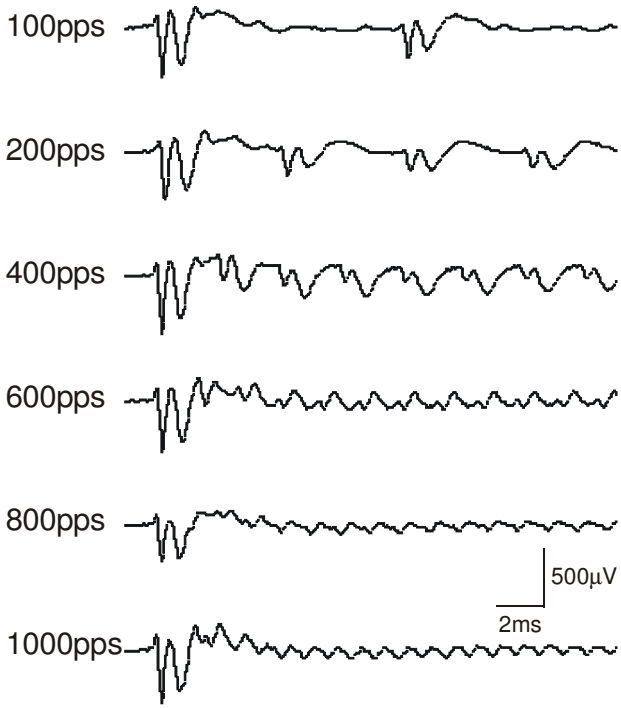

Figure 6.6 Averaged ANEPs elicited by 250-ms trains of repetitive clicks presented at six different rates at 50 dB SPL (Rat 6). Note that responses overlap at rates of 600 pps and above. For clarity's sake, only the first 20 ms of the response trace to each train are shown.

2.3 Histology

The location of the recording electrode in the VCN was verified at the end of the experiment (three months after implantation) in all rats. The animals were deeply anaesthetized with an overdose of pentobarbital (Vetanarcol®, 80 mg / kg, intraperitoneal). Immediately afterwards, a continuous positive current (10 µA) was passed through the recording electrode for 10 min. The animals were then perfused through the heart with 0.9% saline solution followed by a 4% paraformaldehyde solution in

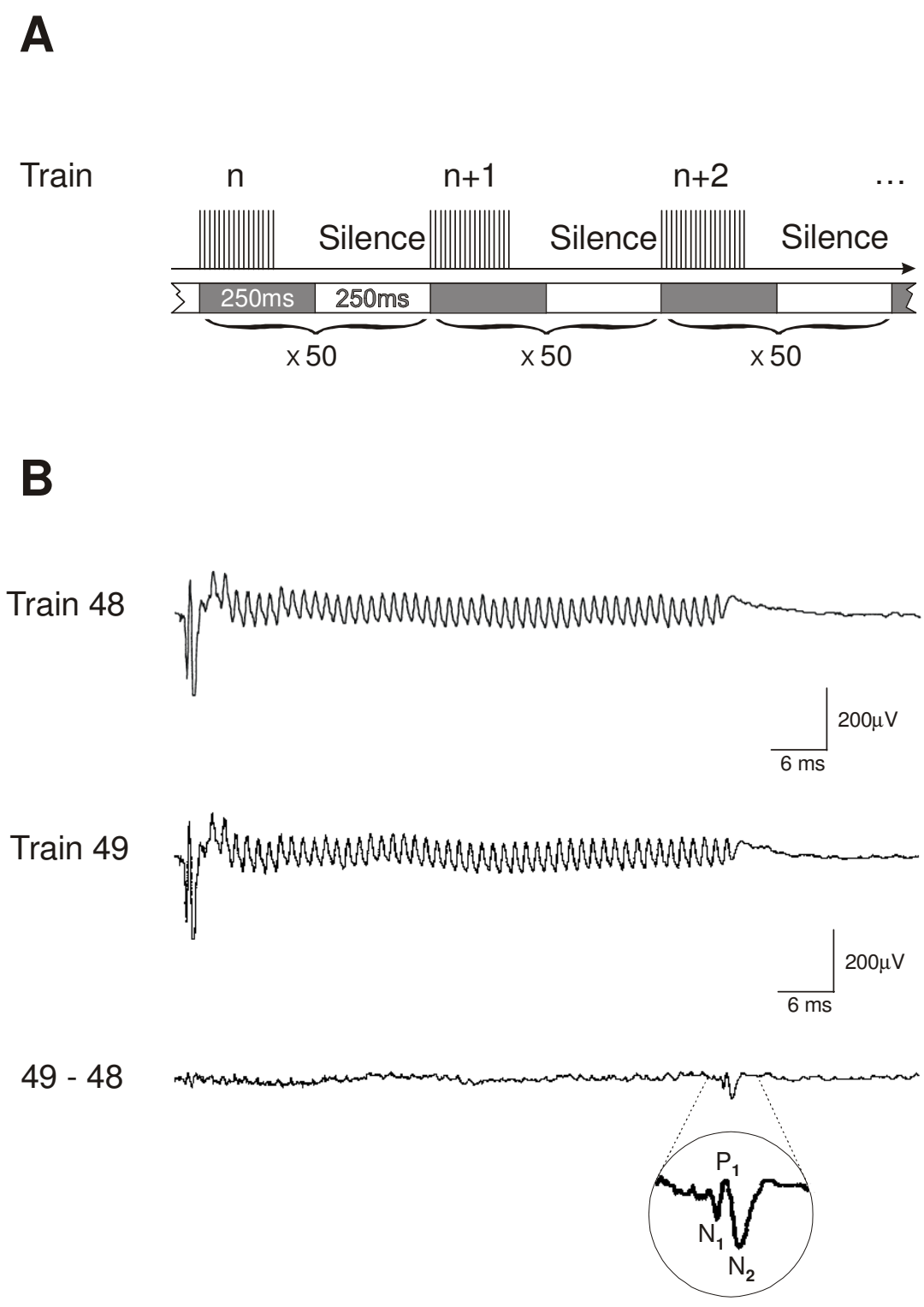

Figure 6.7 (A) Time structure of the stimulus paradigm: each 250-ms click train was followed by a silent interval of equal duration. The combination of the two was repeated 50 times for each train. (B) Illustration of the procedure used to isolate the 49th click of an 800-pps train stimulation: the averaged response obtained for a train consisting of 48 clicks was subtracted from the one evoked by a train with 49 clicks in order to expose the ANEP in response to click 49. Modified from Loquet and Rouiller, 2002.

phosphate buffer (0.1 M at pH = 7.4). After decapitation, the brain was removed, postfixed one night in the fixative solution and kept the next day in a 30% sucrose solution at 4°C for cryoprotection. Frozen coronal sections (50 µm) were cut, washed in phosphate buffer and mounted on slides. Finally, sections were counterstained with cresyl violet (Fluka, 0.06%), coverslipped with Eukitt and observed in light microscopy.

VII RESULTS

1 Auditory Near-Field Evoked Potentials in Response to Tone Bursts

The ANEPs recorded from the VCN in response to pure tone bursts typically showed two negative peaks (N_1 and N_2) separated by a positive deflection (P_1; Fig. 6.4). The latency of the first peak depended on stimulus intensity and was approximately 2.5 ms (for example, 2.43 ms at 16 kHz at threshold). Mean ANEP threshold values obtained from six animals at 11 frequencies are shown in Fig. 7.1. Sensitivity was greatest in the range from 16 to 24 kHz (threshold at 25 dB SPL) and decreased at higher and lower frequencies. The pattern of the curve is quite similar to that obtained by other authors in Long-Evans rats using both electrophysiological (Loquet and Rouiller, 2002) and behavioral techniques (Heffner et al., 1994).

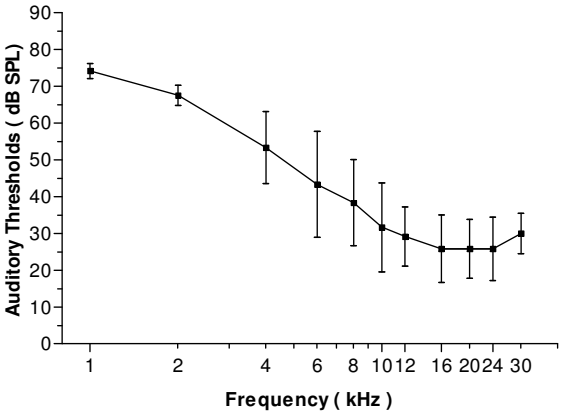

Figure 7.1 Mean ANEP thresholds derived from all six rats. The bars represent standard deviations.

2 Auditory Near-Field Evoked Potentials in Response to Clicks

Similarly to the results obtained with pure tones, ANEP recordings in response to clicks showed two negative peaks (N_1 and N_2) separated by a peak of opposite polarity (P_1; Fig. 6.5). The N_1 peak was more pronounced with respect to P_1 and N_2 than when using tone bursts. The latencies of both N_1 and N_2 at various stimulus intensities are given in Table 7.1. At every intensity, fifty single clicks were presented to and then averaged for each animal. The table displays mean data from all animals. There is a clear tendency for response latency of both N_1 and N_2 to decrease with increasing stimulus intensity, the delay between the two peaks remaining rather constant, however. Note that the standard deviations (SDs) are very small.

	N_1 latency (ms)		N_2 latency (ms)		N_2 - N_1 (ms)	
Intensity	Mean	SD	Mean	SD	Mean	SD
5 dB SPL	1.87	0.05	2.67	0.07	0.80	0.06
10 dB SPL	1.79	0.05	2.60	0.07	0.81	0.08
30 dB SPL	1.65	0.04	2.45	0.05	0.81	0.06
50 dB SPL	1.49	0.04	2.29	0.06	0.79	0.04
70 dB SPL	1.39	0.07	2.17	0.10	0.78	0.08

Table 7.1 Latencies of peaks N_1 and N_2 as well as the delay between these two peaks at various stimulus intensities. SD: standard deviations.

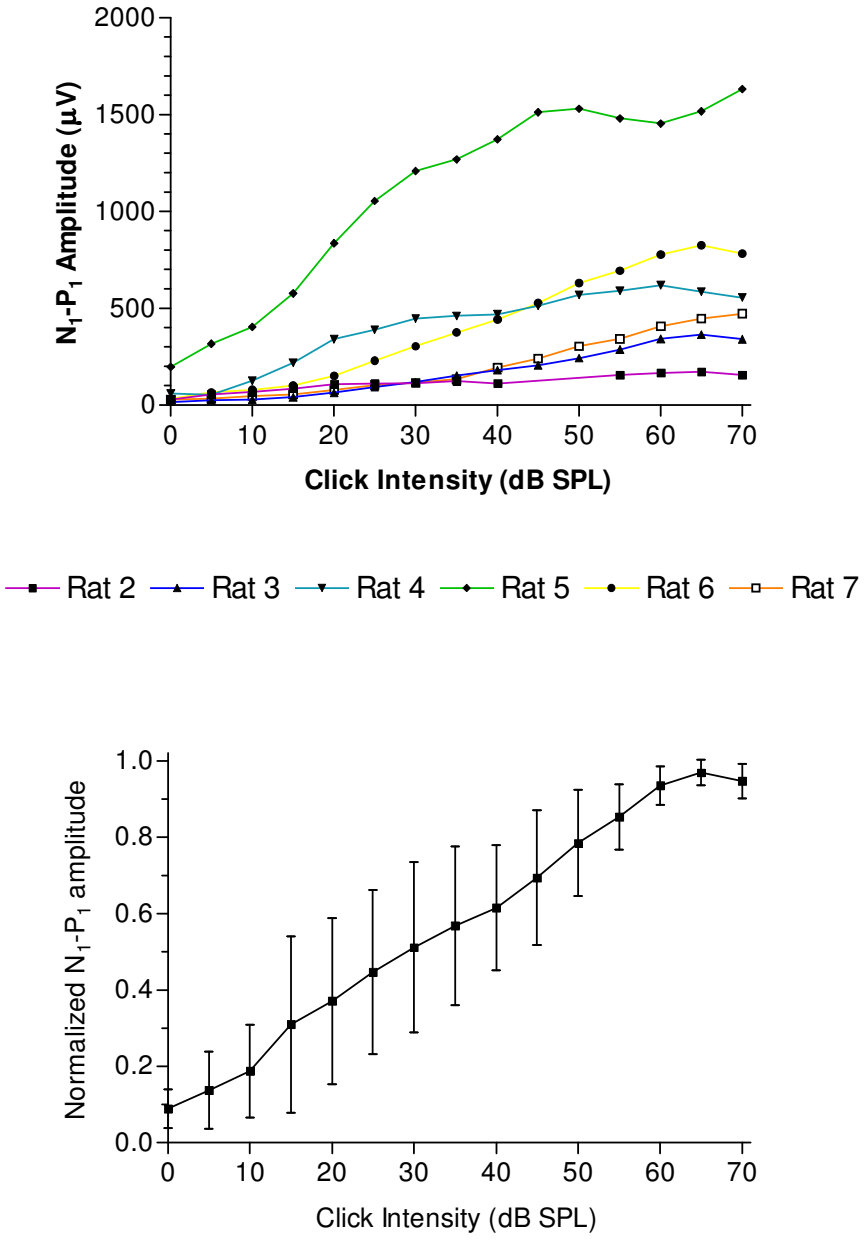

Figure 7.2 Upper panel: N_1-P_1 amplitudes displayed as a function of intensity for each one of the six experimental animals. Lower panel: mean N_1-P_1 amplitude-intensity function incorporating normalized data from all six rats (see text for method). The error bars represent SDs.

Intensity functions established for all six rats by averaging 50 measurements of the N_1-P_1 amplitude of the ANEP in response, each time, to a single click presented at increasing intensities are shown in Fig. 7.2 (upper panel). In order to eliminate the large inter-individual variability and to present an averaged growth function, amplitudes of all responses obtained for a given rat were normalized with respect to the highest ANEP observed for that animal. The averaged growth function is presented in the lower panel of Fig. 7.2. It can be noted that ANEP amplitudes increased as a function of stimulus intensity, and that the relationship was almost linear in the range from 0 to 65 dB SPL.

3 Auditory Near-Field Evoked Potentials in Response to Repetitive Clicks

3.1 N_1-P_1 Component of the Auditory Near-Field Evoked Potential

3.1.1 General Time Course

Fig. 7.3 shows ANEPs in response to the first five clicks of a 250-ms stimulus train presented at 70 dB SPL and 200 pps. It can easily be recognized that both negative peaks (N_1 and N_2) are highest in response to the first stimulus, and that all subsequent potentials are smaller in amplitude. For both peaks, this decrease was quantified by measuring the N_1-P_1 and P_1-N_2 amplitudes, respectively, in response to the individual clicks in a train (Fig. 7.4.A) and then displaying them as a function of the click position within the train (Fig. 7.4.B). In order to be able to compare individual animals, the highest response amplitude (usually the one evoked by the first click) was set to 1 and all subsequent responses were normalized with respect to it. For the N_1-P_1 component, the phenomenon of adaptation manifested itself by a three-stage decrease in time (Fig. 7.4.B): there was an abrupt decrease of response amplitude at train onset (rapid adaptation; lasting 10 to 20 ms in the case of Fig. 7.4), followed by a slower decrease (short-term adaptation; taking around 80 ms in the example), and a steady state. A previous study, conducted by Loquet and Rouiller (2002), observed similar three-phase adaptation curves and demonstrated that they could be well fit by the equation $A(t) = y_1 \cdot e^{-t/K_1} + y_2 \cdot e^{-t/K_2} + \text{plateau}$, where A(t) was the response amplitude at time t, y_1 and y_2 were the y-intercepts of the rapid and the short-term adaptation components, respectively, plateau stood for the average N_1-P_1 amplitude during the steady-state, and K_1 / K_2 were the decay time constants of the two postulated adaptation components. Since, in the present study, fitting the N_1-P_1 adaptation time courses with the above equation also yielded very good coefficients of correlation in most cases, we adopted it in order to determine the time constants of both rapid and short-term adaptation (Fig. 7.4.C). Curve fitting was carried out with GraphPad Prism® 3.02 software using the Levenberg-Marquardt method. The deviation from the model was assessed by considering the coefficient of correlation between the empirical values and the calculated curve ($R^2 \geq 0.70$) and by assessing the Gaussian distribution of the residuals around the curve ($P > 0.1$). The magnitude of the plateau was determined by averaging the ANEP-amplitude values obtained during the last 170 ms of a stimulus train.

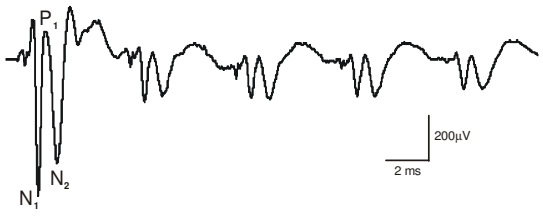

Figure 7.3 ANEPs elicited by a 250-ms train of repetitive clicks presented at 70 dB SPL and 200 pps (Rat 6). Only the first 25 ms of the response are shown.

In non-mathematical terms, we thus postulated both rapid and short-term adaptation to follow an exponential time course and to be linearly superposed to each other and to a steady-state component. Note that in a few cases, empirical curves could be better fit by the one-time-constant exponential-decay equation $A(t) = y_0 \cdot e^{-t/K} + \text{plateau}$. Yet other response traces followed a time

course that was not at all compatible with an exponential decay pattern: they displayed an extremely pronounced rapid adaptation component with very low data points immediately following stimulus train onset. This response behavior shall be discussed in detail in section VIII.5.3.4.

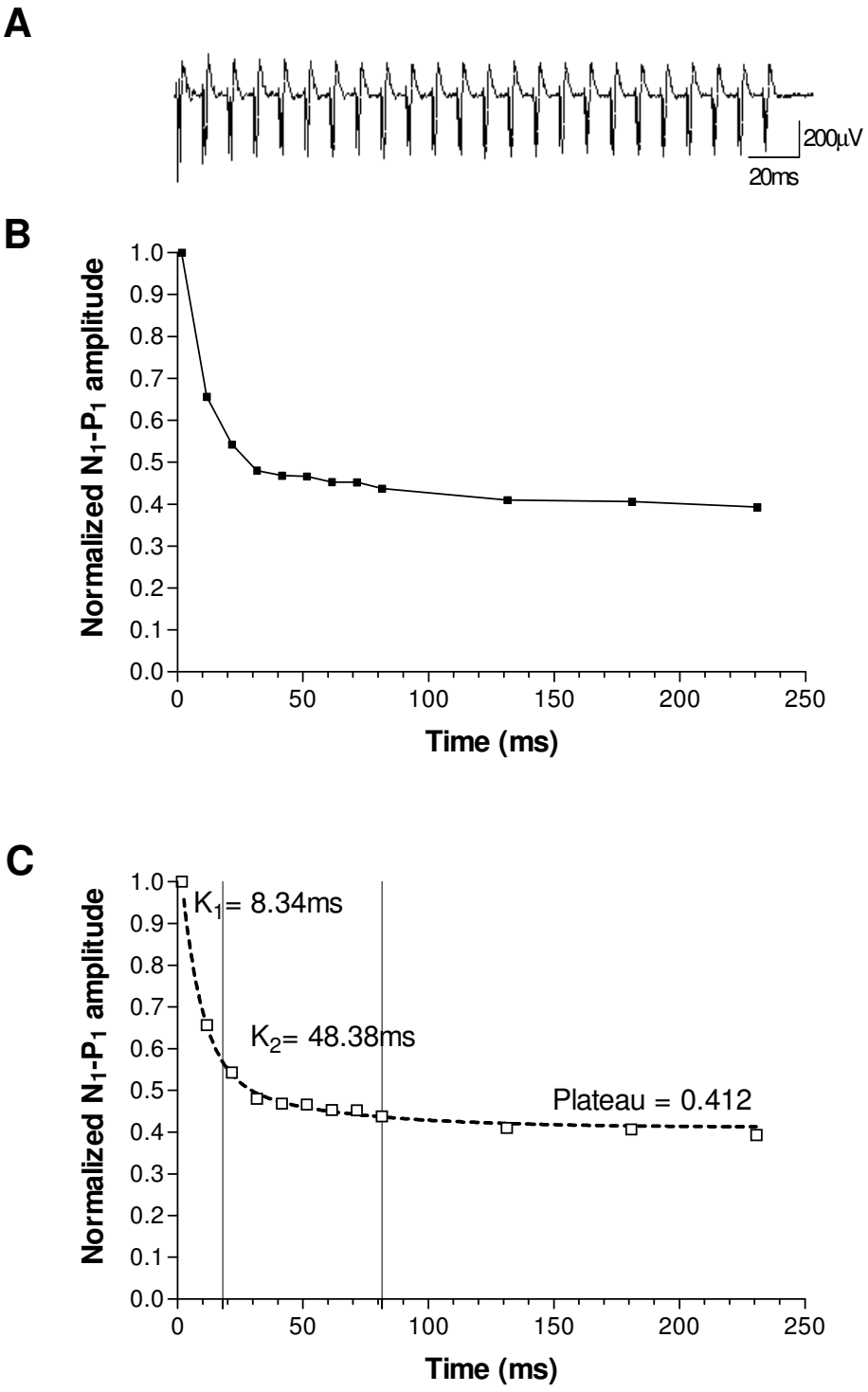

Figure 7.4 (A) Averaged ANEPs elicited by a 250-ms train of repetitive clicks presented to Rat 6 at 100 pps and 30 dB SPL. (B) Plot of the normalized N_1-P_1 amplitudes as a function of the position of the stimulating click in the train. (C) Curve from (B) fit by a two-time-constant exponential-decay equation. The coefficient of correlation for the fitted curve is 0.99.

3.1.2 Effects of Stimulus Repetition Rate

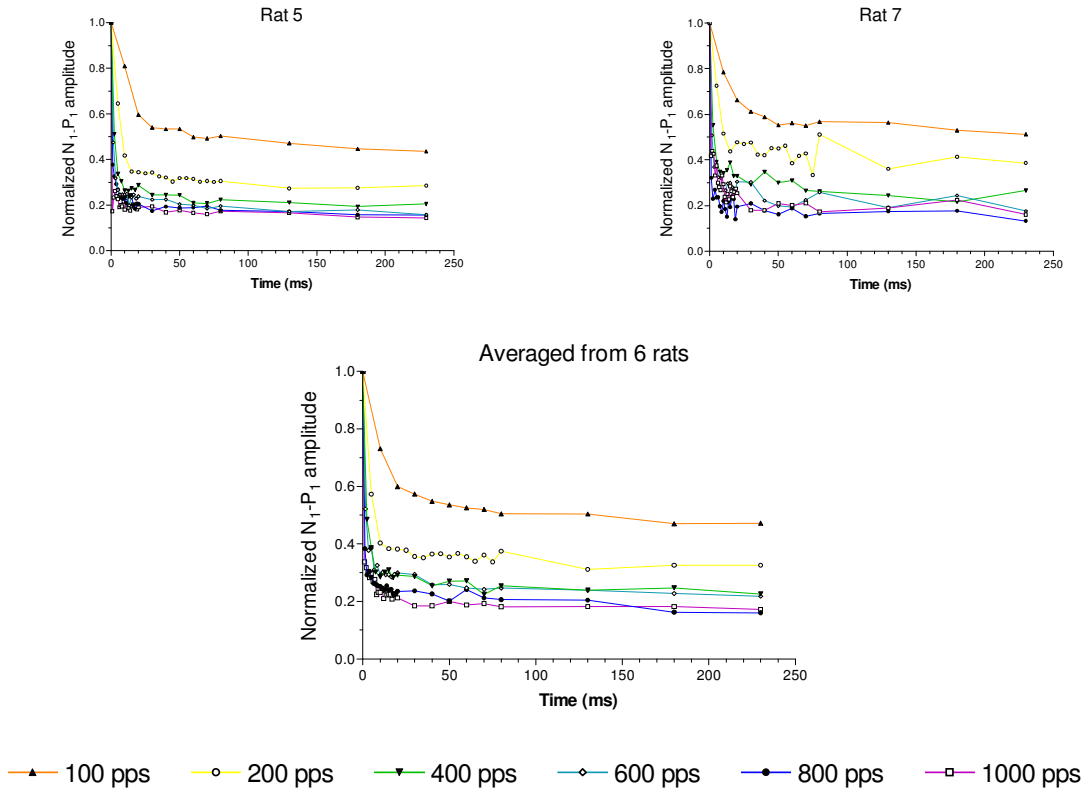

Figure 7.5 Adaptation time course of the N_1-P_1 component of the ANEP as a function of repetition rate. Stimulus trains were presented at 30 dB SPL and pulse rates ranging from 100 to 1'000 pps. Upper panel: data collected from two individual animals; lower panel: data averaged from all six rats.

The behavior of the N_1-P_1 amplitudes as they diminish during a click train was plotted for various stimulus repetition rates (Fig. 7.5). Generally, it can be said that the exponential decrease of the curves became more pronounced as stimulus rate was increased; adaptation was thus rate-dependent. In order to quantify this phenomenon, the rapid (K_1) and short-term (K_2) adaptation time constants were extracted from the adaptation curves at all repetition rates. Table 7.2 displays averaged data taken from five animals. Both time constants exhibited a progressive decrease as a function of stimulus rate. This decrease was more marked for the rapid than for the short-term component. A large inter-individual variability was observed at all rates tested.

Rate (pps)	Rapid time constant (K_1; ms)		Short-term time constant (K_2; ms)	
	Mean	SD	Mean	SD
100	12.2	5.5	49.9	12.1
200	4.6	1.4	54.8	16.0
400	2.2	0.7	54.6	15.5
600	1.2	0.6	30.2	23.4
800	0.7	0.2	28.6	21.8
1000	0.3	0.3	15.0	11.8

Table 7.2 Adaptation time constants as a function of stimulus rate. K_1 and K_2 were determined with non-linear regression fitting curves (see text for method). Mean values and SDs were calculated from data obtained at 30 dB SPL in five rats.

The effect of stimulus repetition rate on adaptation was not only quantified in terms of the time constants of the exponential decays but also in form of the ANEP amplitude measured during the steady-state stage (last 170 ms) of a response. The plot of plateau level across click rate (Fig. 7.6) shows that the former decreases as a function of the latter. This behavior was most pronounced at low repetition rates; at high rates the curve tended to flatten out. Note that the effect of repetition rate was – qualitatively – the same also at stimulus intensities other than 30 dB SPL (for data see section VII.3.3.1).

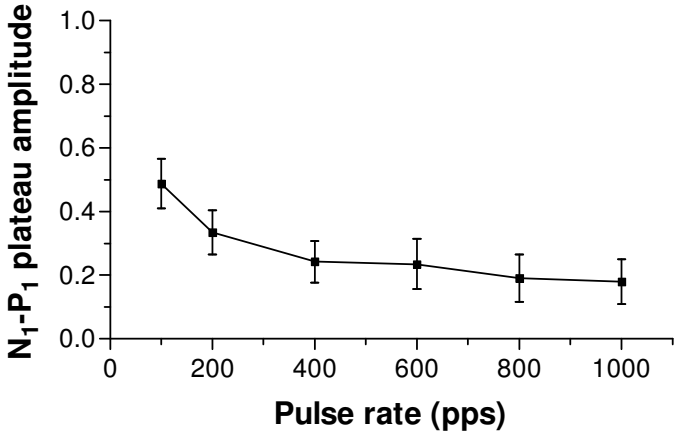

Figure 7.6 Plateau amplitudes of the N_1-P_1 component of the ANEP averaged from all six animals plotted as a function of stimulus repetition rate. All responses were obtained in response to click trains presented at 30 dB SPL. The bars represent SDs.

3.1.3 Effects of Stimulus Intensity

The traces presented in Fig. 7.7 show that an augmentation of stimulus intensity yielded a marked increase of the amplitude of the response to the first click in a train. Even though the subsequent potentials were also influenced by stimulus level, an accentuation of the amplitude difference between the first and the following responses was observed. Thus, as a general statement, it can be said that adaptation became more pronounced when increasing stimulus intensity. This effect was obtained for each

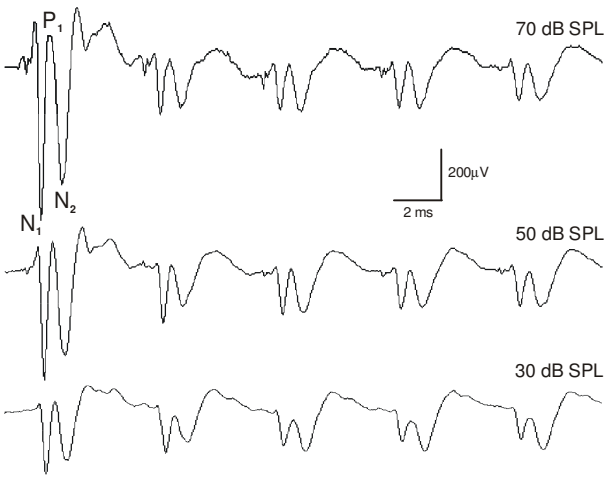

Fig. 7.7 Responses evoked by 250-ms trains of repetitive clicks presented at a rate of 200 pps and three different intensities (indicated to the upper right of each trace). Only the first 25 ms of the responses are shown. Data recorded from Rat 6.

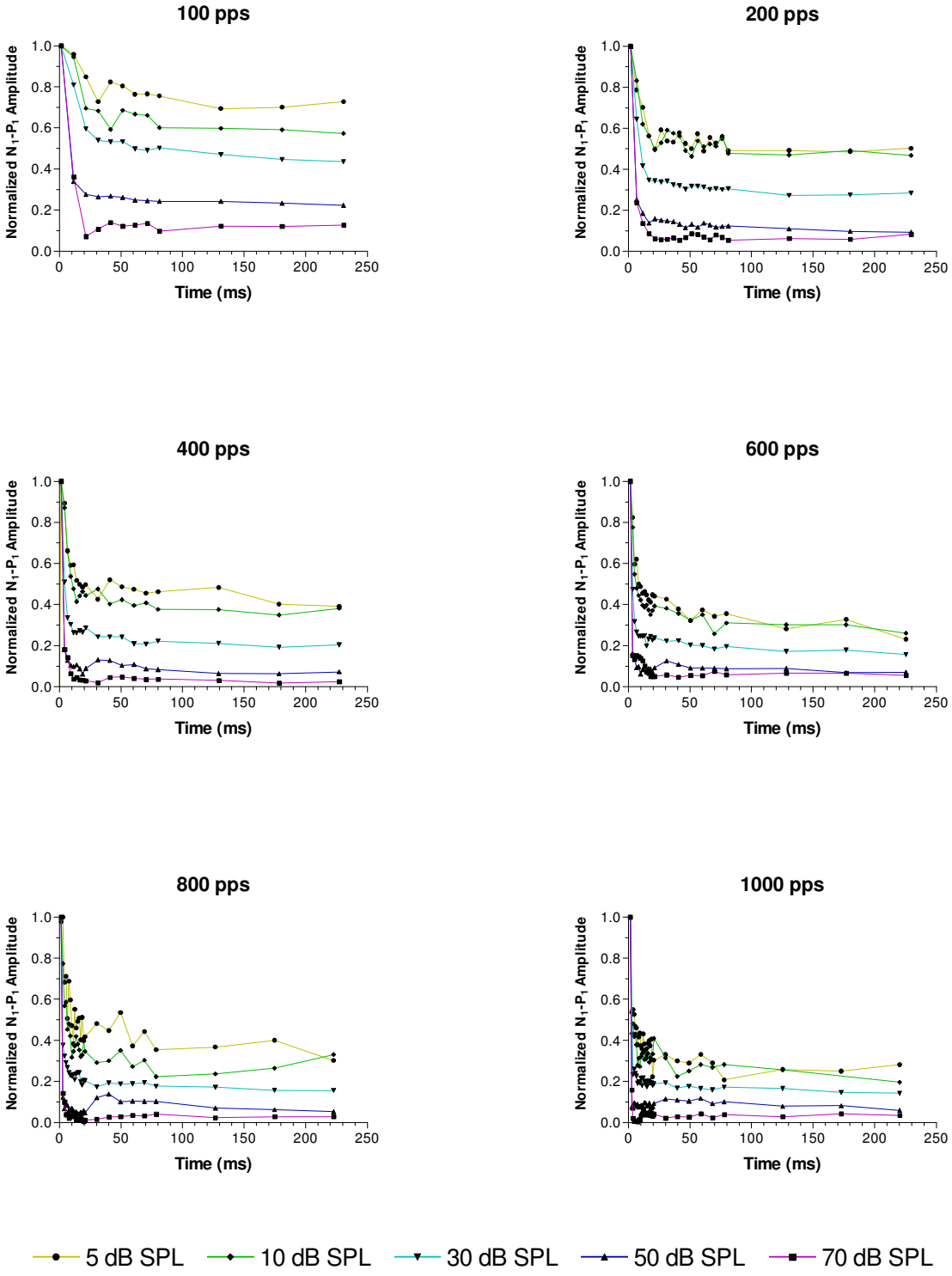

Fig. 7.8.A Adaptation time courses of the N_1-P_1 component of the ANEP in response to 250-ms click trains presented at repetition rates between 100 and 1'000 pps and intensities ranging from 5 to 70 dB SPL. Data obtained from Rat 5.

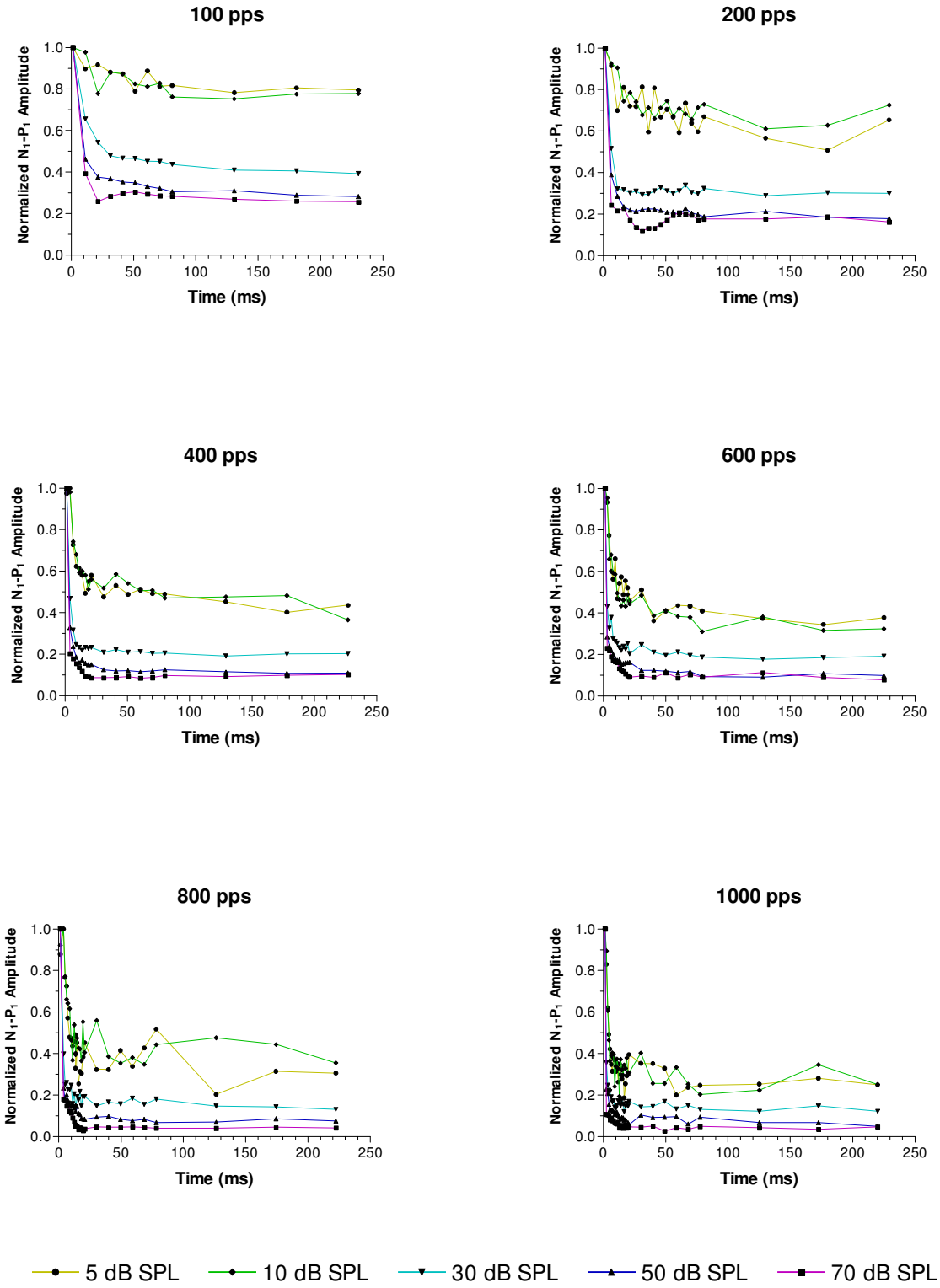

Fig. 7.8.B Adaptation time courses of the N_1-P_1 component of the ANEP in response to 250-ms click trains presented at repetition rates between 100 and 1'000 pps and intensities ranging from 5 to 70 dB SPL. Data derived from Rat 6.

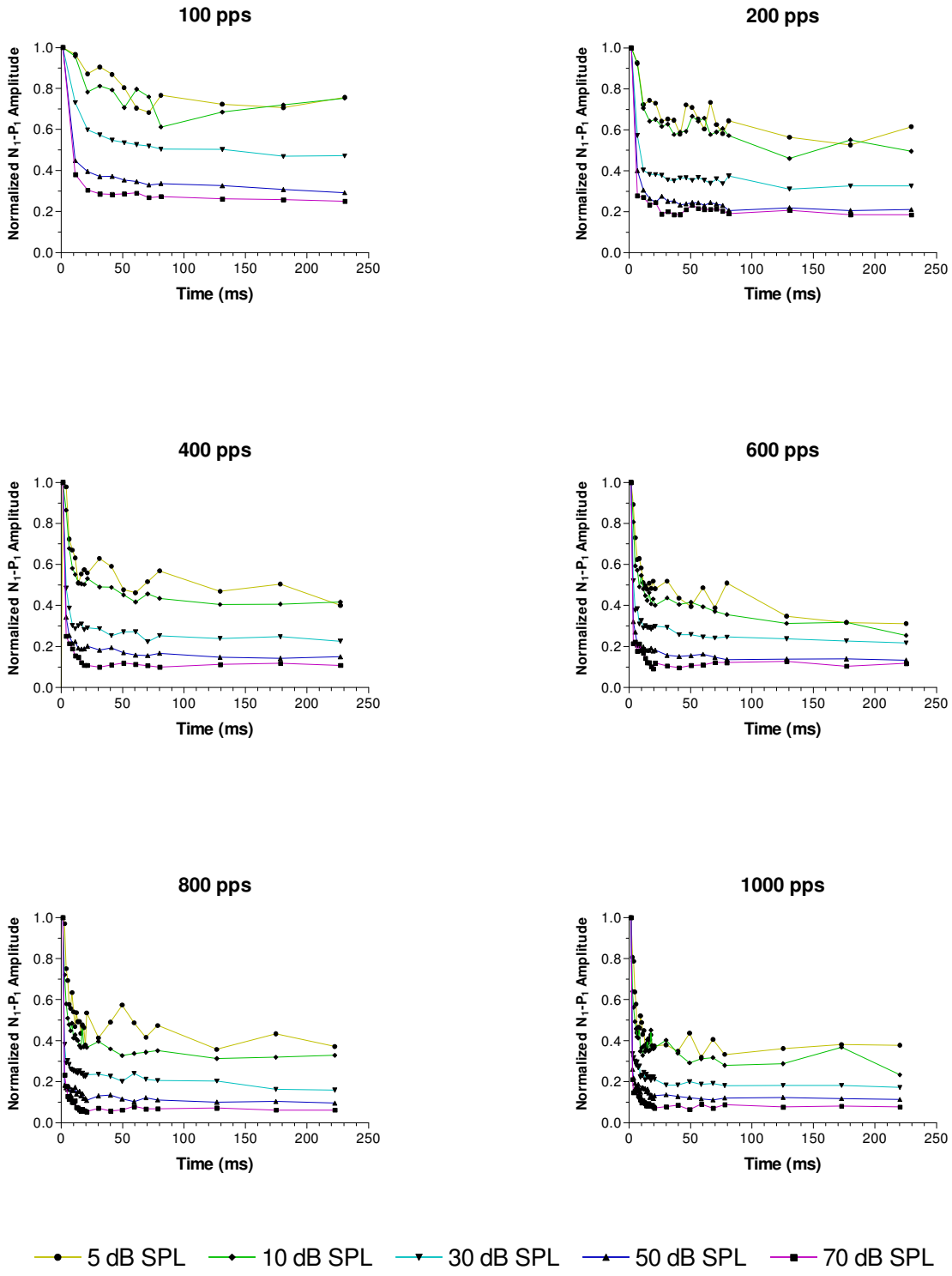

Fig. 7.8.C Adaptation time courses of the N_1-P_1 component of the ANEP in response to 250-ms click trains presented at repetition rates between 100 and 1'000 pps and intensities ranging from 5 to 70 dB SPL. Data averaged from all six rats.

Rate (pps) \ Intensity		5 dB SPL		10 dB SPL		30 dB SPL		50 dB SPL		70 dB SPL	
		K_1	K_2	K_1	K_2	K_1	K_2	K_1	K_2	K_1	K_2
100	Mean	15.5 *	46.6 *	11.4	61.2	12.2	49.9	5.3	50.6	2.4	48.1
	SD	*	*	3.8	17.1	5.5	12.1	3.4	8.1	3.2	12.6
200	Mean	6.5	74.4	9.7	64.0	4.6	54.8	2.8	41.4	2.4	44.0
	SD	1.5	25.7	4.3	37.1	1.4	16.0	1.2	21.1	1.6	34.1
400	Mean	4.4	64.5	4.6	66.4	2.2	54.6	1.4	36.4	0.5	6.3
	SD	2.3	25.5	1.4	21.2	0.7	15.5	0.5	36.9	0.5	2.7
600	Mean	3.8	52.2	3.1	45.9	1.2	30.2	0.8	46.4	0.2	6.8
	SD	1.2	15.1	1.6	25.4	0.6	23.4	0.2	49.4	0.2	0.9
800	Mean	2.6	100.0	1.6	38.5	0.7	28.6	0.2	28.1	0.1	4.9
	SD	1.4	100.8	1.0	24.9	0.2	21.8	0.2	18.8	0.1	2.7
1000	Mean	1.5	54.5	1.1	49.7	0.3	15.0	0.3	8.8	0.2	5.1
	SD	1.6	62.5	0.8	55.3	0.3	11.8	0.3	5.4	0.1	0.9

* Adaptation time course could be fit by a two-time-constant equation in only one animal.

Table 7.3 Rapid and short-term time constants as a function of stimulus rate and intensity. K_1 and K_2 were determined with non-linear regression fitting curves (see text for method). Mean values and SDs were calculated from data obtained in five rats. The few curves better described by a one-time-constant equation were not included in the table.

animal at each rate tested (100 to 1'000 pps), as is apparent from Fig. 7.8: as stimulus intensity was increased from 5 to 70 dB SPL, the initial decrease of ANEP amplitude was more pronounced and plateau level was lower at all repetition rates tested.

A quantification of this trend was carried out by averaging K_1 and K_2 values obtained from five rats. The results are summarized in Table 7.3. It can be noted that at all repetition rates tested, K_1 decreased as stimulus intensity increased. This reduction was maximal at 100 pps (from 15.5 to 2.4 ms), and generally less pronounced, in absolute terms, at higher pulse rates (e.g. from 1.5 to 0.2 ms at 1'000 pps). In order to better visualize this trend, K_1 values were presented logarithmically as a function of stimulus intensity (Fig. 7.9). Most of the resulting plots were approximately linear.

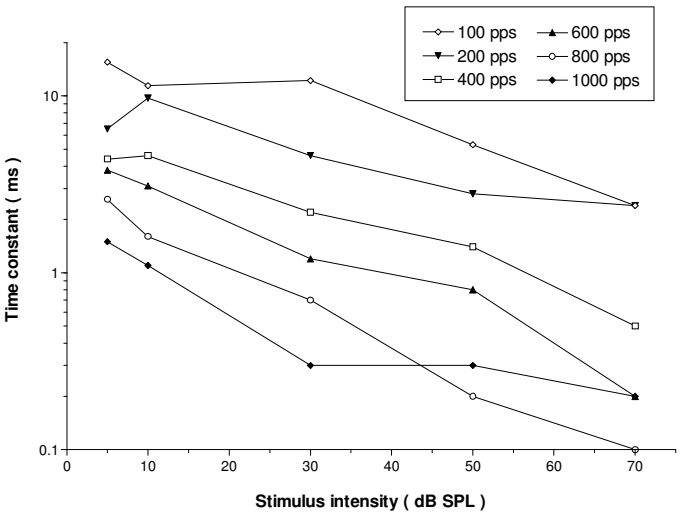

Fig. 7.9 Mean fit rapid-adaptation time constant (K_1) displayed as a function of stimulus rate and intensity. SD bars were removed for the sake of clarity but the values can be found in Table 7.3.

The behavior of the short-term time constant was less uniform. Being nearly independent of intensity at 100 pps, K_2 also showed a tendency to diminish

with increasing stimulus level at higher pulse rates. At 800 and 1000 pps, this decrease was monotonic. At 400, 600, and 800 pps, intensity dependence was most pronounced between 50 and 70 dB SPL.

In order to further quantify the effects of stimulus intensity on neural adaptation, we assessed in all recorded traces the amplitude ratio between the first and the average steady-state response. Fig. 7.10 shows the plots of these quotients as a function of stimulus level for all repetition rates. To the right of the curves, an adaptation indicator has been introduced to underline the fact that a small ratio indicates a large amount of adaptation. The general trend of the curves is a progressive decrease from the left to the right, suggesting that there was more adaptation at high stimulus levels. At 100 and 200 pps, increasing stimulus level from 5 to 70 dB SPL led to an augmentation of adaptation of about 50 % and 40 % of the first-response amplitude, respectively. For higher repetition rates (400 to 1000 pps), this augmentation of adaptation remained steady around 30 % of first-response amplitude. Thus, in what concerns steady-state amplitude, the effects of stimulus intensity on adaptation seem to be more pronounced at low than at high repetition rates. The same observation can be made from Fig. 7.8: the responses traces in the low-rate graphs are more widely spread than those in high-rate graphs.

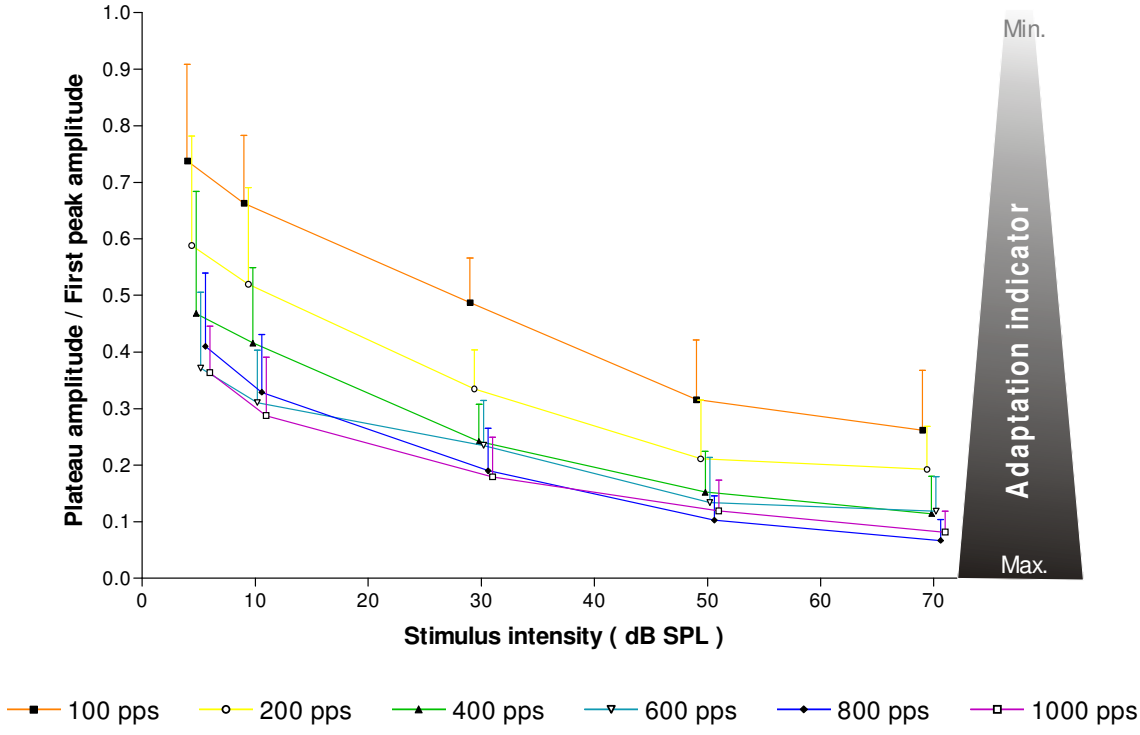

Fig. 7.10 Amount of adaptation of the N_1-P_1 component of the ANEP, expressed in terms of the ratio of the plateau to the first-peak amplitude, as a function of stimulus intensity. Mean values were derived from six animals, the error bars representing SDs. Note that for the sake of clarity, data points of the individual traces were slightly shifted one from another even though they all represent values determined at 5, 10, 30, 50, and 70 dB SPL.

3.2 P_1-N_2 Component of the Auditory Near-Field Evoked Potential

3.2.1 General Time Course

In the same way as it was done for the N_1-P_1 component, P_1-N_2 amplitudes were measured in six rats in response to pulse trains presented at all stimulus repetition rates and intensities. Fig. 7.11 displays a typical response trace (recorded from Rat 7 at 400 pps and 50 dB SPL). As is apparent from the figure, P_1-N_2 response traces typically showed the same three adaptation components described above for N_1-P_1: a rapid decrease of response amplitude during the first few milliseconds of the stimulus train, followed by another, slower decline and a steady state.

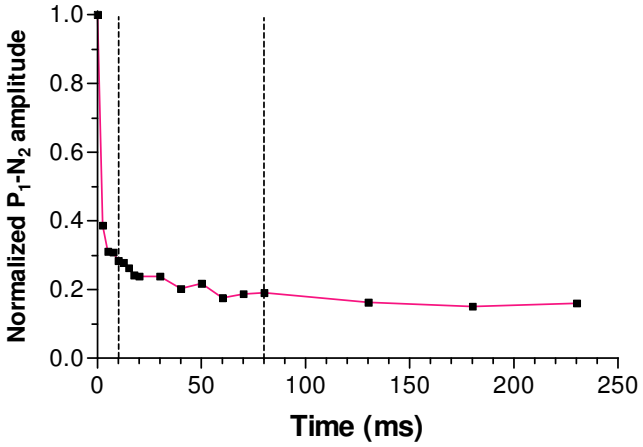

Fig. 7.11 Behavior of the P_1-N_2 component of the ANEP during a click train presented at 400 pps and 50 dB SPL. Data derived from Rat 7.

Although no curve fitting procedure was carried out for the P_1-N_2 component, it seemed reasonable in most cases to assume that rapid and short-term adaptation followed approximately exponential time courses, as it was the case for the N_1-P_1 component. The curve depicted in Fig. 7.11, for example, would certainly yield quite high a coefficient of correlation when fit with a two-time-constant exponential-decay equation. However, in some other cases – most frequently at high stimulus intensities and repetition rates – we observed traces which did not follow such a time course but exhibited an extremely pronounced rapid adaptation, resulting in very low (sometimes barely existing) response amplitudes for the clicks immediately following stimulation onset. Fig. 7.12 represents an example of such a trace. As it was mentioned above, such low data points right after stimulus onset were also, though less frequently, observed in response traces established for the N_1-P_1 component of the ANEP. A possible explanation for this observation will be discussed in section VIII.5.3.4.

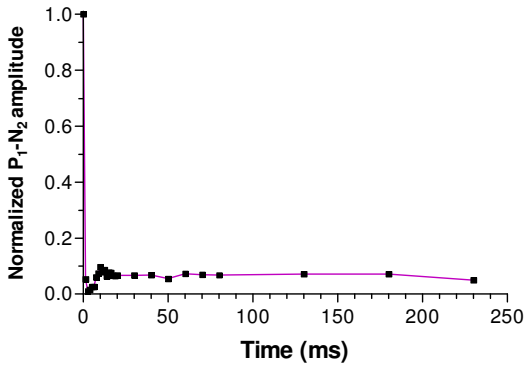

Fig. 7.12 P_1-N_2 trace recorded from Rat 5 in response to a stimulus train presented at 800 pps and 70 dB SPL. Note the very low response amplitudes immediately following train onset.

3.2.2 Effects of Stimulus Repetition Rate

Fig. 7.13 displays the adaptive behavior of the P_1-N_2 component of the ANEP in response to stimulus trains presented at various repetition rates but at a fixed intensity of 30 dB SPL (the upper panels representing data recorded from Rats 5 and 7, respectively, the lower panel displaying averaged values from all six animals). Two statements about the dependency of the adaptation time course on click repetition rate can be deduced from the figure: first, the initial decrease in response amplitude occurred faster as stimulus repetition rate was increased. (It seems safe to say that there is a general tendency for the time constant of the rapid adaptation component to decrease with

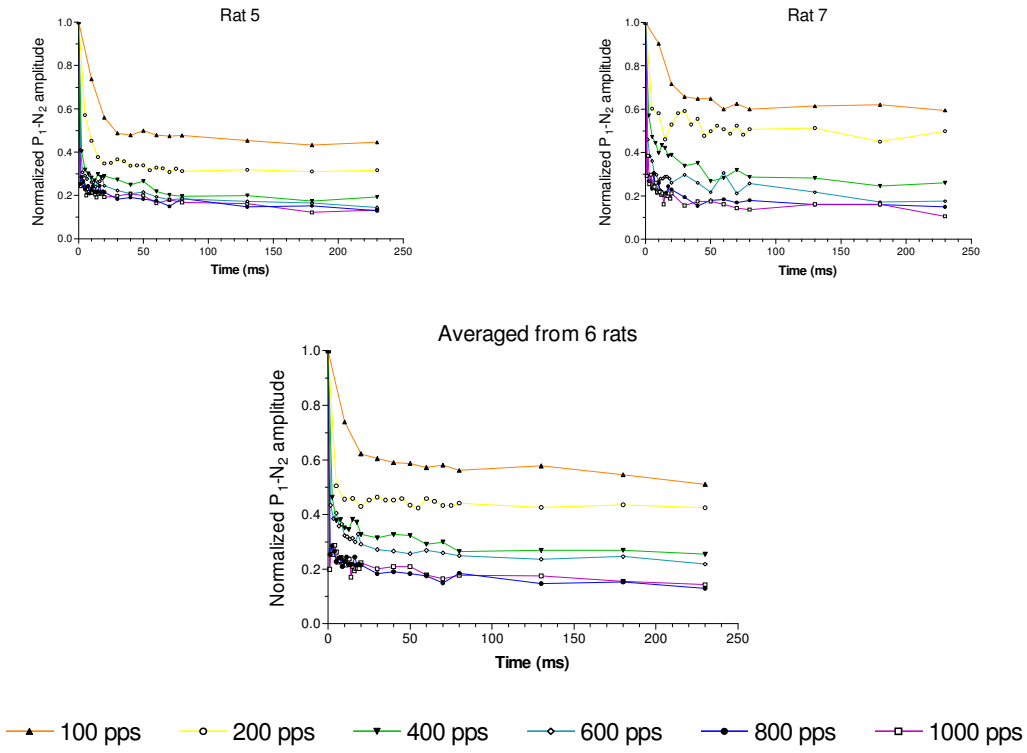

Fig. 7.13 Behavior of the P_1-N_2 component of the ANEP as a function of stimulus repetition rate. Trains were presented at 30 dB SPL and rates ranging from 100 to 1'000 pps. Upper panels: data obtained from two individual animals; lower panel: data averaged from all 6 rats.

increasing repetition rate, although as mentioned above, no mathematical quantification was carried out. The trends for short-term adaptation are less obvious; a statement as to the behavior of its time constant would need mathematical curve fitting procedures.) Second, it is evident that, at higher pulse rates, the steady state in response amplitude established itself at a lower level. In order to quantify the latter observation, the steady-state amplitudes in Fig. 7.13 (lower panel) were plotted as a function of stimulus repetition rate (Fig. 7.14; note that analogous data for the N_1-P_1 component was presented in Fig. 7.6). At 30 dB SPL, an increase of repetition rate from 100 to 1'000 pps resulted in a descent of the steady-state amplitude from around 55 to 16 % of first-peak amplitude. It should be noted that an increase in repetition rate lowered plateau amplitude not only at 30 dB SPL but at all intensities tested (see section VII.3.3.1).

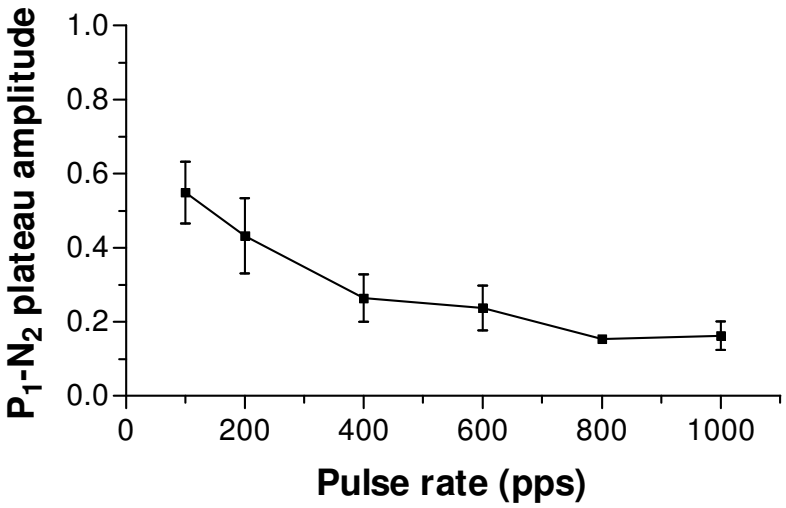

Fig. 7.14 Plateau amplitudes of the P_1-N_2 component of the ANEP averaged from all six animals plotted as a function of stimulus repetition rate. All responses were obtained in response to click trains presented at 30 dB SPL. The bars represent SDs. The SD at 800 pps is too small to be visible.

3.2.3 Effects of Stimulus Intensity

Further above it was said that an increase in stimulus intensity resulted in a more pronounced adaptation for the N_1-P_1 component, in other words, in an accentuation of the difference in amplitude between the first response to a series of clicks and those to follow. Considering once again Fig. 7.7, it becomes evident that this trend also held for the P_1-N_2 component: although an augmentation of stimulus level lead to an increase of all response amplitudes, the effect on the first response was greater than that on those to follow, resulting in a more pronounced adaptation pattern at high stimulus intensities.

Fig. 7.15 confirms this observation. At all repetition rates tested, adaptation clearly occurred faster, and the steady-state amplitude was lower, when stimulus intensity was increased. This effect was clearly more pronounced at low than at high repetition rates, an observation also apparent from Fig. 7.16 which (analogously to Fig. 7.10) displays the plateau-to-first-peak ratios at different repetition rates as a function of intensity: whereas at 100 pps, an increase of intensity from 5 to 70 dB SPL resulted in a descent of the plateau from around 90 to about 30 % of first-response amplitude, the decrease only went from around 25 to somewhat below 10 % at 1'000 pps.

Note that many of the 70-dB-SPL traces in Figs. 7.15.A and B display one or several very low data points immediately following stimulus train onset, in the way displayed above in Fig. 7.12. For the P_1-N_2 component, as mentioned, this phenomenon was observed quite frequently at high stimulus intensities and can therefore also be detected, even though less clearly, in the averaged data set represented in Fig. 7.15.C.

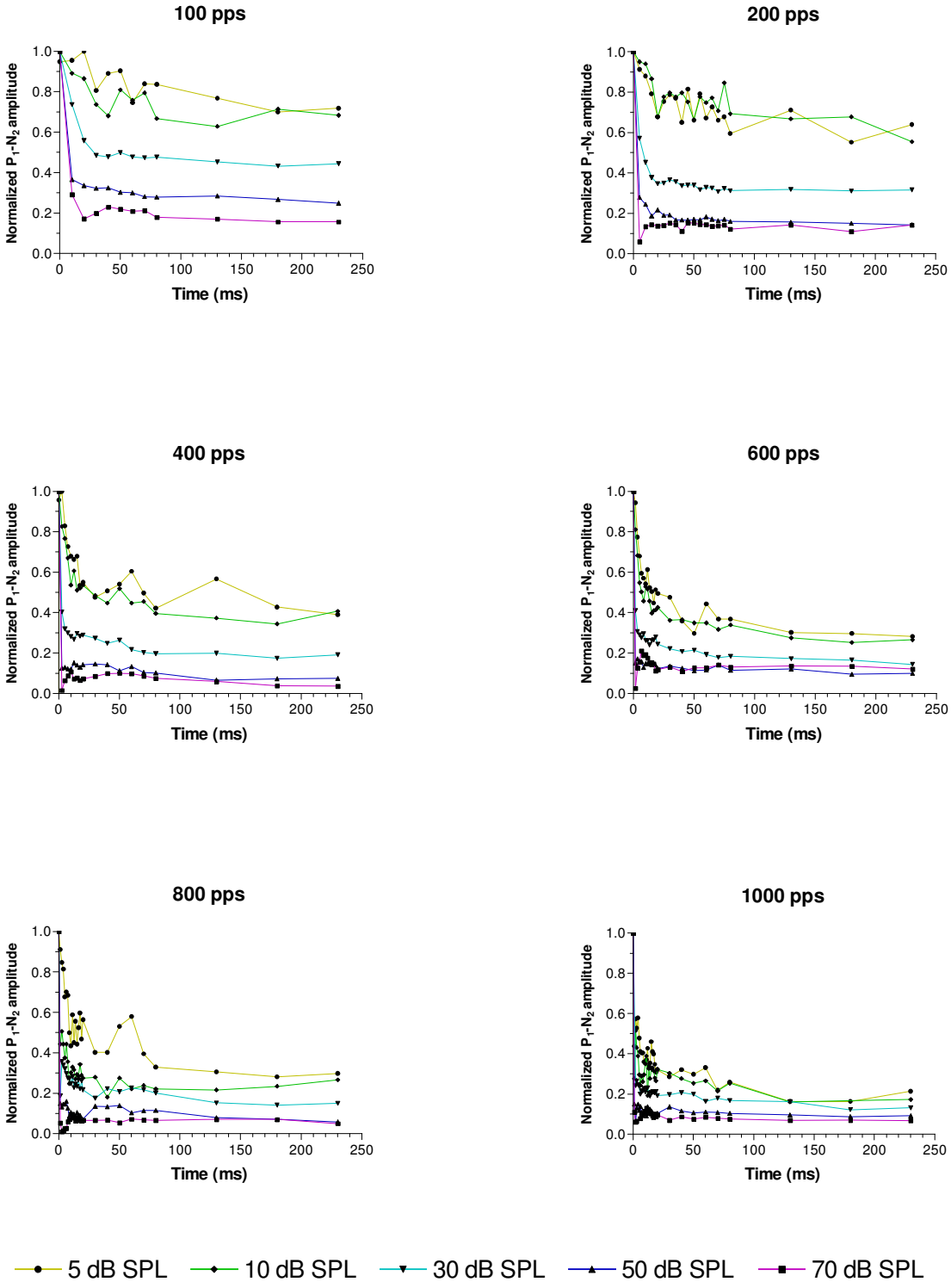

Fig. 7.15.A Adaptation time courses of the P_1-N_2 component of the ANEP in response to 250-ms click trains presented at repetition rates between 100 and 1'000 pps and intensities ranging from 5 to 70 dB SPL. Data recorded from Rat 5.

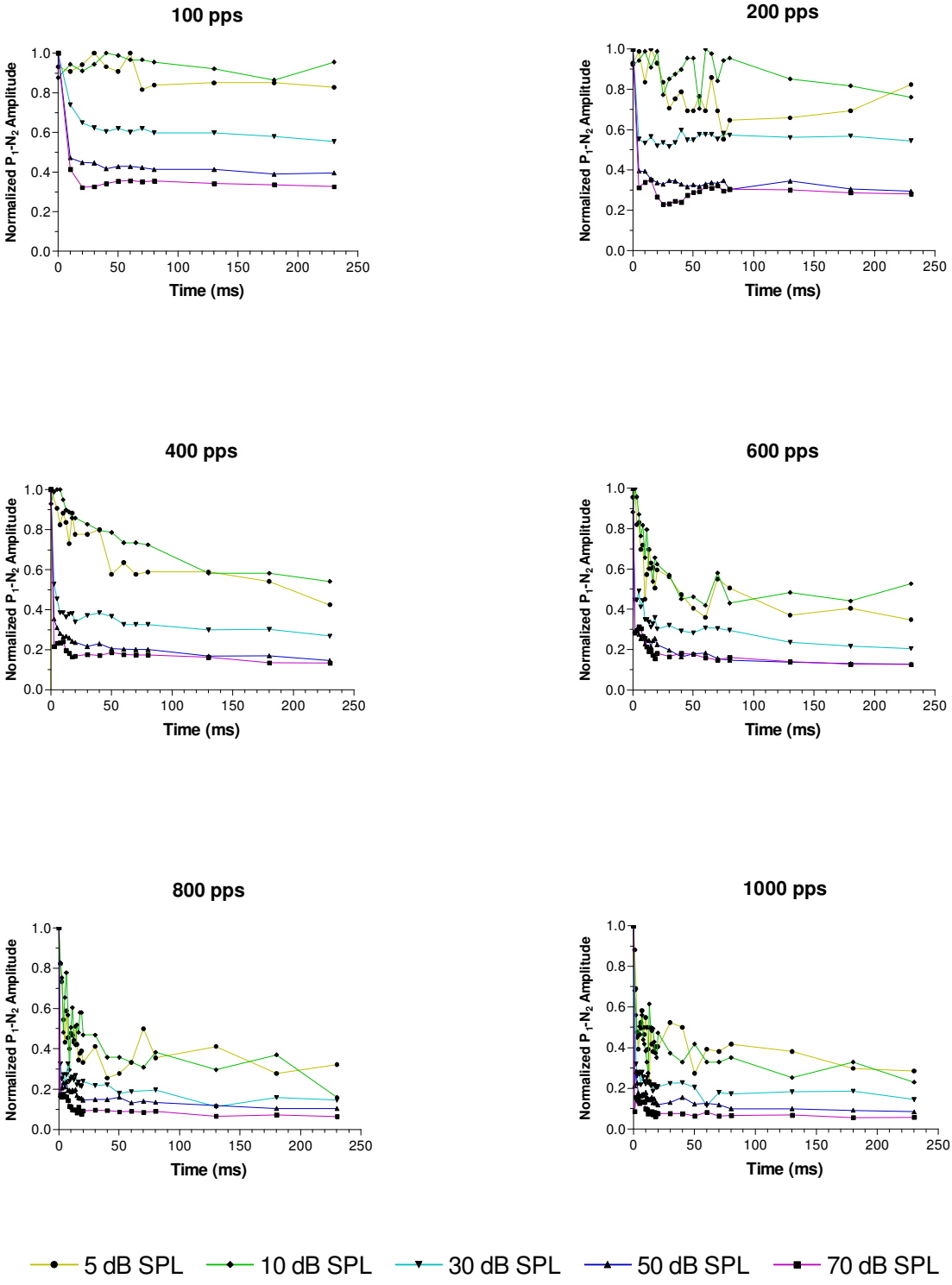

Fig. 7.15.B Adaptation time courses of the P_1-N_2 component of the ANEP in response to 250-ms click trains presented at repetition rates between 100 and 1'000 pps and intensities ranging from 5 to 70 dB SPL. Data recorded from Rat 6.

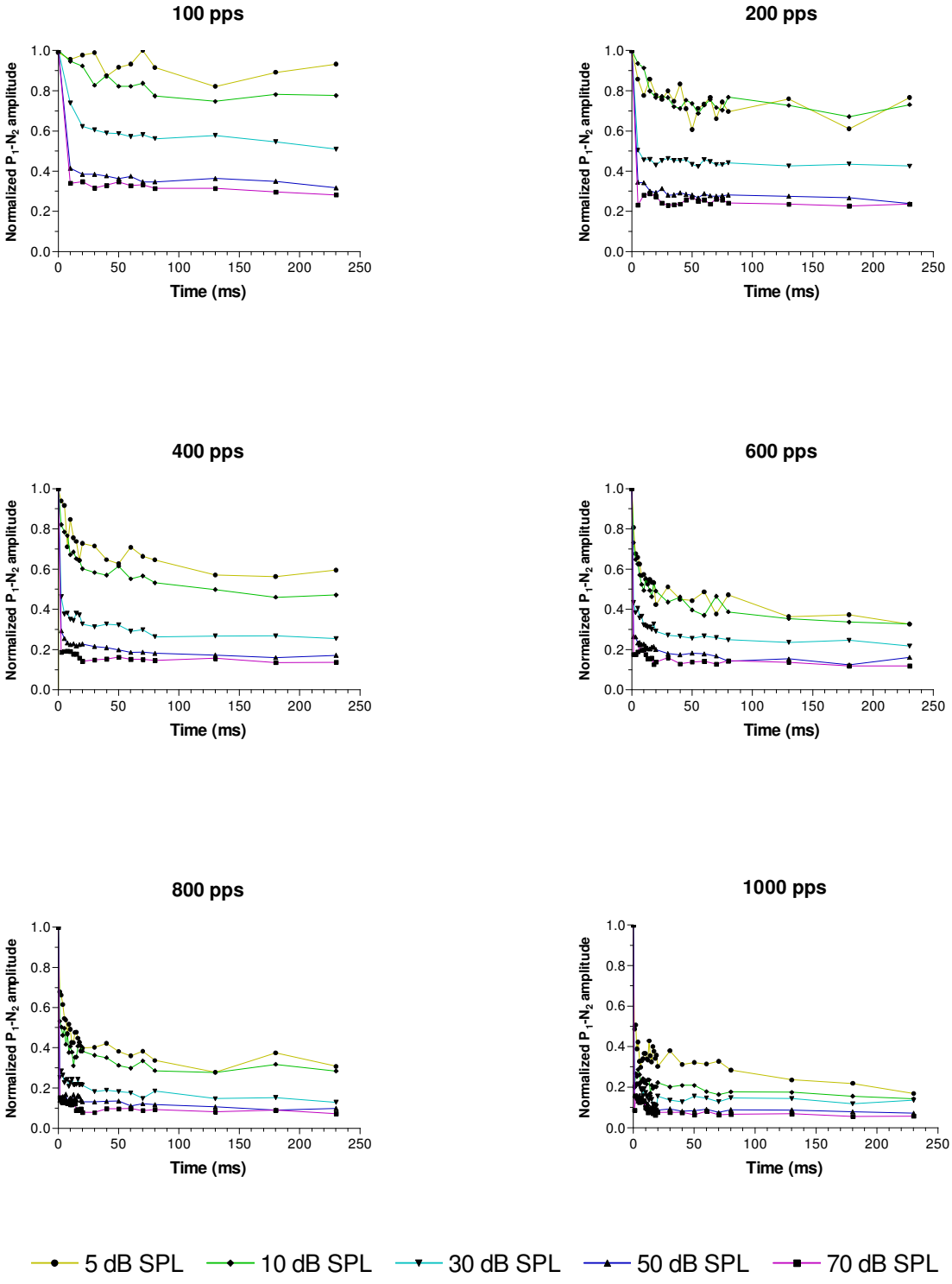

Fig. 7.15.C Adaptation time courses of the P_1-N_2 component of the ANEP in response to 250-ms click trains presented at repetition rates between 100 and 1'000 pps and intensities ranging from 5 to 70 dB SPL. Data averaged from all six rats.

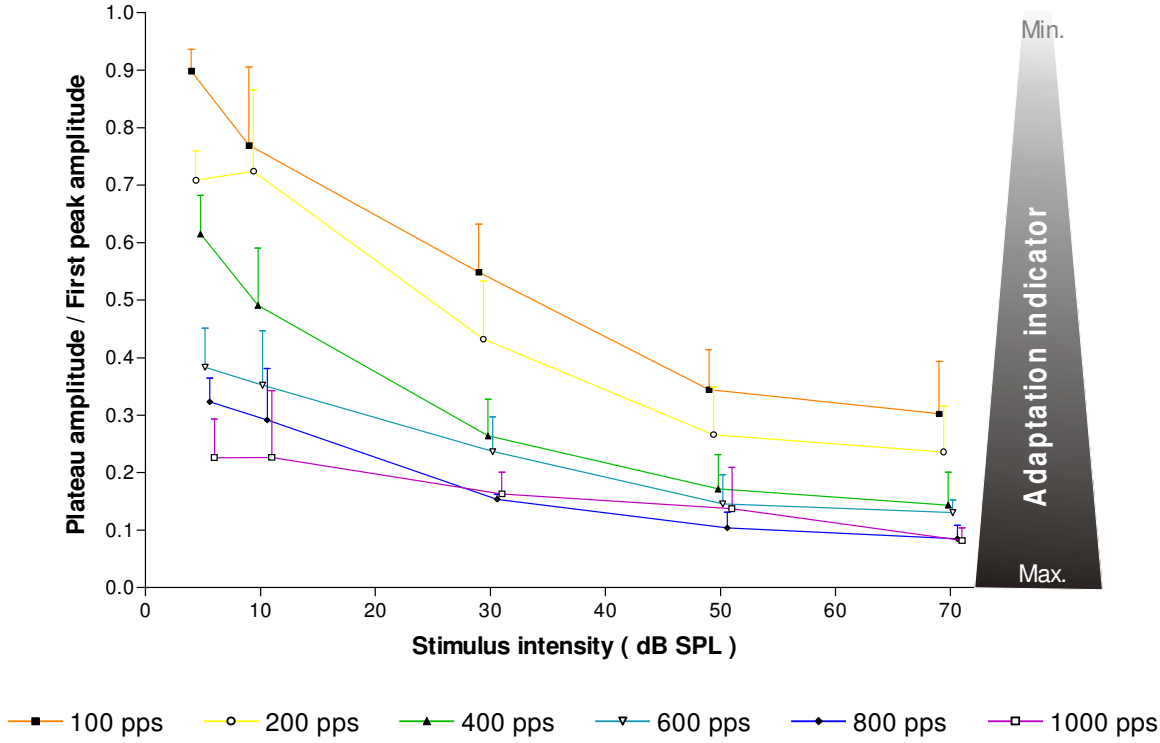

Fig. 7.16 Amount of adaptation of the P_1-N_2 component of the ANEP, expressed in terms of the ratio of the plateau to the first-peak amplitude, as a function of stimulus intensity. Mean values were derived from six animals, the error bars representing SDs. Note that for the sake of clarity, data points of the individual traces were slightly shifted one from another even though they all represent values determined at 5, 10, 30, 50, and 70 dB SPL.

3.3 Comparison of the Adaptation Properties of the N_1-P_1 and P_1-N_2 Components of the Auditory Near-Field Evoked Potential

3.3.1 Effects of Stimulus Repetition Rate

The fact that the amount of adaptation in response to click trains at various stimulus intensities and repetition rates was quantified for both the N_1-P_1 and the P_1-N_2 components of the ANEP allows for a quantitative comparison of the adaptation patterns between these two ANEP deflections. Fig. 7.17 represents a synthesis of Figs. 7.8.C and Fig. 7.15.C: it displays the response traces obtained for both ANEP components at all stimulus intensities and repetition rates tested. It is evident from the figure that, as has been said before, an augmentation of stimulus repetition rate led to more pronounced adaptation patterns for N_1-P_1 as well as for P_1-N_2. In quantitative terms, however, there seemed to be minor differences between the two components. Whereas at low repetition rates there appeared to be a small but consistent tendency for the P_1-N_2 component to display less adaptation than the N_1-P_1 component, the very opposite was the case at high repetition rates: the steady-state amplitudes of the P_1-N_2 component were usually somewhat lower than those of the N_1-P_1 component. Going from top to

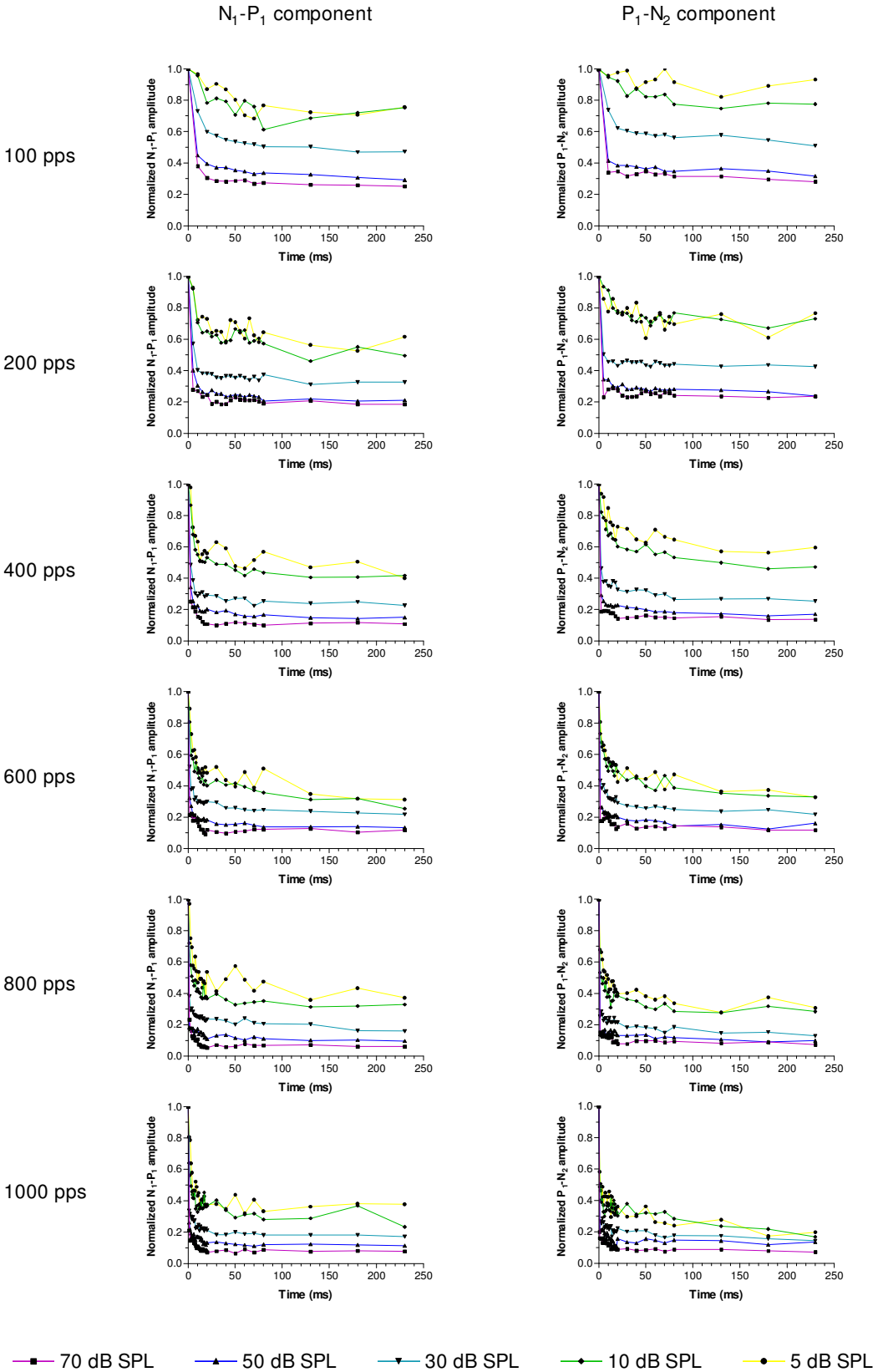

Fig. 7.17 Adaptation time courses for the N_1-P_1 (left panel) and P_1-N_2 (right panel) components of the ANEP at all stimulus intensities and repetition rates tested. The displayed data represents a synthesis of Figs. 7.8.C and 7.15.C (averaged data from all six rats).

bottom of Fig. 7.17, this change occurred progressively and was more pronounced for low- than for high-intensity stimulation. The two graphs representing the amplitudes measured at 600 pps are almost identical.

Thus, stimulus repetition rate had a slightly greater influence on the behavior of the P_1-N_2 than on that of the N_1-P_1 component. This observation is confirmed by Fig. 7.18 which displays the plateau-to-first-peak ratios of the curves in Fig. 7.17 as a function of repetition rate. The data points in the right-hand panel representing low repetition rates (on the left side of the graph) are more widely spread than their counterparts in the left-hand panel. As repetition rate increases, the P_1-N_2 curves descend more quickly and, at 70 dB SPL, lie closer together than the traces for N_1-P_1.

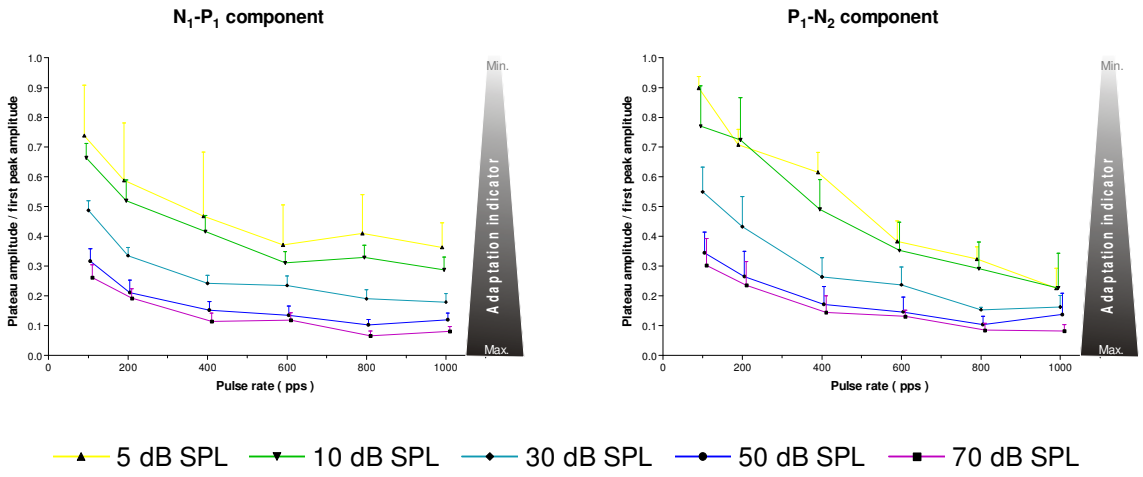

Fig. 7.18 Comparison of the effects of click repetition rate on the steady-state amplitudes of the N_1-P_1 (left panel) and P_1-N_2 (right panel) components of the ANEP for all stimulus intensities. Note that for the sake of clarity, data points of the individual traces were slightly shifted one from another even though they all represent values determined at 100, 200, 400, 600, 800, and 1'000 pps.

In order to verify if this observation could be confirmed statistically, the data displayed in the above graphs was analyzed using paired-value two-way analysis of variance (two-way ANOVA). Two-way ANOVA determines how a certain response – steady-state amplitude, in our case – is affected by two parameters – stimulus repetition rate and ANEP component (N_1-P_1 vs P_1-N_2). The former of these two factors obviously has a great influence on plateau amplitude; the corresponding P values were therefore not included in Table 7.4 (they were all extremely significant). Most interesting in our concern are the P_{int} values: they indicate if the two factors at issue interact; in non-mathematical terms: whether or not stimulus repetition rate has the same influence on steady-state amplitude for both ANEP components. At 5, 10, and 30 dB SPL, P_{int} is significant. This confirms the observation made in Fig. 7.18: at these intensities, the curves for P_1-N_2 are indeed more susceptible to the influence of stimulus repetition rate than those for N_1-P_1. Graphically speaking, the former have a higher slope than the latter. Even though this also seems to be the case at 50 and 70 dB SPL, this trend is not statistically significant, as pointed out by the corresponding P_{int} values.

Intensity	P_{int}	P_{comp}
5 dB	0.011	0.198
10 dB	0.005	0.009
30 dB	0.017	0.064
50 dB	0.666	0.023
70 dB	0.491	0.002

Table 7.4 Output values of paired-value two-way analysis of variance performed on plateau-amplitude data for the two parameters stimulus repetition rate and ANEP component (N_1-P_1 vs P_1-N_2). See text for explanations.

It is interesting to note the significant P_{comp} values at 50 and 70 dB SPL. They indicate that at these intensities, steady-state amplitudes for one ANEP component were systematically higher than those for the other one (independently of repetition rate) – those for P_1-N_2 were above those for N_1-P_1 as is revealed by a closer look at Fig. 7.18. This finding shall be mentioned again in section VIII.3.2. (The P_{comp} value at 10 dB SPL is also significant; it should be noted, however, that as P_{int} is also very low at this intensity, indicating an interaction between the two parameters under consideration, an isolated interpretation of P_{comp} is no longer possible.)

3.3.2 Effects of Stimulus Intensity

Taking another look at Fig. 7.17, it turns out that the differences in effects of intensity on the two ANEP components cannot be as uniformly described as those of repetition rate. Considering the low-repetition-rate diagrams (top panels), the traces for P_1-N_2 seem to be slightly wider spread than those for N_1-P_1, indicating the latter ANEP component to be less subject to stimulus intensity than the former. At high repetition rates (lower panels) however, the opposite seems to be the case: the traces obtained for P_1-N_2 at 800 and 1'000 pps are more closely grouped than those for N_1-P_1. Thus, at high stimulus rates, stimulus intensity seems to have a greater influence on the first one of the two negative ANEP components.

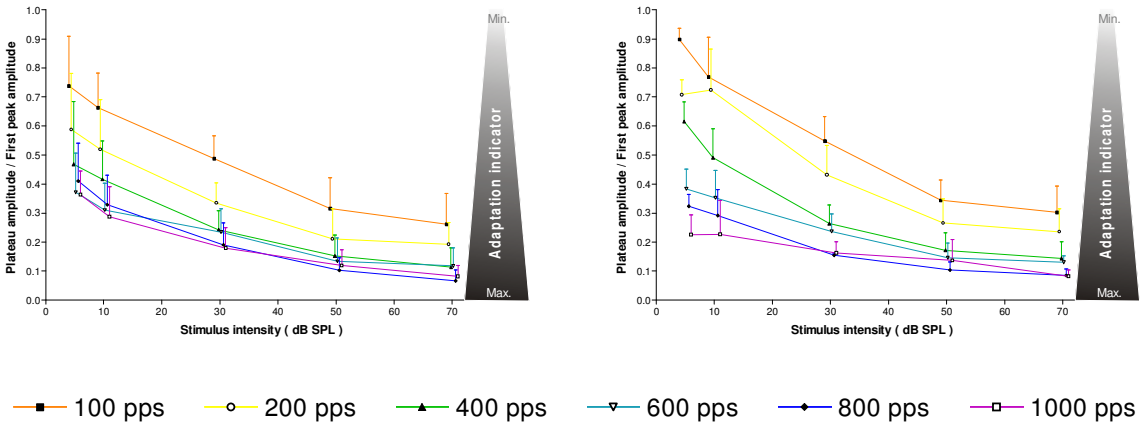

Fig. 7.19 Comparison of the effects of stimulus intensity on the adaptive behavior of the components N_1-P_1 (left) and P_1-N_2 (right) of the ANEP. The represented data is identical to that in Figs. 7.10 and 7.16.

Fig. 7.19 contains the same data as Figs. 7.10 and 7.16, and thus allows for a direct comparison of the effects of stimulus intensity on the adaptive behaviors of both the N_1-P_1 and the P_1-N_2 components. The observations made above are confirmed: the low-repetition-rate graphs (100, 200, and 400 pps) display greater slope for P_1-N_2 than for N_1-P_1. At high repetition rates (800 and 1'000 pps), the relationship is reverse: the curves representing P_1-N_2 are flatter than those representing N_1-P_1. No statistical evaluation was carried out to compare the individual curves at each repetition rate.

4 Histology

The photomicrographs presented in Fig. 7.20 show the location of the tip of the chronic recording electrode within the VCN for three rats. A variation in insertion depth was observed but did not exceed 700 µm.

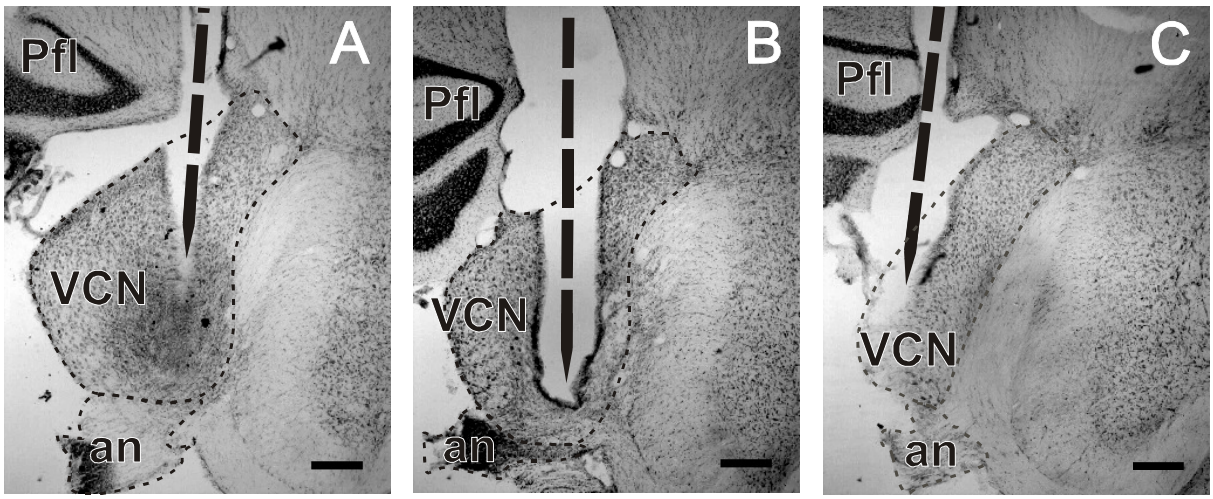

Fig. 7.20 Photomicrographs of frontal sections through the brain stem of three implanted rats, showing the location of the tip of the chronic recording microelectrode in the left VCN: (A) Rat 4, (B) Rat 5 and (C) Rat 6. an: auditory nerve; Pfl: paraflocculus; VCN: ventral cochlear nucleus. The dotted arrow represents the electrode track. Scale bar: 300 µm.

VIII DISCUSSION

1 Preface

The present study assessed the adaptive properties displayed by the peripheral auditory system in response to acoustic stimulation consisting of repetitive click stimuli. The study's results suggest that the adaptation time courses for both the N_1-P_1 and the P_1-N_2 components of the ANEP consist of three superposed components, namely rapid adaptation, short-term adaptation, and a steady state. Quantitatively, all three of these components depended on both stimulus intensity and repetition rate.

Although the position of the recording electrode within the AVCN was verified histologically, there can be no certainty as to the neural populations generating the responses we observed. Therefore, in the first part of this section, different lines of evidence will be discussed which could link the individual waves of the recorded traces to their neural correlates. In the next two parts, the adaptation patterns we found for both ANEP components shall be discussed first with respect to each other and then with regard to previous studies dealing with adaptation in both the AN and the CN. In the last part, several questions about the nature of adaptation will be discussed: at which point along the auditory pathway does adaptation occur? Are there any regularities in the adaptive processes which can be modeled mathematically? And finally, to what extent are the answers to the above questions compatible with the empirical findings of this investigation?

2 Origin of the Recorded Activity

2.1 Position of the Recording Electrode

Because of the position of the recording electrode in the AVCN, the near-field potentials we obtained can most likely be attributed either to cell bodies located in this region (mainly those of spherical and globular bushy cells, as well as those of stellate cells), or then to the ascending branches of incoming AN fibers. Paolini et al. (2001) reported that when advancing electrodes on a dorsal-to-ventral track through the AVCN, AN fibers were usually encountered at greater depths (i.e. more ventrally) than the cell bodies of CN units. Unfortunately, this information is not useful in our concern since our electrodes, due to their larger tip, recorded from a less restricted area than those used in the mentioned report. Even an extremely accurate determination of our electrodes' positions within the VCN would therefore not yield any valuable information, and the anatomical site of our recordings thus does not allow us to attribute them with certainty to either AN fibers or CN units.

2.2 Latencies of the N_1 and the N_2 Peaks of the Auditory Near-Field Evoked Potential

More meaningful than their spatial provenience might be the temporal pattern of the recorded responses. The latency of units in the peripheral auditory system (in both the AN and the CN) depends on various parameters of both the stimulus used and the unit recorded from. Single-unit studies revealed, for example, that units with high CFs usually display shorter latencies than those with low

CFs (e.g. Kiang et al., 1965a; Møller, 1976; FitzGerald et al., 2001). This observation can be explained in terms of the longer travel time of low-frequency stimuli along the BM. Moreover, our results suggest that latencies decrease as stimulus intensity increases (Table 7.1), a finding which is in accordance with prior reports (e.g. Møller, 1975; FitzGerald et al., 2001) and likely due to the faster rise of the EPSP at higher stimulus levels (Møller, 1981a). Also, a higher sound level causes a widening of the traveling wave along the BM and thus a spread of excitation towards higher-CF regions of the cochlea. This, again, will decrease travel time along the BM and, therefore, response latency. Furthermore, latency data varies between species and, at last, clicks usually evoke faster responses than tone bursts because they reach their maximum intensity almost immediately whereas tone bursts have a certain rise time. Given all these influences, one should be cautious when comparing latency values drawn from different reports.

Study	Stimulus	Site of Recording	Latency (ms)
Møller, 1976	Amplitude-modulated tones	CN	1.1 – 1.7*
Møller, 1983	Amplitude-modulated tones	Not stated	0.5 – 1.8
FitzGerald et al., 2001	Clicks, 90 dB SPL	AVCN	1.5 – 3 (depending on CF)
Paolini et al., 2001	Clicks, 100 dB SPL	AVCN	1.4 – 2.7

Table 8.1 Latency data from single-unit studies of AN units. * Averaged values.

Tables 8.1 and 8.2 summarize some of the existing single-unit latency data for the AN and the CN, respectively. All of the mentioned studies were carried out in the rat. Note that latency values obtained with continuous, amplitude-modulated tones are usually somewhat shorter than those observed in response to clicks or short tone bursts (Møller, 1981a). This might explain the rather low AN latencies obtained by Møller (1976, 1983).

Study	Stimulus	Site of Recording	Latency (ms)
Møller, 1975	Rapid onset tone bursts, 42 – 102 dB SPL	CN	2.5 – 4.5 (depending on stimulus intensity)
Møller, 1976	Amplitude-modulated tones	CN	2.4 – 2.7* (depending on CF)
Møller, 1983	Amplitude-modulated tones	Not stated	2.0 – 3.0
Friauf and Ostwald, 1988	Tone pulses, 30 dB above threshold	Ventral and intermediate aoustic striae	2.5 – 2.6* (primary-like), 2.2* (on)
FitzGerald et al., 2001	Clicks, 90 dB SPL	AVCN	2 – 4 (depending on CF)
Paolini et al., 2001	Clicks, 100 dB SPL	AVCN	1.7 – 4

Table 8.2 Latency data from single-unit studies of CN units. * Averaged values.

When comparing our results (see Table 7.1) to the data of the tables, one is tempted to conclude that N_1 represents the activity of the AN whereas N_2 would be caused by the secondary auditory neurons located in the CN. This assumption is substantiated by the fact that in the case of ABR recordings in the rat, there is general consensus that the first and the second wave observed in these traces represent the AN and the CN, respectively. Shaw (1990) measured latencies of 1.27 and 1.99 ms for these two peaks. Taking into account that the intensity of the click stimulation he used exceeded even the highest stimulus levels applied in this study, his results are in good agreement with ours. Likewise, Møller (1981a, 1981b, 1983), who recorded EPs either from the round window or from the CN, found waveforms and peak latencies that were well comparable to ours. He suggested the same respective origins for the two waves and substantiated this hypothesis by comparing traces obtained before and after removal of the CN. After abolishing the nucleus, the trace recorded at the round window changed from a triphasic (N_1, P_1, N_2) to a monophasic, negative potential. The difference between the two curves, a trace exposing two peaks of opposite polarization, was thus supposed to reflect the behavior of the CN. If thesecond one of these two deflections was assumed to stand for the activity of secondary auditory neurons, what could the first peak (the middle one in the original trace) be attributed to? One of the possibilities is the prepotential which is sometimes observed in single-unit recordings of primary-like units (e.g. Kiang et al., 1965b; Romand and Avan, 1997). Prepotentials have most often been witnessed in the anterior subdivision of the AVCN which contains many spherical bushy cells contacted by large synapses called endbulbs of Held. It is therefore hypothesized that the prepotential is caused by the activity of this large synaptic endbulb of the AN fiber whereas the subsequent spike (at a delay of about 0.5 ms) is attributed to the CN unit (Fig. 8.1). Taking this into account, we could tentatively summarize N_1, P_1, and N_2 to correspond to the activity of AN fibers, pre-synaptic terminals, and secondary auditory neurons, respectively.

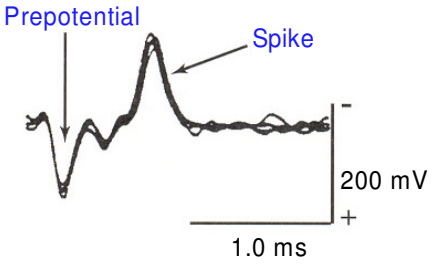

Fig. 8.1. Waveforms recorded by an extracellular metal electrode in the AVCN. Note that negativity is upward. (Modified from Brown, 1999)

However, there cannot be any certainty about this. For example, one may doubt that the data represented in Table 8.1 actually reflects the behavior of AN fibers. For the distinction between primary and secondary auditory neurons, the authors of the mentioned studies based themselves on different criteria. One of the indicators they used was the form of the recorded traces, a single monophasic deflection with a fast rise and a slower decay being a criterion in favor of an AN fiber. They also took into account how well a unit fit into its surroundings tonotopically: whereas the CF of a CN unit is usually close to that of the neighboring cells, this does not have to be the case for an AN fiber just running through a certain area. However, another decisive factor for distinction was latency itself; had this been the only feature used, the data found would evidently lose its meaning in the respect we are using it here.

It should also be noted that the relationship between neural populations and the waves observed in recordings such as ours need not be one-to-one. In other words, it cannot be precluded that a single wave represents the superposed activities of more than one cell population.

In summary: it seems probable that the N_2 peak can be attributed to neurons of the CN. The origins of N_1 and P_1 are less clear. Although the latter two could result from the activity of more than one cell population, we will, conceptually, stick to the assignation made further above since we are not aware of any data that would directly contravene it.

3 Comparison of Adaptation Patterns of the N_1-P_1 and P_1-N_2 Components of the Auditory Near-Field Evoked Potential

3.1 General Time Courses

In response to 250-ms trains of repetitive clicks, the ANEPs we recorded were highest at the onset of stimulation and then declined. This was the case for both N_1-P_1 and P_1-N_2. For both components, the decrease in amplitude could be characterized using three stages: rapid adaptation, short-term adaptation, and a steady state.

In the case of N_1-P_1, further mathematical analysis permitted to characterize the adaptation process to consist, in most cases, of a linear superposition of two exponential decays and a steady state. For P_1-N_2, no mathematical fitting procedure was carried out. However, since in most cases the general shape of the adaptation curves obtained for this component resembled very closely the one observed for the N_1-P_1 traces, it seems plausible for its adaptation to follow the same time course.

As was mentioned in section VII, there sometimes were, more often for P_1-N_2 than for N_1-P_1, adaptation curves not compatible with the above description. Mostly at high stimulus intensities and repetition rates, we observed a very pronounced rapid adaptation with the data points immediately following stimulation onset being suppressed to below the point expected from an exponential decrease. Obviously, in those cases, the adaptation process could not be described by the above scheme. In our opinion, such a response suppression right after stimulus train onset could likely be due to the refractory properties of AN fibers and CN neurons. This hypothesis shall be further explored in section VIII.5.3.

Nonetheless, in summary, it can be said that in what concerns the general time course of adaptation, components N_1-P_1 and P_1-N_2 of ANEPs recorded from the AVCN display very comparable features. If the assumptions made in the preceding section hold true, this means that, in as far as its general time course is concerned, auditory adaptation in response to repetitive acoustic click stimuli is very comparable in the AN and the AVCN.

3.2 Steady-State Amplitude

Whereas adaptation time constants were only calculated for the N_1-P_1 component, plateau amplitudes were assessed for both ANEP peaks and therefore allow for a mathematical comparison of the adaptation patterns displayed by them. Looking again at Table 7.4, it may seem surprising that at the two highest stimulus intensities used, N_1-P_1 actually displayed more pronounced adaptation patterns than P_1-N_2 (significant P_{comp} values at 50 and 70 dB SPL). After all, if the two ANEP components indeed represent the AN and the CN, it would seem that adaptation patterns for P_1-N_2 should be at least as marked as those for N_1-P_1 since the output of the neurons at the basis of the latter component is the input to those related to the former. Thus, even if the synapse between primary and secondary auditory neurons did not participate in the adaptation process at all, how is it possible that the steady-state response of CN neurons is actually higher than that of AN fibers?

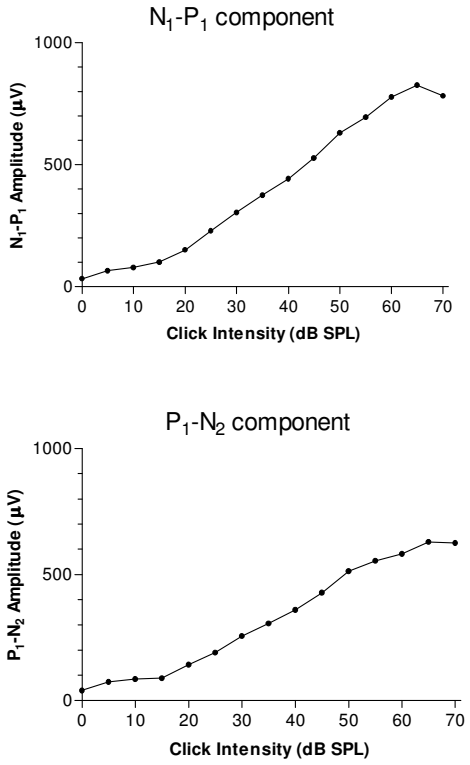

Fig. 8.2 Amplitude-intensity functions for both components of the ANEP established for Rat 6 (same data as in Fig. 7.2).

One possible explanation for this observation would be different amplitude-intensity curves for the AN and the CN. Consider a pulse train presented at 70 dB and 1'000 pps to Rat 6: the very first click of this train will – theoretically – evoke a response of around 780 µV in the AN and of 625 µV in the CN (Fig. 8.2). Looking at Fig. 7.8.B (purple trace of bottom right panel), it turns out that the AN responses to such a pulse train obtained during the steady state average 4.5 % of first-peak amplitude, thus about 35 µV in absolute terms. This potential is about equal to one evoked by a single click presented to the same animal at 0 dB SPL (32.6 µV; see Fig. 8.2, top panel). Thus, the input to the CN produced by a single click at 0 dB SPL is equivalent to that evoked by a 70-dB-SPL click presented towards the end of a 250-ms stimulus train. In the CN, an isolated click presented at 0 dB SPL produced a potential of 40.4 µV (Fig. 8.2, bottom panel); if the synapses between primary and secondary auditory neurons did not display any adaptation, the same response should thus be observed during the steady state in response to a click train presented at 70 dB SPL. Thus, the CN response would present a first peak at 625 µV and a steady state at 40 µV, resulting in a steady-state-to-first-peak ratio of 6.4 %. Another look at Figs. 7.8.B reveals that this corresponds strikingly well with the empirically observed value (6.2 %).

Thus, for the example given, slight discrepancies in the shape of the amplitude-intensity curves (the tendency for the CN curve to level out slightly at high intensities, see again Fig. 8.2) could

account for the differences in plateau amplitude. Does this theory work for the other animals, too? There are some facts that suggest it does, and there are some that imply it does not. Strengthening the theory is, for example, the fact that if one carries out the above reckoning for Rat 2 (also at 70 dB and 1'000 pps), it turns out that, this time, the plateaus observed for N_1-P_1 should be situated above those for P_1-N_2. Indeed, the individual response traces established for Rat 2 (data not shown) suggest it to be the only one out of six experimental animals to actually display higher N_1-P_1 than P_1-N_2 amplitudes.

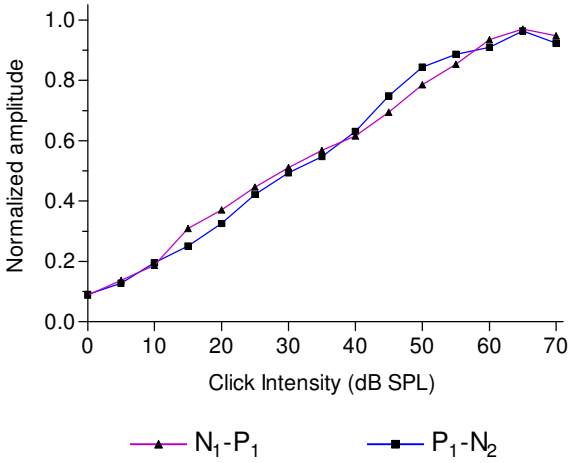

Fig. 8.3 Superposed averaged and normalized growth functions for both N_1-P_1 and P_1-N_2.

On the other hand, when doing the mathematics with averaged amplitude intensity curves (Fig. 8.3), at least at first glance, the theory does not hold. The data point obtained at 70 dB SPL for N_1-P_1 is indeed somewhat higher up than the corresponding value for P_1-N_2. The two curves coinciding almost perfectly at low intensities, this will result in a slightly higher ratio between a high- and a low-intensity response, and ultimately in a somewhat higher plateau amplitude, for P_1-N_2, as described in the example above. It seems, however, that this difference in low-to-high-intensity ratios is too small as to be the cause of the observation at issue. Even more disturbing is the fact that at 50 dB SPL, the normalized response obtained from the CN is actually slightly higher than that of the AN. This would result in a plateau-amplitude relationship between N_1-P_1 and P_1-N_2 reverse to the one we are trying to explain. It has to be noted, however, that many of the amplitudes we measured for the N_1-P_1 component during the steady state of the response to a stimulus train were even lower than those recorded in response to a single 0-dB-SPL stimulus (in terms of Fig. 8.3, they were located to the left of the graph). We do not have any information about the shape of the two amplitude-intensity curves in that range. One may doubt that there are significant differences between their shapes, considering that they are very similar in the range around 0 dB SPL. It must be noted, however, that just small differences in the response behavior to very low stimuli can result in large variations of the ratio between low- and high-intensity responses, since the potential amplitudes are very close to zero.

There is certainly not enough evidence for a secure embracing of the above theory as an explanation for the sometimes higher plateau-to-first-peak ratios in the CN than in the AN. However, it

is clear that if one searches for an accurate quantification of the adaptation behavior of a given relay in a serial system (such as the CN in the auditory periphery), the input to this structure either must be kept constant or then its amplitude as a function of time has to be perfectly known. In our case, the input to the CN (the output of the AN) is not constant. Even though we know the input amplitude's behavior as a function of time with a fair amount of precision (because we have quantified the adaptation properties of the AN), we do not know very well how the CN reacts to this input even in the absence of any adaptive behavior of the synapses between first- and second-order auditory neurons. In order as to obtain an absolutely unbiased quantification of the CN neurons' contribution to the overall time course of adaptation, we would have to hold the input to it (the output of the AN) strictly constant. This task is not as simple as it may seem, because even when stimulating the AN directly with repetitive constant-intensity electrical pulses, it displays a certain amount of adaptation as is apparent from studies carried out in our laboratory (Haenggeli et al., 1998; Loquet et al., 2004).

Another possible explanation for higher plateau amplitudes in the CN than in the AN would be the so-called build-up units located in the DCN (cf. section IV.1.3.4). Recall that in response to tone bursts, these units do not display activity at stimulus onset but then progressively increase their firing rate during the duration of the stimulus. We are not aware of any single-unit recordings from these neurons in reply to repetitive short stimuli, but it seems conceivable that when responding to high-frequency click stimulation, they may exhibit a firing pattern comparable to that provoked by long pure-tone bursts. If this were so, build-up units could indeed increase the ratio between steady-state and first-response amplitude, since they would not contribute to the potential observed in response to the first stimulus in a train but would influence those during the steady state. It must be said that, a priori, the influence of these units on the potentials we recorded from our electrodes would be taken to be minor. They seem to be located too far away from the electrode's position and their number appears too small in order for them to have a significant effect. Nonetheless, a certain influence cannot totally be ruled out.

There can be no certainty as to whether or not the difference in plateau amplitude between N_1-P_1 and P_1-N_2 can be explained by the above theories. However, it seems rather unlikely that the reliability of the synapses at the level of the AVCN would actually increase as a function of time during a stimulus train, as our results would suggest in case any other influence could be ruled out. In the search for a simple theory, and given that this increase in reliability, if it existed, would be very slight, it seems more appropriate to propose that, in the best of cases, the synapses between primary and secondary auditory neurons relays signals invariably over time.

It was described in section VII.3.3.1 that changes in stimulus repetition rate tended to affect slightly more steady-state-to-first-peak ratio for P_1-N_2 than for N_1-P_1. Again, we think that minor differences between the refractory properties of AN fibers and CN neurons may be at the basis of this finding. This hypothesis shall be further detailed in section VIII.5.3.5.

4 Comparison to Prior Results

Note that many of the studies relevant in our context have already been reviewed in section IV. Therefore, the discussion of our results in the context of prior literature will be kept rather short.

Moreover, it will be restricted to a purely empirical level; attempts to investigate the origins of our findings and the functioning of adaptation shall be made in the next section.

4.1 Adaptation Time Course

The results of this study indicate that in the presence of repetitive acoustic stimulation, the reaction of the peripheral auditory system is maximal in response to the first stimulus of the series and becomes progressively less pronounced in response to those to follow. This is in accordance with the findings of prior investigations carried out both in the AN (Peake et al., 1962a; 1962b) and the CN (Huang, 1981). The time course of adaptation we observed for the N_1-P_1 component, a two-stage exponential decay followed by a steady state, was reported before for the same ANEP deflection by Loquet and Rouiller (2002), also using repetitive click stimulation. The time constants of the exponential decays as well as the steady-state amplitudes of the response curves found in their and in the present studies are very comparable.

A similar two-time-constant exponential decay was also observed in the AN of the Mongolian gerbil and the cat (Westerman and Smith, 1984; Chimento and Schreiner, 1990, 1991). Although the stimulus paradigms of those studies were not identical to ours (continuous tone bursts as opposed to repetitive clicks at high rates), we believe that they were similar enough to justify a comparison of results. The rapid-adaptation time constants we observed (especially those at lower intensities and repetition rates) are in good agreement with the values found for both of the mentioned species (see Table 7.3 and section IV.2.2.2). Likewise, the values we obtained for the short-term time constant at moderate intensities (Table 7.2) fit in among those found in prior investigations for the guinea pig, the chinchilla and the Mongolian gerbil (Smith and Zwislocki, 1975; Smith, 1977; Harris and Dallos, 1979; Westerman and Smith, 1984; see Table 4.1). The effects of stimulus intensity and repetition rate explain why our K_2 values at high levels and repetition rates tend to be rather short.

4.2 Effects of Stimulus Repetition Rate on Adaptation

Our results indicate that adaptation phenomena, for both components of the ANEP, become more pronounced as repetition rate is increased (Figs. 7.5 and 7.13). This is evident, on the one hand, from the rate-induced changes of both adaptation time constants, as quantified for the N_1-P_1 component (Table 7.2). Again, our observations parallel those of Loquet and Rouiller (2002), who also found K_1 and K_2 to decrease as they raised the rate of stimulation. The second working point of rate changes is the level of the steady state (Figs. 7.6 and 7.14); several prior studies reported its amplitude to decrease with increasing stimulus rate both in the AN (Peake et al., 1962a, 1962b; Huang and Buchwald, 1980) and the CN (Huang and Buchwald, 1980; Huang, 1981). It should be noted that Huang and Buchwald (1980) observed rate-amplitude effects to be practically identical in the AN and the CN. As discussed in the preceding section, our results are qualitatively and, except for some minor discrepancies, quantitatively in line with this observation.

Remember that Huang and Buchwald (1980) concluded from their results that inter-stimulus silent interval was the most important determinant of steady-state amplitude. Although silent interval was not

considered one of the main stimulus parameters in this study, varying repetition rate between 100 and 1'000 pps while keeping stimulus duration at 100 µs results in silent intervals ranging from 0.9 to 9.9 ms. Therefore, our results, in accordance with those of the cited study, suggest that a decrease in inter-stimulus interval results in a decrease of steady state amplitude.

4.3 Effects of Stimulus Intensity on Adaptation

The fact that adaptation phenomena become more prominent at higher stimulus intensities has been observed in response to both continuous and repetitive acoustic stimuli, as well as in forward-masking paradigms (see section IV). First of all, our results, again for both components of the ANEP, suggest steady-state amplitude to be lower at higher stimulus intensities (Figs. 7.10 and 7.16). A similar effect was observed in the AN of the cat, also in response to repetitive stimulation (Peake et al., 1962b). Second, for the N_1-P_1 component, both adaptation time constants tended to decrease as stimulus intensity increased (Table 7.3, Fig. 7.9). This effect was more pronounced for the rapid than for the short-term component. In fact, literature on intensity-dependence of adaptation time constants is not unanimous: most but not all (Chimento and Schreiner, 1990) studies carried out in the AN stated the short-term time constant to be independent of intensity. The rapid adaptation component, on the other hand, was observed to depend on intensity with respect to both its time constants (Westerman and Smith, 1984; Yates et al., 1985) and its amplitude (e.g. Smith and Brachman, 1982; Westerman and Smith, 1984; Rhode and Smith, 1985; Yates et al., 1985). Altogether, intensity dependence seems to be more prominent for the rapid than for short-term adaptation component. Our results fit well into this overall picture.

5 The Nature of Adaptation

Evidently, the many experimental paradigms used to find out more about adaptation in the auditory periphery did not only aim at acquiring empirical data but were developed also in an endeavor to get to know more about what was behind the bare results.

What are the physiological mechanisms at the basis of the adaptation phenomena we observe? There are two distinct approaches to the answer of this question. The first, direct way is to move along the peripheral auditory pathway, from the external ear all the way to the CN, and to check at every stage if anything has changed about the observed response patterns. Many authors have used this method to determine the site of adaptation; the most important studies shall be reviewed further below. The other, somewhat less evident way is to model adaptation. If the adaptive properties of the auditory periphery were a little black box with an input and an output opening, what kind of transformations would have to occur inside in order to produce the known empirical data?

These two ways of approaching the nature of adaptation are usually not independent of each other. Once there are hints as to the site of adaptation, this may allow better interpretation of mathematical models. Inversely, a mathematical model may provide new clues as to what it is exactly that happens at a certain anatomical site.

5.1 Models of Adaptation

When working on a mathematical model for adaptation, one usually ponders the following two questions: 1. Is there any scheme or, even better, a concrete mathematical equation underlying my empirical results (in terms of the black box: can its output be predicted based on a mathematical relation involving one or several parameters of its input)? 2. If the first question can be answered yes, are there physiological mechanisms in the auditory periphery whose nature would allow for them to be at the basis of the found equation, or of some of its individual parts?

5.1.1 Is Adaptation Additive or Multiplicative ?

When presenting a stimulus to a system without any adaptive properties, the envelope of the response of the system would mirror the shape of the envelope of the stimulus (except for a component due to SA; Fig. 8.4, panels 1 and 2). In what way could adaptation change this "raw response" to produce the typical adapted PSTH? One of the possibilities would be to think of adaptation as a multiplication factor whose magnitude varies along the time axis (Fig. 8.4, panel 3). At every moment during the response to a stimulus, the primary, unadapted response of the system would be multiplied by this factor to produce the final output (Fig. 8.4, panel 5). This adaptation mechanism would thus be multiplicative. However, there is another possible way in which adaptation could modulate the unadapted response envelope. Instead of performing a multiplicative change on the amplitude of the raw PSTH, it could also manipulate the basic firing rate by simply subtracting from it a certain value ("a certain number of spikes per second"). Adaptation could thus be thought of as a decrement whose magnitude varies along the time axis (Fig. 8.4, panel 4). In this case, the final output of the system would result from an additive superposition of the unadapted firing rate of the system and a decrement due to adaptation (Fig. 8.4, panel 6). As is apparent from Fig. 8.4 (panels 5 and 6), the final responses produced by the two mechanisms do not differ greatly from one another. (Note that in the case of an additive adaptation, firing rate would temporarily drop to zero after stimulus offset. This is in accordance with empirical data (Fig. 4.16).) However, only the additive model agrees with the results of Smith and Zwislocki (1975) who found that when superposing an intensity increment to a pedestal stimulus, the response to this increment is independent of the delay at which it is presented (see section IV.2.2.4). In the case of a multiplicative adaptation mechanism, such a sudden increase in firing rate, in the same way as the rest of the response, would be affected by the multiplication factor. The latter becoming smaller with time (Fig. 8.5, panels 1 and 2), so would the rise in firing rate in response to an intensity increment (Fig. 8.5, panels 3 and 4). This is in direct contradiction to the empirical results of Smith and Zwislocki (1975). In case of an additive adaptation mechanism, however, the increment in firing rate would be independent of the delay between pedestal and increment onsets, as is evident from Fig. 8.6 (panels 3 and 4). Smith and Zwislocki (1975) therefore suggested adaptation to be additive. This would mean that at any point during the response to a stimulus, the ultimate PSTH amplitude results from the superposition of an unadapted firing rate and a decrement due to adaptation. This decrement builds up during the stimulus and then disappears progressively when stimulation has ceased (Fig. 8.6, panels 1 and 2; Smith, 1977). Moreover, it has been mentioned in section IV.2.2.2 that in what concerns short-term adaptation, the amplitudes of the

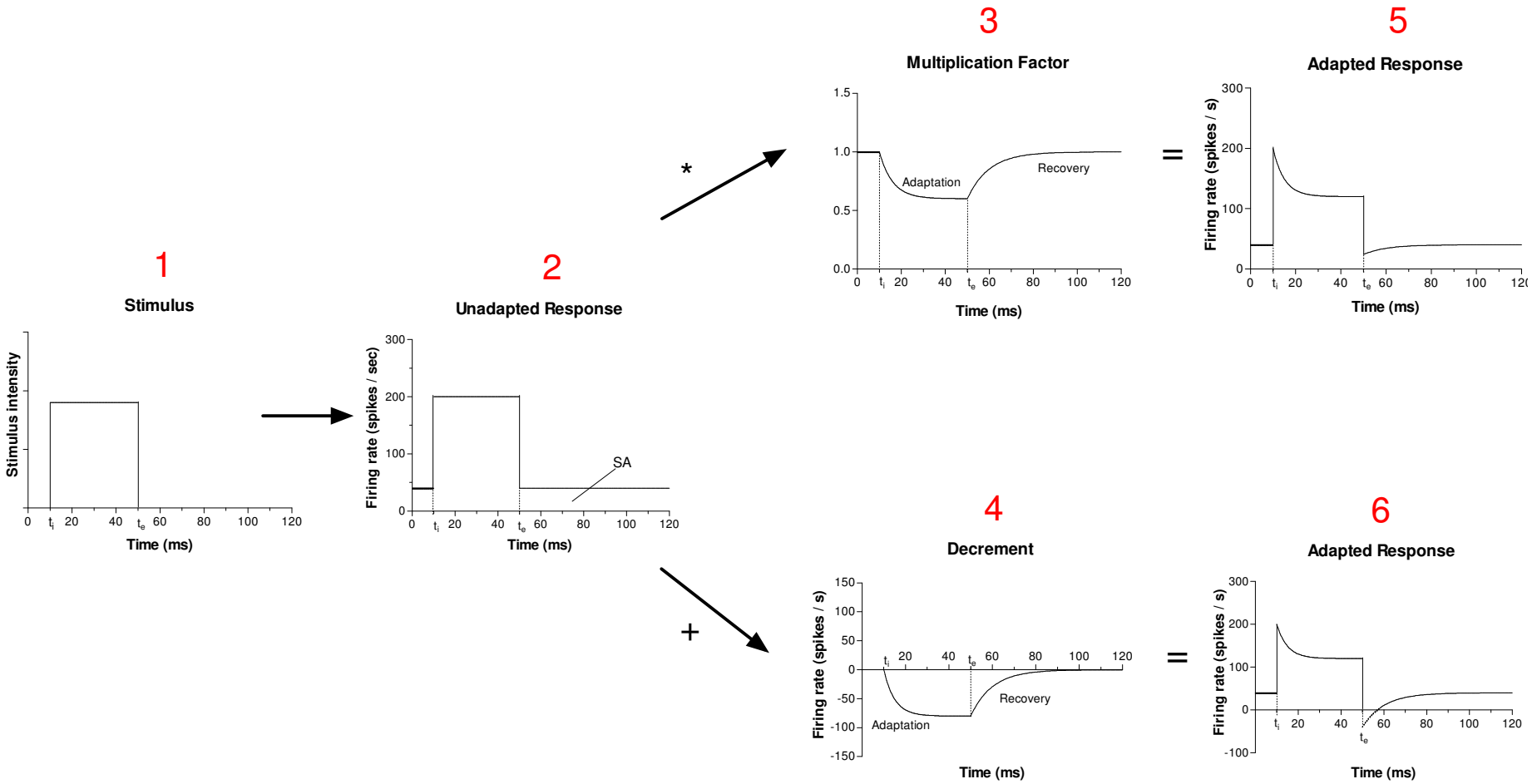

Fig. 8.4 Conceptual presentation of both a multiplicative (top) and an additive (bottom) adaptation mechanism. A stimulus (panel 1) first produces an unadapted response (panel 2) whose envelope mirrors the shape of the stimulus itself (except for SA). This unadapted response can then either be multiplied with a factor varying over time (panel 3) or superposed to an additive decrement (panel 4). Both mechanisms produce resembling adapted PSTHs (panels 5 and 6). t_i: time of stimulus onset; t_e: time of stimulus end.

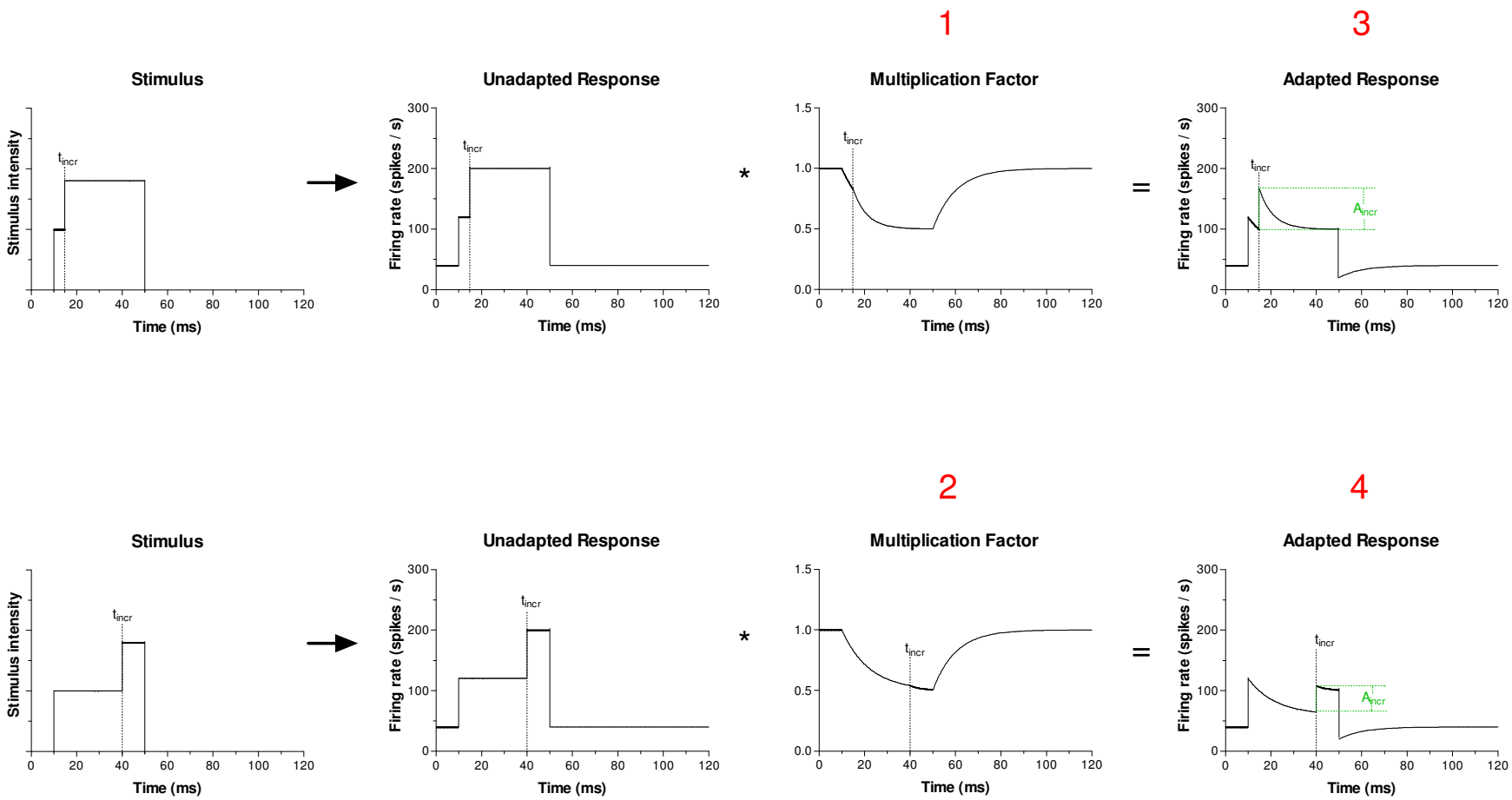

Fig. 8.5 Multiplicative adaptation model. Input consists in tone pedestals with superposed intensity increments. The increase in firing rate depends on the delay after pedestal onset at which the increment is presented. A_{incr}: increase in response amplitude at presentation of the intensity increment; t_{incr}: time of presentation of the intensity increment.

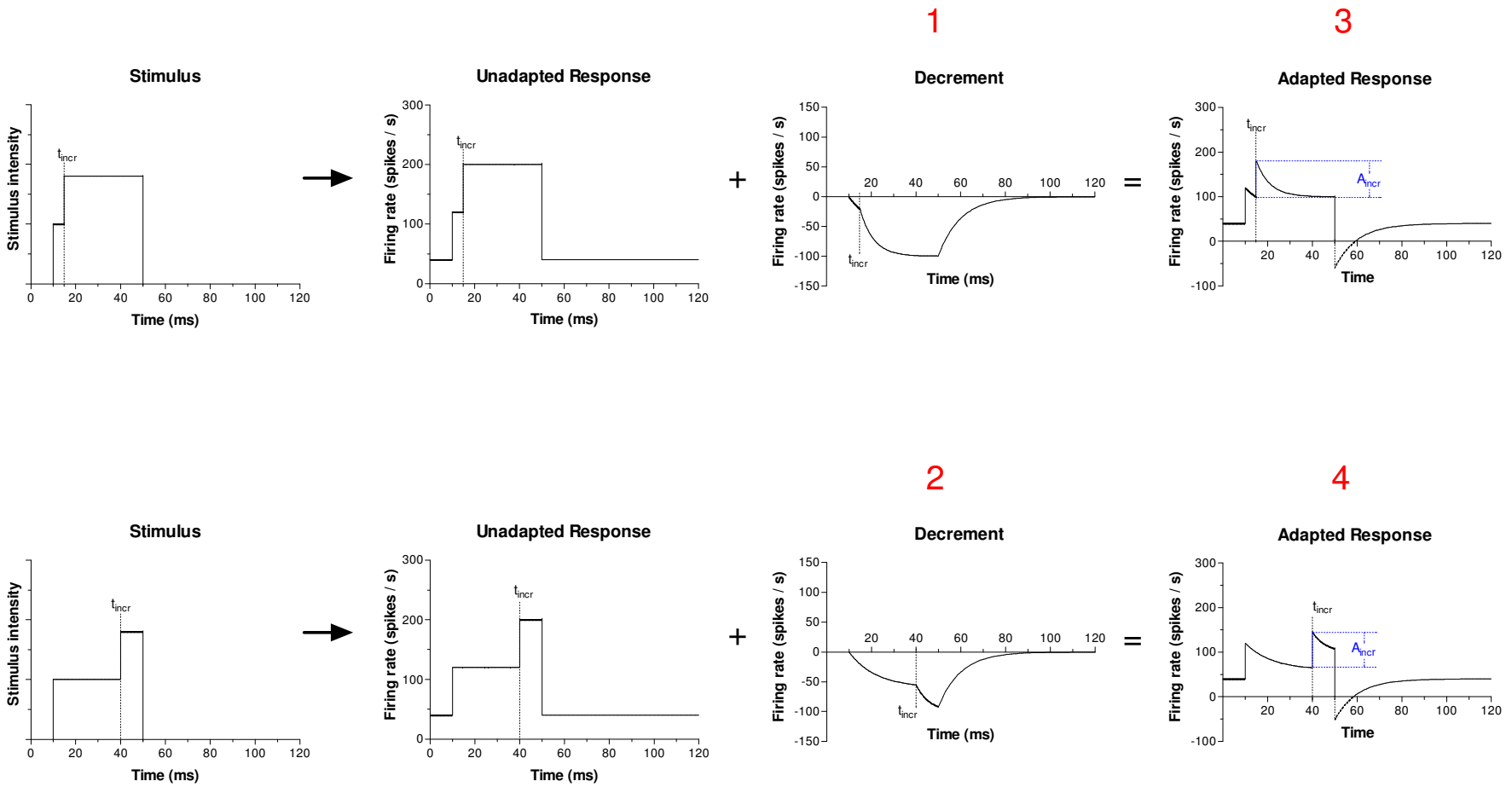

Fig. 8.6 Additive model of adaptation. Input is identical to that in Fig. 8.5. The increase in firing rate is independent of the time delay after pedestal onset at which the intensity increment is presented. A_{incr}: increase in response amplitude at presentation of the intensity increment; t_{incr}: time of presentation of the intensity increment.

onset and the steady-state responses are proportional to one another. This implies that the maximum amplitude of the decrement is also proportional to both of these values (Smith, 1979).

5.1.2 Neurotransmitter Kinetics

The conceptual properties of adaptation were thus established, but how could they be related to physiological events occurring in the auditory periphery? As will be further explained below, early studies (Furukawa and Matsuura, 1978; Furukawa et al., 1978) had already pointed out the synapses between hair cells and afferent dendrites as a possible site of adaptation. In accordance with this, Smith and Brachman (1982) suggested a multi-stage depletion of neurotransmitter to be at the origin of adaptation (Fig. 8.7). Briefly, the model consists of three transmitter reservoirs. The first one of them is very small and, secreting transmitter into the synaptic cleft, depletes rapidly. At any moment, firing rate of the AN is proportional to the rate of transmitter release; transmitter release, in turn, is proportional to the amount of transmitter remaining in the store, resulting in an exponential decay of the latter. This immediate store is responsible for the initial, rapid decrease in firing rate. However, it is linked to a larger local store. Since there is free transmitter flow from the local to the immediate store, the level of the latter will never drop below that of the former. Thus, after immediate-store transmitter has rapidly decreased to the initial level of the local store, depletion will decelerate due to the larger content of the local store. In terms of firing rate, this is marked by the transition from rapid to short-term adaptation. Likewise, the amount of transmitter in the local store cannot drop below a certain value because there is free replenishment from a global store which is assumed to be large enough for its transmitter level to remain constant. In terms of response firing rate, this constant amount of transmitter is responsible for the steady state.

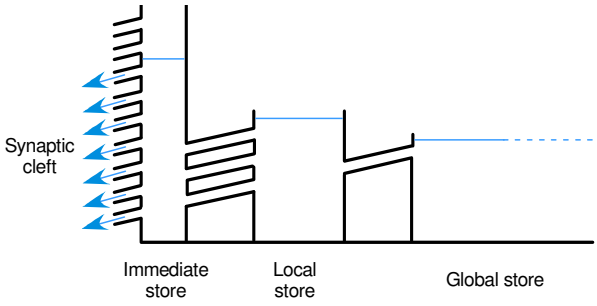

Fig. 8.7 Smith and Brachman's model (1982). Flow from the immediate store is proportional to neurotransmitter left (the higher the transmitter level the more outflow pipes are used).

How does this model fulfill the time-independence of the response to an intensity increment superposed to a pedestal, as it was described above? The immediate store is subdivided into several distinct compartments (Fig. 8.8). These compartments are identical except that every one of them requires a different threshold potential for its activation. A stimulus of a given intensity thus activates a specific number of compartments. If an increase in stimulus intensity is presented at any time, a certain number of additional compartments will be activated, and transmitter flow will therefore increase by an amount proportional to the number of newly activated sites. Prior to presentation of the increment, unactivated compartments do not participate in transmitter release at all and therefore remain full until activation. Therefore, additional transmitter flow due to the increment will be absolutely independent of time.

In addition to mimicking well the behavior of the AN in response to intensity increments and decrements, the multi-stage transmitter-release model reproduced faithfully other typical features of adaptation such as a constant ratio of onset to steady-state rate for the short-term component. Its simplest physiological interpretation would be that each of the three stores represents a separate pre-synaptic compartment in which neurotransmitter, or one of its precursors, are stocked up.

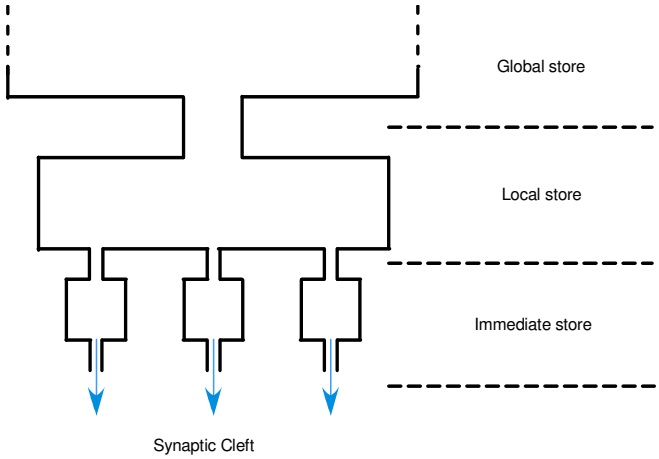

Fig. 8.8 Smith and Brachman's model (1982). The subdivision of the immediate store is responsible for the authentic output of the model in response to intensity increments and decrements.

Somewhat later than the one above, another adaptation model was presented by Meddis (1986; 1988). Again, adaptation was explained on the basis of transmitter flow between various compartments; a flow diagram is given in Fig. 8.9. From a free pool, transmitter is released into the synaptic cleft. The amount liberated depends on the concentration of transmitter in the free pool and on the permeability factor k(t), which is a non-linear function of instantaneous stimulus intensity. From the synaptic cleft, a certain amount of transmitter is lost due to chemical processing and diffusion (at rate l). Additionally, a part of the transmitter substance is re-absorbed into a reprocessing store (at rate

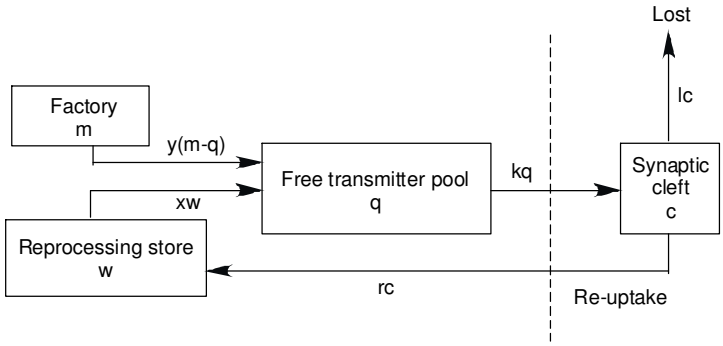

$$\frac{dq(t)}{dt} = y(m - q(t)) + xw(t) - k(t)q(t)$$

$$\frac{dc(t)}{dt} = k(t)q(t) - lc(t) - rc(t)$$

$$\frac{dw(t)}{dt} = rc(t) - xw(t)$$

Fig. 8.9 Meddis' model (1986): Transmitter flow takes place according to the diagram in the upper panel and is quantitatively governed by the three differential equations given in the lower panel. c, m, q, and w denote transmitter concentrations in the respective compartments, k, l, r, x, and y are flow / permeability constants. See text for further details. Modified from Meddis (1986).

r) and, from there, is relayed back to the free pool (at rate x). Additionally, the free pool is replenished from a transmitter factory; flow between the two compartments is governed by their difference of concentration (m-q) and by a constant y. Quantitatively, these descriptions can be summarized by the three differential equations given in Fig. 8.9. It is assumed that spike occurrence in the AN is linearly related to the amount c(t) of transmitter present in the synaptic cleft at a given moment. Evidently, the model's characteristics will vary considerably depending on the numerical values assigned to the various flow / permeability constants (k, l, m, r, x, y).

One of Meddis' model's most impressive features is the fact that, using an appropriate set of parameters, its responses display rapid as well as short-term adaptation, and that the time constants of both of these processes, as well as their dependence on stimulus intensity, are very comparable to the data obtained empirically by Westerman and Smith (1984). Moreover, the model comes up with a time constant of 46 ms for recovery of spontaneous firing rate after the offset of a stimulus, a realistic value, as hinted by the empirical findings of Harris and Dallos (1979; 37 ms) and Westerman (1985; 40 ms). In other points, the model did not agree with experimental findings: for example, although the time constants just mentioned were close, the model could not explain a complete suppression of SA immediately following stimulus offset, as is often observed in practice (see Fig. 4.16). Additional incompatibilities between modeled and empirical responses resulted when applying forward-masking or pedestal-increment paradigms.

In spite of these inconsistencies, Meddis' studies represent an impressive endeavor to model adaptation as it occurs at the synapse between hair cells and AN fibers. Later on, the above considerations about transmitter flow were introduced into a more global model of the auditory periphery, including middle-ear and basilar-membrane mechanics, a mathematical approach to the IHC receptor potential, calcium kinetics of the baso-lateral membrane of the hair cells, the above adaptation model, and refractoriness of the AN (Sumner et al., 2002, 2003). Notably, this appreciation allowed for separate modeling of adaptation for high- and low-SA AN fibers and for off-CF stimulation, coming up with patterns agreeing well with those found in some empirical studies (Rhode and Smith, 1985; Müller and Robertson, 1991; Relkin and Doucet, 1991; see section IV.2.2.2). Another impressive feature of the model is the fact that it produces realistic phase-locking properties; these originate from a combination of low-pass filtering of the hair-cell receptor potential, the dynamics of calcium flow, and transmitter recycling.

5.1.3 Post-Synaptic Receptor Kinetics

Eggermont (1985), in addition to pre-synaptic transmitter flow and AN refractory properties, proposed post-synaptic transmitter kinetics to have an influence on adaptation, too. According to his model, occupation and subsequent liberation (occuring at rates λ and μ, respectively; Fig. 8.10) of post-synaptic receptors are the time-limiting factors of synaptic transmission and therefore mainly responsible for short-term adaptation. The rapid adaptation component is attributed to refractory properties of AN fibers. Pre-synaptic events are not excluded from participating in adaptation: a general transmitter store is suggested to replenish the pre-synaptic vesicles at a rate υ, a process which could account for long-term adaptation. Moreover, the general store is constantly refilled at a

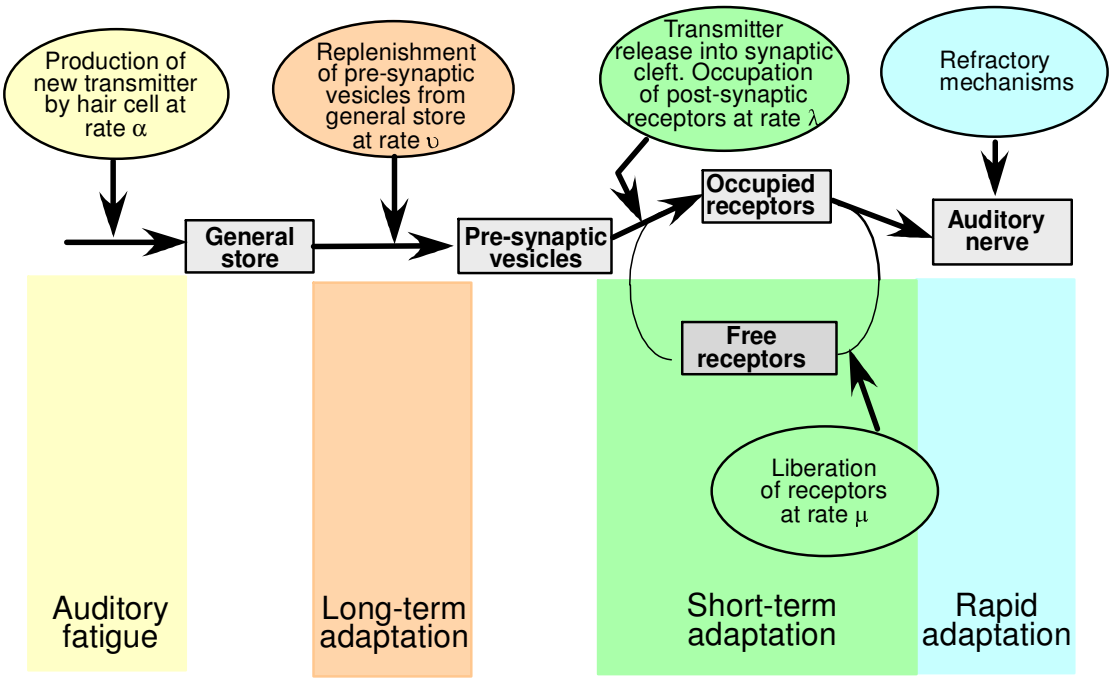

Fig. 8.10 Adaptation model suggested by Eggermont (1985). Both pre- and post-synaptic events, as well as refractory mechanisms in the AN, are responsible for the overall adaptation process.

rate α with new transmitter produced by the hair cell. If this process is in some way limited, it could be the origin of auditory fatigue. As the one of Smith and Brachman (1982), the model of Eggermont (1985) accounts for many of the empirical results obtained in adaptation studies. One of its noteworthy properties, for example, is the fact that the discrepancy between adaptation and recovery time constants observed in many species (see section IV.2.2.2) is intrinsic to it. Note that, whereas Smith and Brachman (1982) suggested both rapid and short-term adaptations to emerge from transmitter kinetics, rapid adaptation is post-synaptic of origin in Eggermont's model.

5.2 Possible Sites of Adaptation

Many sites along the acoustical pathway must be regarded as possible origins of adaptation: the middle ear muscles, cochlear mechanics, hair cells and central-nervous-system influences on them, pre- and postsynaptic events at the hair cell-nerve fiber junction, refractory properties of the AN, the synapse between primary and secondary auditory neurons, or a combination of any two or more of the preceding. Inhibitory interactions at the level of the afferent dendrites or cell bodies of SG neurons were also added to the list of hypothetical mechanisms (Norris et al., 1977).

5.2.1 Middle Ear Muscles and Cochlear Mechanics

The cochlear microphonic is the potential that can be recorded directly from cochlear hair cells. If adaptation were to occur in the middle ear or during the mechanical events taking place in the cochlea, i.e. at a more peripheral site than the hair cells, the cochlear microphonic should display a decrease in amplitude in response to a prolonged stimulus. However, neither the cochlear

microphonic (e.g. Peake et al. 1962a; Norris et al., 1977; Furukawa and Matsuura, 1978) nor intracellular recordings from IHCs (Russel and Sellick, 1978) display such a decrement. Therefore, it seems probable that the events yielding the adaptation patterns we are able to observe at the level of the AN take place after generation of the receptor potential in cochlear hair cells.

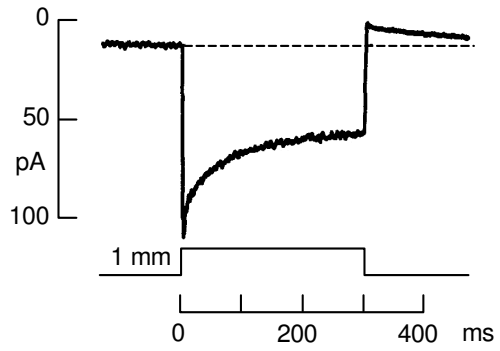

Fig. 8.11 Properties of adaptation of a mouse utricular type II hair cell: in response to a 1-µm deflection, the current across the transduction channels increases rapidly and then progressively declines. Modified from Holt and Corey (2000).

5.2.2 Hair Cells

When cochlear hair cells are artificially stimulated by a prolonged, manual deflection of their hair bundles, there is an abrupt rise in receptor potential followed by a gradual decrease to a plateau level. In other words, the response-deflection relation shifts during a sustained stimulus (Fig. 8.11; Holt and Corey, 2000; Hudspeth, 2000; Hudspeth et al., 2000; for a review see Eatock, 2000). This adaptive behavior may be surprising at first, for, as opposed to other sensory receptors, the vestibulocochlear apparatus does not use a second messenger in its signaling cascades. How is it that a system which uses direct mechanoelectrical transduction displays adaptation nonetheless? Two distinct models have been proposed to explain these findings; they are similar as to the important role of calcium entering through the transduction channels, but quite different with respect to the mechanisms involved and their time constants.

The Active Motor Model

This model suggests the presence of an active motor complex which is linked to the transduction channel and constantly tries to pull it up towards the tip of the stereocilium. When the hair bundle is deflected, the tension in the tip link increases, and the force pulling the channel downward becomes greater than that of the motor pulling it upward (Fig. 8.12). Consequently, the channel slips down, tension in the gating spring decreases and, eventually, the channel will shut, thus reducing inward current and depolarization state of the cell. Inversely, a deflection in the negative direction will reduce gating spring tension, causing all transduction channels to close, and the cell to hyperpolarize. Now, the active motor complex will pull the transduction channel up toward the tip of the cilium. Tension in the gating spring will increase, and some of the channels will return to the open configuration. How is calcium implicated

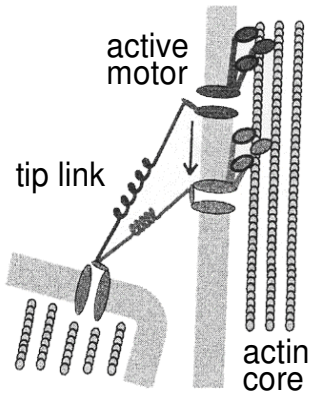

Fig. 8.12 Schematic representation of the active motor model for hair cell adaptation. Taken from Holt and Corey (2000).

in this model? There is evidence that myosin, namely myosin Ib, is responsible for channel movement (Holt and Corey, 2000; Hudspeth et al., 2000). Calmodulin can occupy the light-chain binding sites of myosin and thus confer a calcium dependence to the active motor's activity. High intracellular calcium levels, as occur during a positive deflection, could accelerate the rate of slipping of the active motor and enhance adaptation.

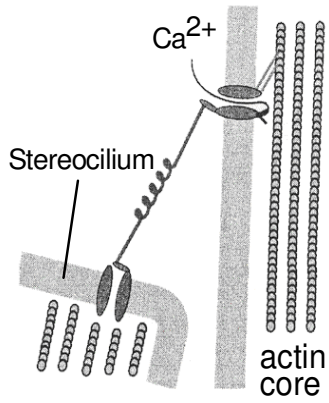

Fig. 8.13 Schematic representation of the calcium-dependent closure model for hair cell adaptation. Modified from Holt and Corey, 2000.

The Calcium-Dependent Closure Model

According to this model, the site of action of the calcium ions is the transduction channel itself. When calcium occupies its binding site, this would change the energetics of the channel in such a way as to favor the closed configuration. Deflection of the hair bundle will open many channels and cause the hair cell to depolarize. At the same time, however, intracellular calcium concentration will rise. Channels tend to close again, and the cell repolarizes (Fig. 8.13).

Electrophysiological data suggest that the active motor model as well as the calcium-dependent closure model may be implicated in the process of adaptation. The latter might operate within delays as short as 0.3 to 5 ms, whereas myosin-slipping would take between 10 and 100 ms.

There seems to be a discrepancy between what has just been described and the fact, mentioned further above, that the hair cell receptor potential is constant during a stimulus. It is important to note that adaptation in a hair cell occurs in response to a mechanical, static deflection of its hair bundles. It seems that, in nature, there is not much use for such adaptive properties, since the hair-bundle movements to natural acoustic stimuli are rapid and balanced about zero (Mac Leish et al., 1999). Thus, although there is an adaptation component in hair cells, it does probably not account for the phenomena observed in the AN or the CN.

5.2.3 Influence of the Olivo-Cochlear Bundle on Hair Cells

It has been shown that activation of the olivocochlear bundle can lower the receptor potential of IHCs and decrease CAP amplitude in the AN in response to sounds (Brown and Nuttal, 1984). It could therefore be hypothesized that activation of this system a short time after stimulus onset could be responsible for the response envelopes observed in the AN in reply to tone bursts. However, it has been shown that adaptation still occurs when the AN is cut (Norris et al., 1977). Since, in this case, all fibers of the olivocochlear bundle are sectioned, there must be a different mechanism underlying the adaptation phenomena.

5.2.4 Hair Cell-Nerve Fiber Synapse

On the one hand, as mentioned before, intracellular recordings from IHCs as well as the cochlear microphonic remain constant in response to continuous acoustic stimulation, indicating that there is no adaptive component occurring peripherally to the IHCs. On the other hand, the EPSPs picked up from dendrites of SG neurons are observed to clearly exhibit adaptive behavior (Furukawa and Matsuura, 1978; Furukawa et al., 1978). Therefore, the site (or one of the sites) of adaptation must be located at the synapse between the IHCs and the afferent dendrites. Concretely, the search focused on two mechanisms: pre-synaptic liberation of neurotransmitter and binding of transmitter molecules to receptors in the post-synaptic membrane. As described above, both of these possibilities have been considered in an endeavor to model adaptation mathematically.

5.2.5 Auditory Nerve

There is clear evidence that the events taking place at the synapses between hair cells and primary auditory neurons are not the only ones responsible for the adaptation patterns observed in the AN. When stimulating the eighth nerve directly (electrically), thus bypassing the hair cells and the afferent synapses, adaptation phenomena are still present. In response to pulsatile electrical stimulation, Haenggeli et al. (1998) observed the AN to display an initial rapid decrease in CAP amplitude during the first 5 ms, followed by a more progressive decay during the next 50 ms, approximately, and a steady state. Additionally, there was a long-term adaptation effect (considered by the authors to result of fatigue) that manifested itself over at least 6 minutes. Adaptation, again expressed as the ratio of steady-state to onset-response amplitude, clearly became more pronounced as pulse rate increased, a finding which is in accordance to results obtained from the AN in response to acoustical stimulation (Peake et al., 1962a, 1962b; Huang and Buchwald, 1980, present study). The absolute decrements found in the mentioned acoustic and electric adaptation studies cannot directly be compared since the durations of the individual pulses used in the former were greater than those applied in the latter. However, a study carried out recently in our laboratory (Loquet et al., 2004) showed the adaptation pattern of the N_1-P_1 component of the ANEP to be clearly less pronounced in response to repetitive electrical stimulation than to acoustic stimuli. Furthermore, the recovery of the AN occurs a lot faster during an electrical forward-masking paradigm than when evaluated by analogous acoustic stimulation (Haenggeli et al., 1998; Chimento and Schreiner, 1990). Together, this data suggests that refractoriness of AN fibers does play a role in the adaptation phenomena but cannot explain them all by itself.

5.2.6 Signal Transmission from Primary to Secondary Auditory Neurons

The two main types of synapses in the AVCN are the endbulbs of Held (contacting spherical bushy cells) and the so-called modified endbulbs (contacting globular bushy cells; Bourk, 1976; Guinan, Jr. and Li, 1990; Trussell, 2002; Kopp-Scheinpflug et al., 2002). Both of these synapses have a reputation of being very reliable, i.e. practically every AP that gets to the pre-synaptic terminal will be relayed to the post-synaptic membrane (one-to-one ratio). Therefore, the temporal pattern of a spike train arriving from an AN fiber is well preserved as it is transmitted from the primary to the secondary auditory neuron. This is evident, for instance, from the comparable phase-locking properties classically

observed in the AN and the AVCN. An equally good preservation of adaptation properties across these synapses, as suggested by the many similarities we observed in the present study for the N_1-P_1 and P_1-N_2 adaptation data, is therefore not surprising.

Nonetheless, we have found minor quantitative discrepancies between the adaptation patterns of the two ANEP peaks, notably a slightly different susceptibility to the influence of stimulus repetition rate. It is important to note that the very synapses in the CN are not the only site at which such dissimilarities may be generated: as detailed further below (section VIII.5.3.5), refractory properties of secondary auditory neurons may also lie at their basis.

5.3 Implication of Auditory-Nerve Refractoriness in Adaptation

As we have seen, both approaches potentially leading to a better understanding of the mechanisms underlying adaptation (mathematical modeling and the specific search for possible anatomical sites) head in a similar direction. The hair cell-nerve fiber synapse as well as the AN itself (due to refractoriness) seem likely to be the main sites of adaptation.

This concept raises some interesting question with respect to the results of this study. To what extent, for example, could a theory invoking refractory mechanisms justify the shape of our adaptation curves? Furthermore, could refractoriness come up with plausible explanations for some of the effects of stimulus intensity and repetition rate on adaptation? Could it possibly explain the slight quantitative differences between the adaptation patterns of components N_1-P_1 and P_1-N_2 of the ANEP?

5.3.1 A Model of Refractoriness

All of the following considerations shall be based on a simple model. The ANEPs we recorded represent the summed activity of many individual neurons. We will assume that these units have fluctuating instead of fixed thresholds, and that for all of them, depending on stimulus intensity, there is a certain probability of responding to a stimulus. Thus, when stimulated by a click train of a given intensity, a certain number of neurons will respond to the first stimulus and become refractory thereafter. The group of cells being able to respond to the second stimulus consists of those which either have not responded to the first one or then already have overcome their refractory period. Out of all these, the same fraction as before will respond to the second click, since its intensity is identical to the first one's (it is essential to realize that fluctuating thresholds are a necessary prerequisite for such a constant response fraction). Since the group of possible responders is smaller for the second than for the first click, the compound response to the second stimulus will be lower than that to the first one. For the third stimulus, the accessible neuronal population consists of cells which have not responded to either one of the preceding clicks and, again, those which are not refractory anymore. Note that this time, more neurons have surmounted the refractory period (especially some of those activated by the first click), so that the difference in response amplitude will be smaller between the second and the third than between the first and the second stimulus. At some point, as the sequence goes on, a dynamic equilibrium will be established, with the number of neurons overcoming their refractory state and that of cells entering it (because of a stimulus) being equal. This will result in responses of constant magnitude; in other words, in a steady state.

5.3.2 Absolute and Relative Refractory Periods

In order to model the above considerations, we need to establish the time course according to which the refractory neurons recover. It is very important to realize, though, that in terms of the model, the question to be asked is a slightly different one: how does the number of neurons in the „ready-to-respond group“ recover? Nevertheless, it is clear that the answer to this question depends directly on the behavior of individual nerve fibers. Fig. 8.14 displays the excitation thresholds of three imaginary AN fibers as a function of time. In a fully recovered state, they display thresholds between 10 and 40 dB SPL. At time zero, a stimulus is presented to them, its intensity high enough to cause all of them to fire. Their thresholds immediately go up to infinity, and for a certain period, no stimulus, whatever its intensity, will be able to evoke a response from any one of them. This interval is referred to as the absolute refractory period (ARP; gray zone in Fig. 8.14). In AN fibers of the guinea pig, Mulheran (1999) found the ARP to last about 0.85 ms, whereas Brown (1994) came up with values sometimes even below 0.5 ms. In the cat AN, the ARP was reported to last between 0.56 and 0.86 ms (Li and Young, 1993). Miller et al. (2001) found a mean ARP as low as 0.33 ms. The interval after the ARP, when a fiber is again able to respond but still has an elevated threshold, is the so-called relative refractory period (RRP). The RRP varies considerably between fibers: in the guinea pig, it can be almost as short as the ARP but may also reach values of at least 5 ms (Brown, 1994). (Note that in Fig. 8.14, the purple and the dark blue fibers have inverse thresholds after recovery from the stimulus. This is intended to illustrate the fact that fluctuating thresholds are required in order for the model of refractoriness to work properly.)

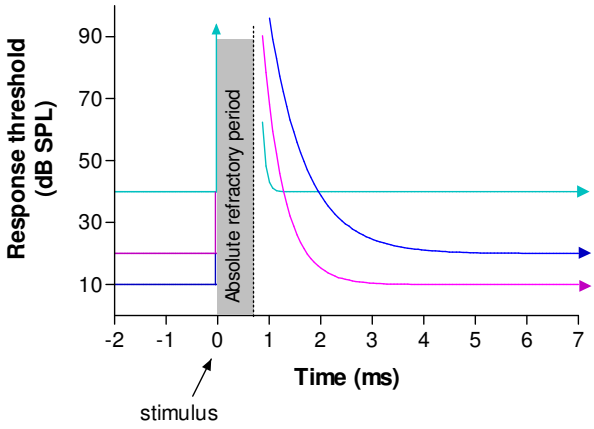

Fig. 8.14 Excitation thresholds of three imaginary AN fibers before and after a stimulus occurring at time 0. The light blue fiber recovers fastest, the dark blue one slowest. The inversion of thresholds for the purple and the dark blue fibers is intended to underline the fact that fluctuating thresholds are a prerequisite for proper functioning of the model.

Based on guinea pig data, we have established the recovery function given in Fig. 8.15 for our model. Again, it is important to note that this graph does not directly represent the behavior of nerve cells, but simply indicates the number of neurons becoming “responders” again as a function of time after a stimulus. For example, 1.67 ms after a stimulus – thus at the time of the second click of a 600-pps train – 67 % of the neurons having responded to the first stimulus would have rejoined the ready-to-respond group. Note that the shape of the recovery curve cannot be less arbitrary than the very concept of “responder” and “non-responder”; there is no justifiable answer to the question at which point a neuron has recovered enough in order to become a responder again. At any rate, it is important to emphasize that this simple model does not aim at an accurate quantification of the

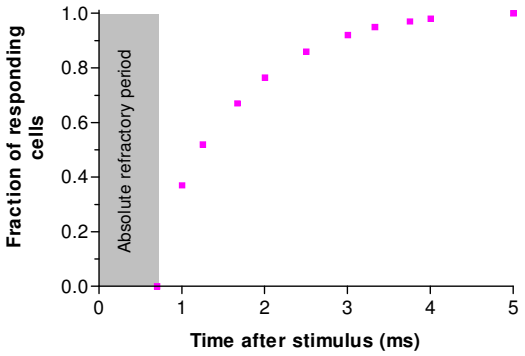

Fig. 8.15 "Recovery curve" displaying the fraction of AN fibers again ready-to-respond as a function of time. It is important to note that, although not independent of it, this figure does not indicate threshold behavior.

response behavior of the AN; it shall simply be used in order to conceive an idea about the qualitative aspects of the influence of refractoriness on adaptation.

5.3.3 Raw Output of the Model of Refractoriness

Fig. 8.16 shows the model's output for a train of clicks presented at 1'000 pps and an intensity at which, each time, 18 % of the neurons which are ready to respond will actually fire. From Fig. 7.2, it is apparent that this would correspond to a stimulus intensity of about 10 dB SPL if ANEP amplitude could be assumed to be approximately proportional to the number of individual AN fibers responding. (In this context, it should be noted that in single-unit recordings in response to forward-masking paradigms, spike amplitude to the probe tone was actually observed to decrease with the masker-probe interval (Miller et al., 2001). This suggests that the amplitude of a compound potential may not be a reliable indicator for the number of contributing neurons. Since our model is not intended to allow for accurate quantitative analysis, however, a possible non-linearity between the number of neurons and the resulting potential is of minor concern.)

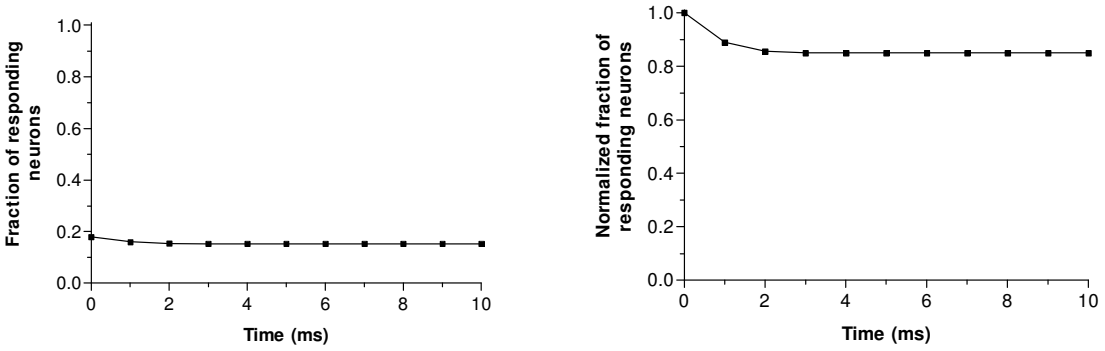

Fig. 8.16 Model output in response to a train of stimuli evoking, each time, a response in 18 % of the total neuronal population. Adaptive processes at the hair cell-nerve fiber synapse are disregarded. Whereas the left-hand panel displays the number of responding neurons as a fraction of the whole cell population, the right-hand panel represents the same values normalized with the first response set to 1.

Whereas the left-hand panel of Fig. 8.16 shows the number of responding neurons as a fraction of the whole population at issue, the right-hand panel represents the same curve normalized with the first response set to 1. Evidently, for the given stimulus train, the influence of refractoriness is not very pronounced; the steady state establishes itself at almost 90 % of first-peak amplitude. This is the case because only a low percentage of neurons responds to the individual stimuli with a large part of the population being constantly ready-to-respond.

Fig. 8.17 represents the model's output in response to stimulus trains presented at 1'000 pps and intensities ranging from 5 to 70 dB SPL. As click intensity is increased, a higher percentage of the ready-to-respond cell group will fire in response to a stimulus (the amplitude-intensity curve presented in Fig. 7.2 was used to estimate the responding fraction of neurons at each intensity). This results in a quicker decrease in number of these responders after stimulus train onset and, therefore, in a faster initial decay of the adaptation curve. Moreover, the equilibrium at which the number of cells becoming refractory equals the one of neurons becoming responders again, thus the steady state of the adaptation curve, will establish itself at a lower level. Note that for the 50- and the 70-dB-SPL traces, the number of neurons in the ready-to-respond group is so low just after stimulation onset that the second data points are actually the lowest ones of the whole response curve. 80 and 95 %, respectively, of all neurons respond synchronously to the first click at these stimulus intensities, in a way as for almost the whole population to be refractory right afterwards. Since the neurons will then recover at very different rates, no stimulus later in the train will be able to evoke spikes in as many nerve fibers, and, as before, a steady state will be reached at a certain point.

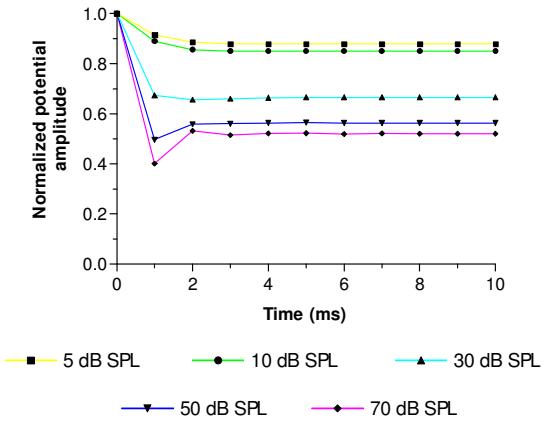

Fig. 8.17 Output of the model in response to click trains presented at 1'000 pps and intensities ranging from 5 to 70 dB SPL.

Fig. 8.18 represents the model's responses to stimulus trains presented at constant intensities of 70 and 30 dB SPL (left- and right-hand panel, respectively) and repetition rates varying between 400 and 1'000 pps. Note that the traces for 100 and 200 pps would not display any adaptation since, according to the recovery function the model is based on, all neurons will have rejoined the ready-to-respond group after 5 ms. Only at 400 pps the second one of two consecutive stimuli starts to invade

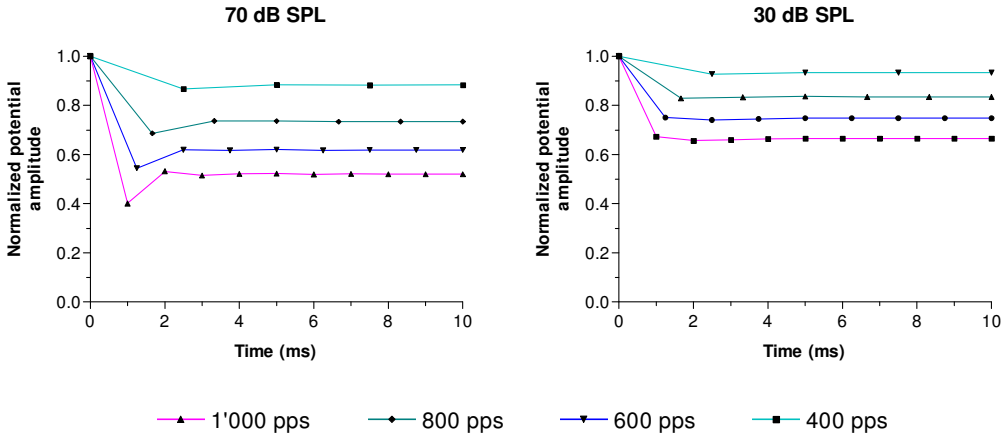

Fig. 8.18 Effect of stimulus repetition rate on model output. Only repetition rates at and above 400 pps are displayed since the traces for 100 and 200 pps would not display any adaptation at all.

the RRP of the AN fibers and therefore encounters a reduced number of neurons in the responders' group. As the inter-stimulus interval is further shortened (at increasing repetition rates), ever fewer neurons will have recovered after a response by the time the subsequent stimulus is presented. This will result in a faster decrease of the model's response at the onset of a stimulus train as well as in a lower steady state. As illustrated by Fig. 8.18, this effect is – qualitatively – the same at all stimulus intensities. Again, the left-hand panel of the figure demonstrates the fact that, at high stimulus intensities, the response to the second stimulus in a train may be the lowest one of all.

Thus, it can be said that the model invoking AN refractory properties in the adaptation process comes up with qualitatively coherent effects of stimulus parameters on adaptation. An augmentation in both stimulus repetition rate and / or intensity causes the initial decrease in potential amplitude to occur more rapidly and the steady state to establish itself at a lower level.

It has to be noted that the above curves were produced by feeding the model constant-intensity stimuli, a situation which could only be reproduced in reality by stimulating the AN electrically. When using acoustic stimulation, however, the hair cell-nerve fiber synapse will participate in the adaptation process, and the input to the AN fibers will therefore not be constant. In terms of our model, we would not have to abandon the notion of responders and non-responders, but we would be obliged to revise the concept of a constant fraction of neurons in the ready-to-respond group actually firing in reply to a stimulus. Instead, the response fraction would depend on the output of a first function representing synaptic adaptation. This somewhat more complicated situation shall be discussed just below. It is important to note, however, that the qualitative effects of stimulus intensity and repetition rate as they were just discussed will not be changed by the introduction of a time-variable response fraction and are therefore perfectly valid.

5.3.4 Refractoriness Applied on the Adapted Output of the Hair Cell-Nerve Fiber Synapse

As has been said just above, if synaptic events are to be included into the model of refractoriness, the fraction of neurons in the ready-to-respond group actually firing in response to a click train would have to be calculated individually for each stimulus based on the output function of the hair cell-nerve fiber synapse. If we knew the exact shape of this function, we would be able to test our model quantitatively. For instance, it would be interesting to see if we would come up with realistic steady-state amplitudes were we to use the "real" synaptic output for our calculations.

However, the lack of information about the output of the hair cell-nerve fiber synapse renders quantitative testing of the model impossible. All we have is the data obtained by Furukawa and colleagues (Furukawa and Matsuura, 1978; Furukawa et al., 1978; see section VIII.5.2.4) who found the adaptation time course of the EPSPs in large saccular afferent fibers of the goldfish to be exponential. Even without more ample information, applying the model of refractoriness on such an exponentially decreasing "output curve" of a hair cell may yield some interesting pieces of (purely qualitative) information. For example, is the shape of the resulting curves compatible with the empirical adaptation time courses found in this study?

The right-hand panel of Fig. 8.19 shows the model's output for a click train presented at 70 dB SPL and 1'000 pps, assuming the input to the model – in other words, synaptic output – to follow the time course indicated in the left-hand panel of the figure (consider the purple trace in Fig. 8.17 for a "raw" version of the model's response to such a stimulus train). The parameters of the exponential synaptic output are not purely arbitrary but were chosen in order as to produce a curve which reached a realistic steady-state level (somewhat below 10 % of first-response amplitude) at a reasonable time after stimulus onset (around 20 ms). Fig. 8.19 only displays the first 50 ms of the response to the stimulus train.

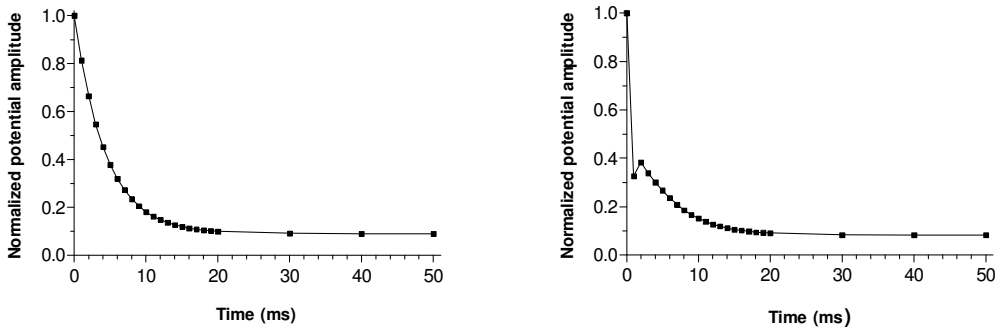

Fig. 8.19 The curve on the left is supposed to represent synaptic output in response to a stimulus train presented at 70 dB SPL and 1'000 pps. This function is then fed to the model of refractoriness, using the recovery function displayed in Fig. 8.15. The final output of this procedure is given in the right-hand panel. Only the first 50 ms of the response to the stimulus train are shown.

Note that the effect of refractoriness is almost exclusively evident during the first few milliseconds of response. At first, it may seem surprising that the steady states in the two panels of Fig. 8.19 are almost identical in amplitude, given the considerable reduction of the ready-to-respond group evident from Fig. 8.17. In this respect, it is important to realize that by the time the steady state has established itself, synaptic output has declined to about a tenth of its value at stimulus train onset, as can be derived from the left panel of Fig. 8.19. At such low input to the AN, few fibers will respond to each individual stimulus, and the number of potential responders will therefore be close to 100 %, as was mentioned further above for a stimulus train presented at 10 dB SPL.

An interesting feature of the right-hand graph of Fig. 8.19 is the fact that even when including foregoing synaptic events, the second data point of the curve is still lower than the third one. Obviously, this is in direct contradiction to the main hypothesis used in this report, according to which adaptation can be modeled by a linear addition of two exponential decays. With respect to this, two points are important to note. First, it is very difficult to assess the exact form of the first, rapid decay of ANEP amplitude in empirical response traces. Although fitting it with an exponential decay function resulted in good coefficients of correlation in most cases, this does not have to mean that, in reality, adaptation may not follow a slightly different time course. Second, and more importantly, we actually did observe response traces in which the data points immediately after the first response were very low (as mentioned in sections VII.3.1.1 and VII.3.2.1). Fig. 8.20 displays a typical example of such a trace: clearly, the data points immediately following the first response are too low as to nicely fit a two-

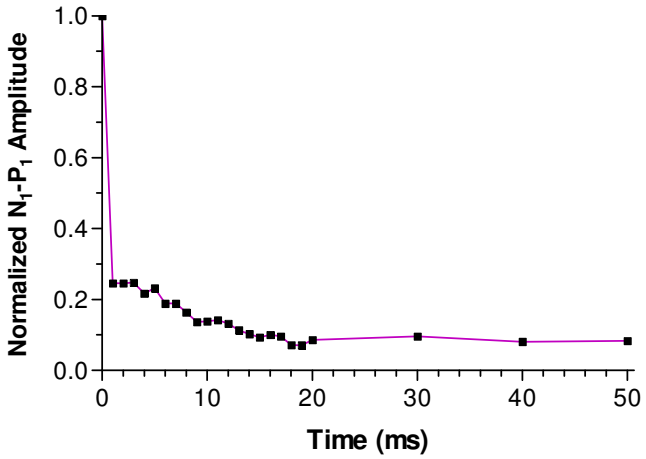

Fig. 8.20 Response to a stimulus train presented at 70 dB SPL and 1'000 pps to Rat 7. Data points obtained 1 to 3 ms after stimulus train onset are clearly too low as to fit a two-time-constant exponential decay.

time-constant exponential decay. The curve's slope is even slightly upward between the data points for the second and the fourth response potential.

Thus, there are indeed similarities between the curves in Figs. 8.19 (right panel) and 8.20. However, it seems that for the curve displayed in Fig. 8.20, post-onset response suppression is more marked and also somewhat longer in time than for the modeled trace in Fig. 8.19. If the first few milliseconds of response in Fig. 8.20 are actually influenced by refractoriness, this would mean that the recovery function (Fig. 8.15) would have to be modified in the sense of a longer RRP. In Fig. 8.21, the recovery function has been modified in a way as for model output to fit as well as possible the time course of the response trace displayed in Fig. 8.20.

Apparently, a minor modification of the recovery time course yields an excellent fit of the empirical data points by the model. The adjusted recovery time course may seem a bit slow when recapitulating the data quoted above about the RRP of AN fibers (section VIII.5.3.2). However, it cannot be precluded that there are in fact neurons displaying incomplete recovery after up to 6 or 7 ms. Furthermore, another important point has to be considered: AN fibers may not be the only relay in the peripheral auditory pathway to display refractoriness. When the adaptation model of Smith and Brachman (1982; Fig. 8.7) was discussed further above, it was said that as soon as transmitter level of the immediate store drops below that of the local store, the former would be refilled from the latter, since there is free transmitter flow between the two compartments. In theory, this transmitter trade-off is instantaneous. However, thinking in physiological terms, it is well conceivable that replenishment of the immediate store – by transport of transmitter vesicles, for example – would need some time to "get going". In this case, for a very short time after stimulation onset, there would be no back-up for the immediate store, allowing transmitter concentration (and therefore also secretion into the synaptic cleft) to go very low. Then, once the refilling process established, a dynamic equilibrium would be reached.

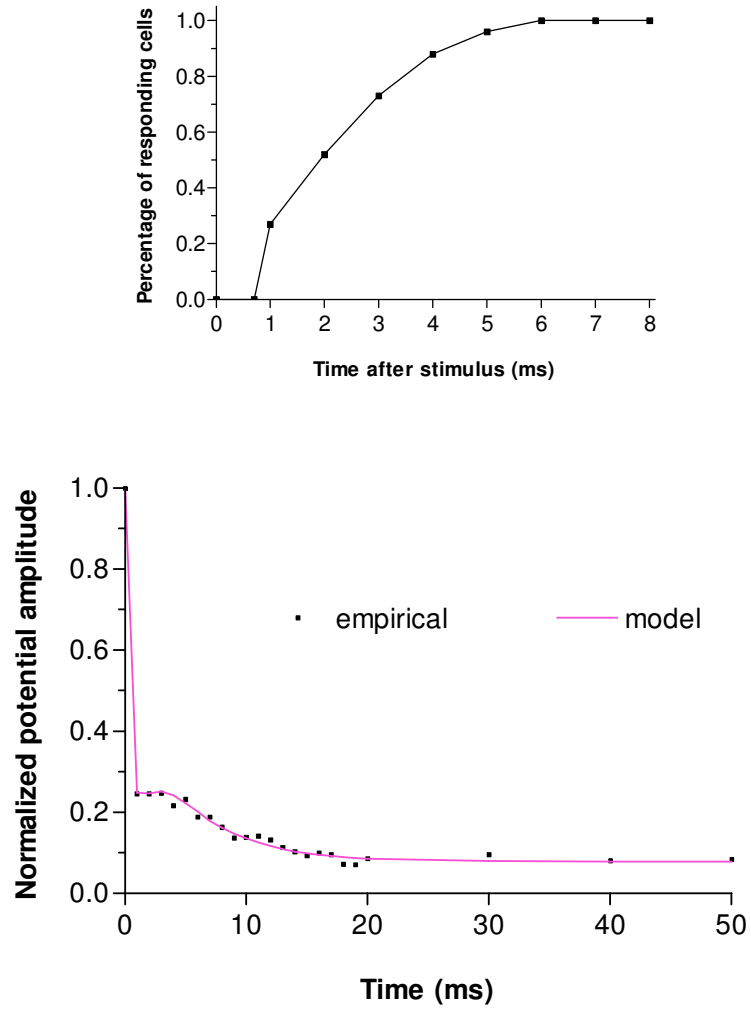

Fig. 8.21 The small black dots in the lower graph represent the same response trace as shown in Fig. 8.20 (stimulus train presented to Rat 7 at 70 dB SPL and 1'000 pps). Superposed to it (purple line) is the output emerging from the model when using a recovery curve adjusted for best fit (upper panel).

5.3.5 Refractoriness at the Basis of Discrepancies between the Adaptation Patterns of the N_1-P_1 and P_1-N_2 Components of the Auditory Near-Field Evoked Potential ?

The graphs depicted in Fig. 8.22 represent the resulting traces when response curves obtained for N_1-P_1 at a given set of stimulus parameters are subtracted from the corresponding traces obtained for P_1-N_2. Assuming our hypothesis about the respective origins of the two negative ANEP components to hold true, the depicted curves thus represent changes in the adaptation pattern occurring between primary and secondary auditory neurons.

Besides demonstrating again the fact that the P_1-N_2 plateaus were often higher than those for N_1-P_1 (as confirmed statistically at 50 and 70 dB SPL, see section VII.3.3.1) these graphs display another very interesting feature: in almost all of them, the data points immediately following stimulus train

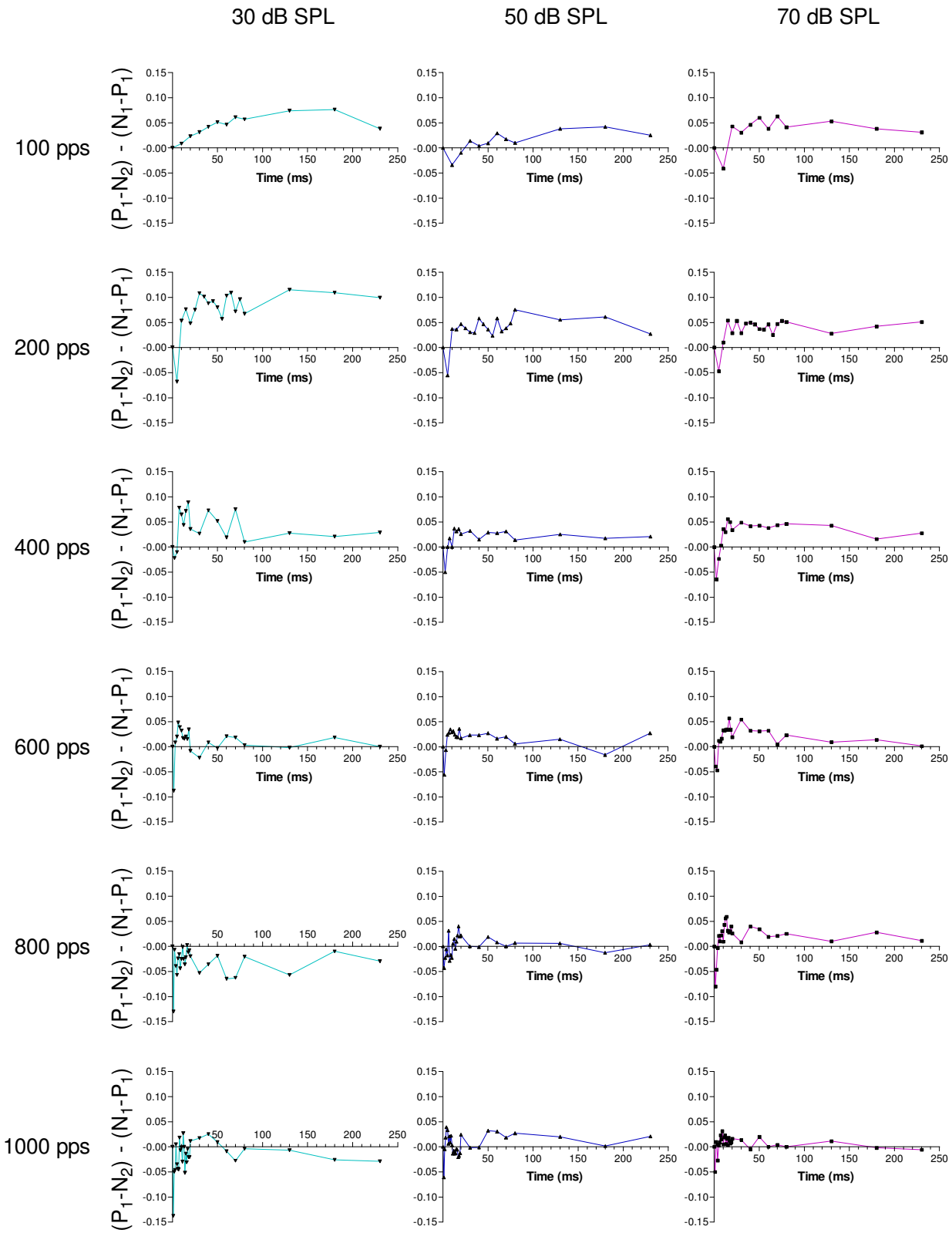

Fig. 8.22 Resulting traces when response curves obtained for N_1-P_1 at certain stimulus intensities and repetition rates are subtracted from the corresponding curves obtained for P_1-N_2. Only curves for 30, 50, and 70 dB SPL are shown.

onset are negative, indicating that the initial, rapid decline in ANEP amplitude was often more prominent in secondary than in primary auditory neurons. Thus, the discrepancies between the adaptation patterns of the two ANEP deflections are most evident during the period of response in which refractoriness exerts most of its influence. If the AVCN neurons at the basis of the potentials we recorded were to recover somewhat slower than AN fibers from the strong response to the first pulse in a stimulus train, this could indeed result in a more pronounced suppression of their activity just after train onset. It was said in section IV.1.3.4 that there is a population of neurons in the AVCN referred to as primary-like with notch units. The short pause in firing rate these neurons exhibit right after stimulus onset is actually attributed to their refractory period supposed to last between 1 and 2 ms. A certain contribution of these units to our ANEP recordings is probable and may contribute to the period of low activity sometimes observed in our P_1-N_2 response traces.

A slow recovery time course of CN units compared to the one observed in AN fibers could explain another one of our experimental findings. It was mentioned in section VII.3.3.1 that the effect of repetition rate on adaptation was more pronounced for the P_1-N_2 than for the N_1-P_1 component. The difference was only statistically significant at lower intensities (5, 10, and 30 dB SPL) but seemed to exist also at 50 and 70 dB SPL. From Fig. 8.18, it follows that, according to the model, an augmentation in stimulus repetition rate leads to a lower steady-state amplitude, because fewer neurons will have enough time to recover between two stimuli. Evidently, if the neurons were to follow a slower recovery time course, this could decrease steady-state amplitude even further. Thus, a slower recovery time course for the neurons responsible for the P_1-N_2 component of the ANEP would be a possible explanation for the low plateau levels observed for that component at high stimulus rates.

5.3.6 Summary

The above section is intended to demonstrate in what way refractoriness may contribute to the manifestation of adaptation as it was found in the present study. Refractoriness provides plausible explanations for a number of the patterns observed. Perhaps the strongest hint suggesting its involvement in adaptation is the fact that it is able to explain the atypical response traces we sometimes observed at high stimulus intensities and repetition rates. The low data points displayed by those curves just after stimulus onset cannot be explained by our original hypothesis which considered the adaptive process to follow a two-time-constant exponential decay. Even if these special response curves were not attributable to refractory properties of AN fibers, there may be other physiological processes susceptible to refractoriness possibly at their basis. The atypical traces were observed too frequently to simply be discarded.

Unfortunately, our ignorance of certain parameters prevents us from an accurate evaluation of the model. Among these parameters are the exact time course of the input to the dendrites of the AN fibers (synaptic adaptation), which we would need to check if refractoriness, applied to it, would produce realistic adaptation time courses for the two ANEP components. Also, our knowledge of the ARP and the RRP of AN fibers and CN units is clearly insufficient for a quantitative analysis of the modeled output. A weakness of the model itself is the fact that it only works if the AN fibers implicated

are assumed to have fluctuating instead of fixed thresholds. In reality, fiber thresholds are not absolutely invariant, but as outlined in section IV.1.3.3, there clearly are fibers with lower thresholds than others.

All in all, it seems to us that refractoriness of some component of the peripheral auditory pathway can probably be invoked to explain such atypical response traces as those shown in Figs. 8.20 or 7.12. There is not enough evidence, however, for a clear statement as to the implication of refractoriness in the other findings cited in this section.

IX CONCLUSION

1 Results of the Present Study

The goal of the present study was a description of the time course of neural adaptation as it occurs in the peripheral auditory relays in response to repetitive acoustic stimulation. In particular, it aimed at a quantification of the effects of changes in stimulus intensity and repetition rate on these adaptation properties. The experiments were carried out in unanesthetized Long-Evans rats and used electrodes chronically implanted in the AVCN. We verified our recording technique by assessing the response thresholds as a function of stimulus frequency, by establishing amplitude-intensity curves, and by an analysis of latency data. All three lines of evidence fit in well among the existing literature, and we therefore concluded our method to be suitable for our purpose.

The adaptation time courses for both the N_1-P_1 and the P_1-N_2 components of the ANEP could be characterized by three stages, namely rapid adaptation, short-term adaptation, and finally a steady state. In the case of N_1-P_1, mathematical fitting of the empirical response traces suggested rapid and short-term adaptations to follow exponential time courses in most cases. No fitting procedures were carried out for the P_1-N_2 component; however, based on the close resemblance of the adaptation time courses for the two wave components, similar exponential decays often seemed plausible. The amount of adaptation was assessed for both N_1-P_1 and P_1-N_2 in terms of the amplitude ratio between the response to the first stimulus of a click train and the potentials observed during the steady state. For both ANEP components, adaptation occurred more rapidly and was more pronounced as either repetition rate or intensity of the stimulating clicks was increased.

In the following, two of the main implications of the above results shall be outlined.

2 Adaptation Patterns in the Auditory Nerve and the Cochlear Nucleus

Two recent reports (Loquet and Rouiller, 2002; Loquet et al., 2003) assumed the N_1-P_1 component of the ANEP recorded from the AVCN mainly to represent activity of secondary auditory neurons located around the tip of the recording electrode. As discussed in the previous section, those investigations yielded an adaptation time course identical to the one described above, namely a pattern consisting of two exponential decays superposed to a steady state. Since several prior studies had found the same adaptation time course in the AN (see sections IV.2.2.2 and VIII.4.1), Loquet and colleagues concluded that the neurons of the AVCN essentially had similar adaptation properties as AN fibers.

However, the latency measurements carried out in the present investigation suggest that the N_1-P_1 component may mainly reflect AN rather than CN activity. For this reason, in addition to the amplitude measurements of the N_1-P_1 component, we also assessed the magnitude of the P_1-N_2 component, the latter being more consistent with CN activity latency-wise. As described in the preceding sections, the assessment of the P_1-N_2 component suggested its behavior to be quite similar to that of the N_1-P_1 deflection. It seems, therefore, that we can now more convincingly conclude that the time courses of

adaptation observed in the AN and the AVCN in response to repetitive acoustic click stimuli are, except for some minor quantitative discrepancies, very comparable (evidently, we can only refer to those neurons which contribute to the ANEP). This would mean that, as opposed to the junctions between hair cells and AN fibers, the synapses between primary and secondary auditory neurons do not play an important role in adaptation. As described in section VIII.5.2.6, this finding is not surprising because the endbulbs of Held and the so-called modified endbulbs located in the AVCN are known to be very reliable in signal transmission.

3 Adaptation Patterns in Response to Acoustic and Electric Stimulation

Another implication of our results, far more important from a clinical point of view than the one described just above, is their applicability in the research field of cochlear implants. Cochlear implants are becoming ever more important in the approach of those cases of sensorineural hearing loss which can no longer be effectively treated by conventional amplifying hearing aids (e.g. Copeland and Pillsbury, 2004).

A cochlear implant basically consists of a microphone, a speech processor, and an array of electrodes which are placed directly in the scala tympani, next to the dendrites of the AN. The sound processor decomposes the sound picked up by the microphone into individual frequency components and converts these components into electrical impulses which are sent out to the electrode array. The electrodes (up to 22 in modern devices) stimulate directly the afferent endings of the AN, taking advantage of the tonotopic arrangement of hair cells along the BM: impulses representing the high-frequency components of the sound spectrum are transmitted by electrodes terminating in basal regions of the cochlea whereas low-frequency components will be treated by longer electrodes ending further up along the BM. In this way, a given sound will excite about the same AN fibers by means of the electrode array as it would were it passed along the BM in form of a traveling wave in a healthy ear (for a review see e.g. Miyamoto, 1996; Rubinstein and Miller, 1999; Dorman and Wilson, 2004).

It is the aim of a cochlear implant, as exemplified in the last sentence, to mimic the structures of the auditory system it replaces: the conductive system, cochlear mechanics, and, more importantly, the hair cells including the synapses between themselves and SG neurons. These synapses, for the reasons exposed in section VIII.5, are held to be responsible for an important part of the adaptation patterns we observe in response recordings from primary and secondary auditory neurons. Being bypassed in the case of an implant, they can no longer convey their influence on the spike train running along the AN, and in an endeavor to evoke authentic firing patterns, we have to make up for the adaptation component thus lost by feeding to our electrodes an already-modified signal. If, for example, it were our intention to provide the more central auditory structures with the information that the ear is currently exposed to a series of constant-intensity clicks, we must not use electric pulses which will evoke in the AN a time-invariant firing pattern. Rather, we need to gather information about how, in an intact auditory system, the AN actually codes such a constant-intensity stimulus train. It was

the goal of the present study to exactly describe this response pattern and its susceptibility to changes in certain stimulus parameters.

Being in possession of this information, how do we go on? If the hair cell-nerve fiber synapse were the only site at which adaptive processes occur, our task would be quite clear: whatever the time course of EP amplitude we would like to produce in the AN, we would simply use an electrical pulse paradigm of identical shape. However, studies carried out in our laboratory (Haenggeli et al., 1998, Loquet et al., 2004) show that the AN itself is in all likelihood responsible for another adaptation component (see section VIII.5.2.5.). In other words, even though we bypass the hair cell-nerve fiber synapses and stimulate directly the dendrites of SG neurons, the response envelope we observe in the AN or the CN will not mirror the shape of the stimulus train. This means that an electrical stimulation paradigm with a signal envelope derived from the adaptation time courses found in this study would not evoke authentic AN response patterns.

Our problem thus becomes slightly more complicated. Speaking again in terms of a black box, we have to feed it an input in order to come up with a certain final output. Although the present study yields information about the outcome required, we are in need of further studies in order to find out more about the interposed machinery. It seems that, in terms of the auditory system, the machinery may correspond to the site in the SG dendrites at which spikes are generated. Our laboratory, in collaboration with a research group in Geneva, has recently made a first effort to develop an electrical stimulus paradigm adjusted in a way as to reproduce the adaptation time courses found in the present study (Loquet et al., 2004).

It is a main objective of cochlear implants to provide their users with reasonable comprehension of speech. Obviously, trains of repetitive clicks represent a strong simplification of the complex acoustic properties of spoken language. We must therefore aim at assessing the adaptive behavior of the auditory periphery also in response to more complex stimulus paradigms such as, for example, click trains having amplitude-modulated envelopes. This kind of stimulation would be of particular interest because its electrical counterpart (amplitude-modulated series of biphasic electrical pulses) is a coding strategy commonly used in modern cochlear implants (continuous interleaved sampling (CIS); Wilson et al., 1991).

For some patients, cochlear implants may not be the solution to their problem. In type II neurofibromatosis, for example, both ANs are invaded by tumors. Patients may become completely deaf due to tumor growth or tumor mass' surgical removal. The only solution to restore at least part of the hearing process in these patients are so-called auditory brainstem implants which stimulate directly the CN (Portillo et al., 1993; Otto et al., 2002; Colletti et al., 2002, 2004; Kuchta et al., 2004). By quantifying not only the adaptive behavior of the AN but also that of the AVCN, the present study therefore offers another line of evidence with clinical implications. However, it is clear that knowing adaptation properties of the CN in response to acoustic stimulation is only the first step on the way to an electrical stimulus paradigm intended to mimic these physiological responses. It has been said above that in the case of the AN, the response envelope evoked by a series of electrical pulses is not similar to the envelope of the pulse train itself, most likely because of AN fiber refractoriness. Likewise,

in the case of CN neurons, it is very hard to predict in what way they react to pulsatile electrical stimulation. If refractory properties of these cells were equal to those of AN fibers, applying an electrical stimulus paradigm designed for the AN (Loquet et al., 2004) to the CN may yield acceptable results. As has been pointed out earlier, however, there are some hints even in this very study suggesting that refractory properties in the first two auditory relays may not be absolutely identical. It seems that the only reliable approach to establishing an electrical stimulus paradigm for the CN would be empirical, the electrical stimulation being applied directly to CN neurons and their responses being recorded, for example, from their axons projecting to the SOC.

As has been pointed out in section IV, a great variety of different response types can be observed among the neurons in the CN. Evidently, the ANEPs we picked up from electrodes placed in the VCN represented the joint activity of numerous cells and did not allow to observe the behavior of individual neurons. Therefore, another way to complement the results of the present report would be single-unit studies, again carried out in an endeavor to ultimately find electrical stimulus paradigms evoking physiological adaptation time courses – not in terms of gross potentials, this time, but for as many individual types of neurons as possible.

X REFERENCES

Abbas PJ. Recovering from Long-Term and Short-Term Adaptation of the Whole Nerve Action Potential. J Acoust Soc Am 1984; 75: 1541-1547.

Boettcher FA, Salvi RJ, Saunders SS. Recovery from Short-Term Adaptation in Single Neurons of the Cochlear Nucleus. Hear Res 1990; 48: 125-144.

Bourk TR. Electrical Responses of Neural Units in the Anteroventral Cochlear Nucleus of the Cat. PhD Thesis. Massachusets Institute of Technology, Cambridge, Massachusets, 1976.

Bredberg G. Cellular Pattern and Nerve Supply of the Human Organ of Corti. Acta Otolaryngol 1968; suppl 236: 1-135.

Brown MC, Nuttall AL. Efferent Control of Cochlear Inner Hair Cell Responses in the Guinea Pig. J Physiol (London) 1984; 354: 625-646.

Brown MC. The Antidromic Compound Action Potential of the Auditory Nerve. J Neurophysiol 1994 ; 71: 1826-34.

Brown MC. Audition. In: Zigmond MJ, Bloom FE, Landis SC, Roberts JL, Squire LR (eds): Fundamental Neuroscience. San Diego, Academic Press, 1999; 791-820.

Chimento TC, Schreiner CE. Time Course of Adaptation and Recovery from Adaptation in the Cat Auditory-Nerve Neurophonic. J Acoust Soc Am 1990; 88: 857-864.

Chimento TC, Schreiner CE. Adaptation and Recovery from Adaptation in Single Fiber Responses of the Cat Auditory Nerve. J Acoust Soc Am 1991; 90: 263-273.

Chimento TC, Schreiner CE. Adaptation and Recovery from Adaptation of the Auditory Nerve Neurophonic (ANN) Using Long Duration Tones. Hear Res 1992; 62: 131-141.

Colletti V, Fiorino F, Carner M, Sacchetto L, Miorelli V, Orsi A. Auditory Brainstem Implantation: The University of Verona Experience. Otolaryngology – Head and Neck Surgery 2002; 127: 84-96.

Colletti V, Carner M, Miorelli V, Guida M, Colletti L, Fiorino F. Cochlear Implant Failure: Is an Auditory Brainstem Implant the Answer? Acta Otolaryngol (Stockh) 2004; 124: 353-357.

Copeland BJ, Pillsbury HC. Cochlear Implantation for the Treatment of Deafness. Ann Rev Med 2004; 55: 157-167.

Coro F, Pérez M, Mora E, Boada D, Conner WE, Sanderford MV, Avila H. Receptor Cell Habituation in the A1 Auditory Receptor of Four Noctuoid Moths. J Exp Biol 1998; 201: 2879-2890.

Cutnell JD, Johnson KW. Physics. New York, John Wiley & Sons, Inc., fourth edition, 1997; 458-493.

Davis H. An Active Process in Cochlear Mechanics. Hear Res 1983; 9: 79-90.

de Ribaupierre F. Acoustical Information Procession in the Auditory Thalamus and Cerebral Cortex. In: Ehret G, Romand R (eds): The Central Auditory System. New York / Oxford, Oxford University Press, 1997; 317-397.

Dorman MF, Wilson BS. The Design and Function of Cochlear Implants. Am Sci 2004; 95: 436-443.

Eatock RA. Adaptation in Hair Cells. Annu Rev Neurosci 2000; 23: 285-314.

Eggermont JJ, Spoor A. Masking of Action Potentials in the Guinea Pig Cochlea, Its Relation to Adaptation. Audiology 1973; 12: 221-241.

Eggermont JJ. Peripheral Auditory Adaptation and Fatigue: A Model Oriented Review. Hear Res; 1985; 18: 57-71.

Evans EF. Cochlear Nerve and Cochlear Nucleus. In: Keidel WD, Neff WD (eds): Handbook of Sensory Physiology, Volume V/2. Auditory System. New York, Springer Verlag, 1975; 1-108.

Fekete DM, Rouiller EM, Liberman MC, Ryugo DK. The Central Projections of Intracellularly Labeled Auditory Nerve Fibers in Cats. J Comp Neurol 1984; 229: 432-450.

Feng JJ, Kuwada S, Ostapoff E-M, Batra R, Morest DK. A Physiological and Structural Study of Neuron Types in the Cochlear Nucleus. I. Intracellular Responses to Acoustic Stimulation and Current Injections. J Comp Neurol 1994; 346: 1-18.

FitzGerald JV, Burkitt AN, Clark GM, Paolini AG. Delay Analysis in the Auditory Brainstem of the Rat: Comparison with Click Latency. Hear Res 2001; 159: 85-100.

Friauf E, Ostwald J. Divergent Projections of Physiologically Characterized Rat Ventral Cochlear Nucleus Neurons as Shown by Intra-Axonal Injection of Horseradish Peroxidase. Exp Brain Res 1988; 73: 263-284.

Frisina RD, Smith RL, Chamberlain SC. Encoding of Amplitude Modulation in the Gerbil Cochlear Nucleus. I. A Hierarchy of Enhancement. Hear Res 1990; 44: 99-122.

Furukawa T, Matsuura S. Adaptive Rundown of Excitatory Post-Synaptic Potentials at Synapses between Hair Cells and Eight Nerve Fibres in the Goldfish. J Physiol 1978; 276: 193-209.

Furukawa T, Hayashida Y, Matsuura S. Quantal Analysis of the Size of Excitatory Post-Synaptic Potentials at Synapses between Hair Cells and Afferent Nerve Fibres in Goldfish. J Physiol 1978; 276: 211-226.

Givois V, Pollack GS. Sensory Habituation of Auditory Receptor Neurons: Implications for Sound Localization. J Exp Biol 2000; 203: 2529-37.

Guinan JJ Jr, Li RYS. Signal Processing in Brainstem Auditory Neurons Which Receive Giant Endings (Calyces of Held) in the Medial Nucleus of the Trapezoid Body of the Cat. Hear Res 1990; 49: 321-334.

Haenggeli A, Zhang JS, Vischer MW, Pelizzone M, Rouiller EM. Electrically Evoked Compound Action Potential (ECAP) of the Cochlear Nerve in Response to Pulsatile Electrical Stimulation of the Cochlea in the Rat: Effects of Stimulation at High Rates. Audiology 1998; 37: 353-371.

Hancock KE, Voigt HF. Intracellularly Labeled Fusiform Cells in Dorsal Cochlear Nucleus of the Gerbil. I. Physiological Response Properties. J Neurophysiol 2002a; 87: 2505-2519.

Hancock KE, Voigt HF. Intracellularly Labeled Fusiform Cells in Dorsal Cochlear Nucleus of the Gerbil. II. Comparison of Physiology and Anatomy. J Neurophysiol 2002b; 87: 2520-2530.

Harris, DM, Dallos P. Forward Masking of Auditory Nerve Fiber Responses. J Neurophysiol 1979; 42: 1083-1107.

Heffner HE, Heffner RS, Contos C, Ott T. Audiogram of the Hooded Norway Rat. Hear Res 1994; 73: 244-247.

Henderson D, Hamernik R, Woodford C, Sitler R, Salvi R. Evoked-Response Audibility Curve of the Chinchilla. J Acoust Soc Am 1973; 54: 1099-1101.

Holt JR, Corey DP. Two Mechanisms for Transducer Adaptation in Vertebrate Hair Cells. Proc Natl Acad Sci 2000; 97: 11730-11735.

Huang C-M, Buchwald JS. Changes of Acoustic Nerve and Cochlear Nucleus Evoked Potentials due to Repetitive Stimulation. Electroencephalogr Clin Neurophysiol 1980; 49: 15-22.

Huang C-M. Time Constants of Acoustic Adaptation. Electroencephalogr Clin Neurophysiol 1981; 52: 394-399.

Hudspeth AJ. Hearing. In: Kandel ER, Schwartz JH, Jessell TM (eds): Principles of Neural Science. New York, McGraw-Hill, fourth edition, 2000; 590-613.

Hudspeth AJ, Choe Y, Mehta AD, Martin P. Putting Ion Channels to Work: Mechanoelectrical Transduction, Adaptation, and Amplification by Hair Cells. Proc Natl Acad Sci 2000; 97: 11765-11772.

Javel E. Long-term Adaptation in Cat Auditory-Nerve Fiber Responses. J Acoust Soc Am 1996; 99: 1040-1052.

Keithley EM, Feldman ML. Hair Cell Counts in an Age-Graded Series of Rat Cochleas. Hear Res 1982; 8: 249-262.

Kiang NY-S. Stimulus Coding in the Auditory Nerve and the Cochlear Nucleus. Acta Otolaryngol 1965; 59: 186-200.

Kiang NY-S, Watanabe T, Thomas EC, Clark EF. Discharge Patterns of Single Fibers in the Cat Auditory Nerve. Research Monograph N° 35. Cambridge, MA, M.I.T. Press, 1965a; 20-15.

Kiang NY-S, Pfeiffer RR, Warr WB, Backus, ASN. Stimulus Coding in the Cochlear Nucleus. Ann Otol Rhinol Laryngol 1965b; 74: 463-485.

Kiang NY-S, Rho JM, Northrop CC, Liberman MC, Ryugo DK. Hair Cell Innervation by Spiral Ganglion Cells in Adult Cat. Science 1982; 217: 175-177.

Kopp-Scheinpflug C, Dehmel S, Dörrscheidt GJ, Rübsamen R. Interaction of Excitation and Inhibition in Anteroventral Cochlear Nucleus Neurons That Receive Large Endbulb Synaptic Endings. J Neurosci 2002; 22 : 11004-11018.

Kuchta J, Otto SR, Shannon RV, Hitselberger WE, Brackmann DE. The Multichannel Auditory Brainstem Implant: How Many Electrodes Make Sense? J Neurosurg 2004; 100: 16-23.

Li J, Young ED. Discharge-Rate Dependence of Refractory Behavior of Cat Auditory-Nerve Fibers. Hear Res 1993; 69: 151-162.

Liberman MC. Single-Neuron Labeling in the Cat Auditory Nerve. Science 1982; 216: 1239-1241.

Liberman MC. Central Projections of Auditory-Nerve Fibers of Differing Spontaneous Rate. I: Anteroventral Cochlear Nucleus. J Comp Neurol 1991; 313: 240-258.

Liberman MC. Central Projections of Auditory-Nerve Fibers of Differing Spontaneous Rate. II: Posteroventral and Dorsal Cochlear Nuclei. J Comp Neurol 1993; 327: 17-36.

Loquet G, Rouiller EM. Neural Adaptation to Pulsatile Acoustical Stimulation in the Cochlear Nucleus of the Rat. Hear Res 2002; 171: 72-81.

Loquet G, Meyer K, Rouiller EM. Effects of Intensity of Repetitive Acoustic Stimuli on Neural Adaptation in the Ventral Cochlear Nucleus of the Rat. Exp Brain Res 2003; 153: 436-442.

Loquet G, Pelizzone M, Valentini G, Rouiller EM. Matching the Neural Adaptation in the Rat Ventral Cochlear Nucleus Produced by Artificial (Electric) and Acoustic Stimulation of the Cochlea. Audiol Neurootol 2004; 9: 144-159.

Lorente de No R. Anatomy of the VIIIth Nerve. Laryngoscope 1933; 43: 327-350.

Mac Leish PR, Shepherd GM, Kinnamon SC, Santos-Sacchi J. Sensory Transduction. In: Zigmond MJ, Bloom FE, Landis SC, Roberts JL, Squire LR (eds): Fundamental Neuroscience. San Diego, Academic Press, 1999; 671-717.

Meddis R. Simulation of Mechanical to Neural Transduction in the Auditory Receptor. J Acoust Soc Am 1986; 79: 702-711.

Meddis R. Simulation of Auditory-Neural Transduction: Further Studies. J Acoust Soc Am 1988; 83 : 1056-1063.

Miller CA, Abbas PJ, Robinson BK. Response Properties of the Refractory Auditory Nerve Fibers. J Assoc Res Otolaryngol 2001; 2 : 216-232.

Miyamoto RT. Cochlear Implants. In: Goldenberg RA (ed): Hearing Aids: A Manual for Clinicians. Philadelphia, Lippincott-Raven Publishers, 1996; 231-246.

Møller AR. Unit Responses in the Rat Cochlear Nucleus to Repetitive, Transient Sounds. Acta Physiol Scand 1969; 75: 542-551.

Møller AR. Latency of Unit Responses in the Cochlear Nucleus Determined in Two Different Ways. J Neurophysiol 1975; 38: 812-821.

Møller AR. Dynamic Properties of Primary Auditory Nerve Fibers Compared with Cells in the Cochlear Nucleus. Acta Physiol Scand 1976; 98: 157-167.

Møller AR. Neural Delay in the Ascending Auditory Pathway. Exp Brain Res 1981a; 43: 93-100.

Møller AR. Latency in the Ascending Auditory Pathway Determined Using Continuous Sounds: Comparison Between Transient and Envelope Latency. Brain Res 1981b; 207: 184-188.

Møller AR. On the Origin of the Compound Action Potentials (N_1, N_2) of the Cochlea of the Rat. Exp Neurol 1983; 80: 633-644.

Mulheran M. The Effects of Quinine on Cochlear Nerve Fiber Activity in the Guinea Pig. Hear Res 1999; 134: 145-152.

Müller M, Robertson D. Relationship between Tone Burst Discharge Pattern and Spontaneous Firing Rate of Auditory Nerve Fibres in the Guinea Pig. Hear Res 1991; 57: 63-70.

Norris CH, Guth PS, Daigneault EA. The Site at Which Peripheral Adaptation Occurs. Brain Res 1977; 123: 176-179.

Osen KK. Cytoarchitecture of the Cochlear Nuclei in the Cat. J Comp Neurol 1969; 136: 453-484.

Ostapoff E-M, Feng JJ, Morest DK. A Physiological and Structural Study of Neuron Types in the Cochlear Nucleus. II. Neuron Types and Their Structural Correlation with Response Properties. J Comp Neurol 1994; 346: 19-42.

Otto SR, Brackmann DE, Hitselberger WE, Shannon RV, Kuchta J. Multichannel Auditory Breinstem Implant: Update on Performance in 61 Patients. J Neurosurg 2002; 96: 1063-1071.

Paolini AG, FitzGerald JV, Burkitt AN, Clark GM. Temporal Processing from the Auditory Nerve to the Medial Nucleus of the Trapezoid Body in the Rat. Hear Res 2001; 159: 101-116.

Paxinos G, Watson C. The Rat Brain in Stereotaxic Coordinates. San Diego, Academic Press, fourth edition, 1998.

Peake WT, Goldstein MH Jr, Kiang NY-S. Responses of the Auditory Nerve to Repetitive Acoustic Stimuli. J Acoust Soc Am 1962a; 34: 562-570.

Peake WT, Kiang NY-S, Goldstein MH Jr. Rate Functions for Auditory Nerve Responses to Bursts of Noise: Effect of Changes in Stimulus Parameters. J Acoust Soc Am 1962b; 34: 571-575.

Portillo F, Nelson RA, Brackmann DE, Hitselberger WE, Shannon RV, Waring MD, Moore JK. Auditory Brain Stem Implant: Electrical Stimulation of the Human Cochlear Nucleus. Adv Otorhinolaryngol 1993; 48: 248-252.

Relkin EM, Doucet JR. Recovery from Prior Stimulation I: Relationship to Spontaneous Firing Rates of Primary Auditory Neurons. Hear Res 1991; 55: 215-222.

Relkin EM, Doucet JR, Sterns A. Recovery of the Compound Action Potential Following Prior Stimulation: Evidence for a Slow Component That Reflects Recovery of Low Spontaneous-Rate Auditory Neurons. Hear Res 1995; 83: 183-189.

Rhode WS, Smith PH, Oertel D. Physiological Response Properties of Cells Labeled Intracellularly with Horseradish Peroxidase in Cat Dorsal Cochlear Nucleus. J Comp Neurol 1983a; 213: 426-447.

Rhode WS, Oertel D, Smith PH. Physiological Response Properties of Cells Labeled Intracellularly with Horseradish Peroxidase in Cat Ventral Cochlear Nucleus. J Comp Neurol 1983b; 213: 448-463.

Rhode WS, Smith PH. Characteristics of Tone-Pip Response Patterns in Relationship to Spontaneous Rate in Cat Auditory Nerve Fibers. Hear Res 1985; 18: 159-168.

Rhode WS, Smith PH. Physiological Studies on Neurons in the Dorsal Cochlear Nucleus of the Cat. J Neurophysiol 1986; 56: 287-307.

Romand R, Avan A. Anatomical and Functional Aspects of the Cochlear Nucleus. In: Ehret G, Romand R (eds): The Central Auditory System. New York / Oxford, Oxford University Press, 1997; 97-191.

Rouiller EM, Ryugo DK. Intracellular Marking of Physiologically Characterized Cells in the Ventral Cochlear Nucleus of the Cat. J Comp Neurol 1984; 225: 167-186.

Rouiller EM, Cronin-Schreiber R, Fekete DM, Ryugo DK. The Central Projection of Intracellularly Labeled Auditory Nerve Fibers in Cats: An Analysis of Terminal Morphology. J Comp Neurol 1986; 249: 261-278.

Rouiller EM. Functional Organization of the Auditory Pathways. In: Ehret G, Romand R (eds): The Central Auditory System. New York / Oxford, Oxford University Press, 1997; 3-96.

Rubinstein JT, Miller CA. How Do Cochlear Prostheses Work? Curr Opin Neurobiol 1999; 9: 399-404.

Russell IJ, Sellick PM. Intracellular Studies of Hair Cells in the Mammalian Cochlea. J Physiol 1978; 284: 261-190.

Ryugo DK, Dodds LW, Benson TE, Kiang NY-S. Unmyelinated Axons of the Auditory Nerve in Cats. J Comp Neurol 1991; 308: 209-223.

Shaw NA. Central Auditory Conduction Time in the Rat. Exp Brain Res 1990; 79: 217-220.

Shore SE. Recovery of Forward-Masked Responses in Ventral Cochlear Nucleus Neurons. Hear Res 1995; 82: 31-43.

Smith PH, Rhode WS. Electron Microscopic Features of Physiologically Characterized, HRP-Labeled Fusiform Cells in the Cat Dorsal Cochlear Nucleus. J Comp Neurol 1985; 237: 127-143.

Smith PH, Rhode WS. Characterization of HRP-Labeled Globular Bushy Cells in the Cat Anteroventral Cochlear Nucleus. J Comp Neurol 1987; 266: 360-375.

Smith PH, Rhode WS. Structural and Functional Properties Distinguish Two Types of Multipolar Cells in the Ventral Cochlear Nucleus. J Comp Neurol 1989; 282: 595-616.

Smith PH, Joris PX, Carney LH, Yin TCT. Projections of Physiologically Characterized Globular Bushy Cell Axons from the Cochlear Nucleus of the Cat. J Comp Neurol 1991; 304: 387-407.

Smith PH, Joris PX, Yin TCT. Projections of Physiologically Characterized Spherical Bushy Cell Axons from the Cochlear Nucleus of the Cat: Evidence for Delay Lines to the Medial Superior Olive. J Comp Neurol 1993; 331: 245-260.

Smith RL, Zwislocki JJ. Short-Term Adaptation and Incremental Responses of Single Auditory-Nerve Fibers. Biol Cybern 1975; 17: 169-182.

Smith RL. Short-Term Adaptation in Single Auditory Nerve Fibers: Some Poststimulatory Effects. J Neurophysiol 1977; 40: 1098-1112.

Smith RL. Adaptation, Saturation, and Physiological Masking in Single Auditory-Nerve Fibers. J Acoust Soc Am 1979; 65: 166-178.

Smith RL, Brachman ML. Adaptation in Auditory-Nerve Fibers: A Revised Model. Biol Cybern 1982; 44: 107-120.

Spoendlin H. Innervation Densities of the Cochlea. Acta Otolaryng 1972; 73: 235-248.

Spoendlin H. Neuroanatomical Basis of Cochlear Coding Mechanisms. In: Round Table Conference on Cochlear Function. Paris, 1974; 383-407.

Spoendlin H. Neural Connections of the Outer Haircell System. Acta Oto Laryngol 1979; 87: 381-387.

Starr A. Suppression of Single Neuron Activity in the Cochlear Nucleus of the Cat Following Sound Stimulation. J Neurophysiol 1965; 28: 850-862.

Sumner CJ, Lopez-Poveda EA, O'Mard LP, Meddis R. A Revised Model of the Inner-Hair Cell and Auditory-Nerve Complex. J Acoust Soc Am 2002; 111: 2178-2188.

Sumner CJ, Lopez-Poveda EA, O'Mard LP, Meddis R. Adaptation in a Revised Inner-Hair Cell Model. J Acoust Soc Am 2003; 113: 893-901.

Trussell LO. Modulation of Transmitter Release at Giant Synapses of the Auditory System. Curr Opin Neurobiol 2002; 12: 400-404.

von Békésy G. In: Wever, EG (ed): Experiments in Hearing. New York, McGraw-Hill, 1960.

Webster, DB. An Overview of Mammalian Auditory Pathways with an Emphasis on Humans. In: Webster DB, Popper AN, Fay RR (eds): The Mammalian Auditory Pathway: Neuroanatomy. New York, Springer Verlag, 1992; 1-22.

West CD. The Relationship of the Spiral Turns of the Cochlea and the Length of the Basilar Membrane to the Range of Audible Frequencies in Ground Dwelling Mammals. J Acoust Soc Am 1985; 77: 1091-1101.

Westerman LA, Smith RL. Rapid and Short-Term Adaptation in Auditory Nerve Responses. Hear Res 1984; 15: 249-260.

Westerman LA. Adaptation and Recovery of Auditory-Nerve Responses. PhD Thesis, Syracuse University, Syracuse, NY; 1985.

Wilson BS, Finley CC, Lawson DT, Wolford RD, Eddington DK, Rabinowitz WM. Better Speech Recognition with Cochlear Implants. Nature 1991; 352: 236-238.

Wilson BS, Finley CC, Lawson DT, Zerbi M. Temporal Representations with Cochlear Implants. Am J Otol 1997; 18: 30-34.

Winslow RL, Sachs MB. Single-Tone Intensity Discrimination Based on Auditory-Nerve Rate Response in Backgrounds of Quiet, Noise, and with Stimulation of the Crossed Olivocochlear Bundle. Hear Res 1988; 35: 165-190.

Winter IM, Robertson D, Yates GK. Diversity of Characteristic Frequency Rate-Intensity Functions in Guinea Pig Auditory Nerve Fibres. Hear Res 1990; 45: 191-202.

Yates GK, Robertson D, Johnstone BM. Very Rapid Adaptation in the Guinea Pig Auditory Nerve. Hear Res 1985, 17: 1-12.

Zenner HP, Zimmerman U, Schmitt U. Reversible Contraction of Isolated Mammalian Cochlear Hair Cells. Hear Res 1985; 18: 127-133.

XI ADDENDUM

Exp Brain Res (2003) 153: 436–442
DOI 10.1007/s00221-003-1689-9

RESEARCH ARTICLE

G. Loquet · K. Meyer · E. M. Rouiller

Effects of intensity of repetitive acoustic stimuli on neural adaptation in the ventral cochlear nucleus of the rat

Received: 6 December 2002 / Accepted: 27 March 2003 / Published online: 22 October 2003
© Springer-Verlag 2003

Abstract To study neural adaptation as a function of stimulus intensity, auditory near-field evoked potentials were recorded from the ventral cochlear nucleus in awake Long Evans rats. Responses to 250-ms trains of repetitive clicks (pulse rates ranging from 100 to 1000 pulses per second) were collected at stimulus intensities of 5, 10, 30, 50 and 70 dB SPL. The amplitude of the first negative (N_1) component of the average evoked potentials to individual pulses in the train was measured by using a subtraction method. The N_1 responses were normalized with respect to the highest cochlear nucleus potential observed in the train, and then plotted as a function of click position in the train. As expected, the general trend of the curves was an exponential decay reaching a plateau more or less rapidly as a function of both intensity and rate of stimulation. Fitting these curves with exponential decay equations revealed that the rapid time constant decreased for increasing stimulus intensities whereas the short-term time constant is relatively independent of intensity. The amount of adaptation (expressed as the ratio of the plateau to the first peak amplitude) was substantially less prominent at low intensities (5–10 dB SPL) and low rates (100–200 pulses per second) than at higher intensities and high rates. These results indicate that adaptation patterns obtained in the ventral cochlear nucleus by using near-field evoked potentials exhibit properties comparable to those already present at the level of the auditory nerve.

Keywords Unanesthetized · Brainstem · Auditory evoked potentials · Click

G. Loquet · K. Meyer · E. M. Rouiller (✉)
Division of Physiology, Department of Medicine, University of Fribourg,
Rue du Musée 5,
1700 Fribourg, Switzerland
e-mail: eric.rouiller@unifr.ch
Tel.: +41-26-3008609
Fax: +41-26-3009675

Introduction

From a psychophysical point of view, the subjective intensity of a pure-tone that lasts more than a few seconds and does not exceed 30 dB SL (sensation level) decreases during stimulation. This loudness decrease, referred to as adaptation, is due to the reduction of neural response to continuous stimulation over time (Gelfand 1997). In profoundly deaf patients, however, the current generation of cochlear implants does not reproduce adaptation properties, so imparting a loss of information which may contribute, at least in part, to the commonly reported low level of speech intelligibility in noisy conditions.

Experimental studies on auditory adaptation at the neural level have generally been conducted in animal models (cat and rodent) by recording compound action potentials (Eggermont and Spoor 1973; Abbas 1984; Chimento and Schreiner 1990, 1992) or action potentials from single auditory nerve fibers (Smith and Zwislocki 1975; Smith 1977, 1979; Harris and Dallos 1979; Westerman and Smith 1984; Rhode and Smith 1985; Yates et al. 1985; Javel 1996). In the auditory nerve (AN), the compound action potential (CAP) in response to a transient sound is characterized by a negative deflection, reflecting the synchronized discharges of several individual fibers. In response to a variety of different stimulus types such as high frequency tones (Gorga and Abbas 1981; Abbas 1984), low frequency tones (Chimento and Schreiner 1990, 1991, 1992), short repetitive tone-bursts (Peake et al. 1962a, 1962b; Eggermont and Spoor 1973; Müller and Robertson 1991), or click trains (Kiang et al. 1965; Wickesberg and Stevens 1998), both techniques (CAP and single unit recordings) yielded similar results, namely an initial rapid decrease of CAP amplitude or firing rate during the first few milliseconds (*rapid adaptation*), followed by a slower decay over tens of milliseconds (*short-term adaptation*), and then an even slower decrease over several seconds (*long-term adaptation*) or minutes (*very long-term adaptation*). The similarity of adaptation patterns to pure tones and to series of clicks could possibly be attributed to the fact that

at high repetition rates, the latter stimulus is close to a cosine-phase harmonic complex (Hafter and Richards 1988). Nevertheless, small differences were reported at the single unit level, especially between high and low spontaneous rate AN fiber populations (Rhode and Smith 1985; Müller and Robertson 1991), suggesting that different mechanisms may underlie adaptation. Moreover, it is important to note that the measures of adaptation were essentially performed in two ways: either over the duration of the stimulus (Peake et al. 1962a, 1962b; Eggermont and Spoor 1973; Westerman and Smith 1984; Müller and Robertson 1991; Javel 1996) or during the recovery period (Gorga and Abbas 1981; Abbas 1984; Chimento and Schreiner 1990, 1991, 1992). However, both approaches are closely related, and thus lead to comparable results (rapid, short-term, and long-term adaptation). Similar to the AN, the near-field evoked potential recorded from the cochlear nucleus (CN) in response to transient sounds is characterized by a negative deflection (with a longer latency), believed to reflect the synchronized discharges of secondary auditory neurons (Møller 1983). With this approach, the measurements of adaptation in the ventral division of the CN (VCN), carried out with short repetitive tone-bursts (Møller 1969; Huang and Buchwald 1980; Huang 1981) or click trains (Møller 1969; Loquet and Rouiller 2002), showed an adaptive pattern similar to that of the AN, with at least three distinct decay components. At the single unit level, only two of the three major response types described in the VCN (primary-like and chopper) exhibited adaptation patterns similar to those reported in the auditory nerve fibers in response to tones (Evans 1975). The same conclusion was reached in studies using a forward-masking paradigm (Boettcher et al. 1990; Shore 1995).

As to the mechanisms involved, adaptation phenomena are still not fully understood. On the one hand, for the auditory nerve, authors agree to consider adaptation to be the result of neural refractory properties and depletion of available transmitter at the hair cell–nerve fiber synapse (for review see Eggermont 1985; Javel 1996). Therefore, the multi-component adaptation may be attributed to a multi-stage transmitter depletion (Smith and Brachman 1982), with transmitter release depending to some extent on the nature of the stimulus. For example, there would be an increase of adaptation in AN fibers when the intensity of a tone stimulation increased (Peake et al. 1962b; Westerman and Smith 1984; Yates et al. 1985; Rhode and Smith 1985; Müller and Robertson 1991). On the other hand, in CN, adaptation was expected to be more complex, mainly because of (1) the variety of afferent inputs, (2) the intrinsic membrane characteristics of each cell type, and (3) inhibitory inputs. Nevertheless, at the single unit level, it was reported that adaptation patterns in firing rate of primary-like and chopper units when the intensity of a tone was increased were similar to those observed in single AN fibers (Boettcher et al. 1990; Shore 1995; Burkard and Palmer 1997). In contrast, there are no studies addressing this issue at the whole CN level based on near-field evoked potentials.

In a recent report (Loquet and Rouiller 2002), we demonstrated that the dynamic properties of adaptation to trains of repetitive clicks in VCN were comparable to those of the AN at a fixed intensity. Whether this similarity persists at various intensity levels needed further investigation. To address this question, VCN near-field evoked potentials were chronically recorded in an animal model (unanesthetized adult rats) in response to pulsatile acoustical stimuli of varying intensities (ranging from 5 to 70 dB SPL) and pulse rates (ranging from 100 to 1000 pulses per second, pps). The results are compared to adaptive properties previously established for the auditory nerve.

Materials and methods

Animals

Experiments were conducted on male adult Long-Evans rats (Janvier Laboratories, Le Genest-Saint-Isle, France) weighing approximately 300 g and aimed at recording auditory evoked near-field potentials from a chronic electrode implanted in the left VCN. The experimental procedure was approved by the Swiss veterinarian authorities and was performed in accordance with the *Principles of laboratory animal care* (US NIH Publication No. 86-23, revised 1985) and the 1964 Declaration of Helsinki for animal care. The procedure was described in detail in a recent report (Loquet and Rouiller 2002) and will only be summarized here. Briefly, before surgery, the animals (n=6) were treated with atropine sulfate (0.05 mg/kg s.c.) to minimize respiratory distress, and with a nonsteroidal anti-inflammatory drug (Carprofen, 4 mg/kg i.m.) to reduce inflammation and pain. Then, they were deeply anesthetized with pentobarbital (Vetanarcol, 40 mg/kg i.p.) and placed in a stereotaxic apparatus (Model 1404; Muromachi Instruments, Japan) in order to implant the chronic recording tungsten electrode (2–4 MΩ impedance) in the left VCN (coordinates: AP=−9.80 mm, ML=4.30 mm, DV=7.99±0.35 mm from bregma). A ground electrode was placed in the rostral cranium on the dura mater, and the two electrodes were soldered to a socket and fixed to the skull with dental cement. The animals were allowed to recover for 1 week before beginning chronic recording. The location of the recording electrode in the VCN was histologically verified in the brains of all rats at the end of the experiment (see Loquet and Rouiller 2002).

Acoustic stimulation

Testing was performed with Tucker-Davis Technologies System II (TDT, Alachua, FL, USA) equipment in a sealed sound proof booth (IAC, Niederkrüchten, Germany) on awake rats placed in a restraining device (Loquet and Rouiller 2002). Acoustic signals were synthesized digitally using TDT SigGen32 software and, after digital-to-analog conversion, fed into a programmable attenuator before delivery to a speaker positioned 10 cm away from the left pinna of the rat. The calibration of the system was carried out with a sound level meter (B&K, model 2231) by measuring the sound pressure level (SPL root mean square re 20 μPa) emitted by the speaker when it was driven by a pure tone signal at 9 V peak level. The sound field was calibrated by positioning the microphone (B&K, model 4155, prepolarized free-field 1/2 inch) at the point normally occupied by the center of the animal's head. Within the audiometric room, the ambient noise level did not exceed 69 dB SPL with regard to the overall spectra linear level, and 38 dB SPL with regard to frequencies above 1 kHz. Cochlear nucleus near-field potentials (CNP) were amplified (2×10^3), bandpass filtered between 30 Hz and 5 kHz and then fed into an analog-to-digital converter.

The TDT data acquisition software BioSig32 was used to automate CNP averaging over 50 presentations and for offline analysis.

Acoustic stimulation consisted of repetitive short condensation-rectangular-pulse clicks (100 μs) delivered in a train of 250 ms duration followed by a pause (silent period) of 250 ms before the next train. The intra-train pulse rates varied from 100 to 1000 pps, and five intensities were tested: 70, 50, 30, 10 and 5 dB SPL. The analysis window stretched over 250 ms, and the amplitude of the N_1 component of the CNP was measured as the voltage difference between the first negative (N_1) and the first positive (P_1) peak. At repetition rates greater than 400 pps, responses to individual clicks started to overlap so that the amplitude of a certain response was influenced by the preceding one. To circumvent this contamination, the 250-ms trains were presented in an order so as to always increment click number in the train by one. The average CNP obtained in response to a certain train (*n* clicks) was then subtracted from the CNP to the following train (*n*+1 clicks), the resulting curve exposing solely the *n*+1 click (see Loquet and Rouiller 2002). Thus, individual clicks could be studied free of contamination. Finally, N_1–P_1 amplitudes were normalized with respect to the highest CNP observed in the train (usually the CNP to the first click), and were plotted as a function of the position of the corresponding click in the train.

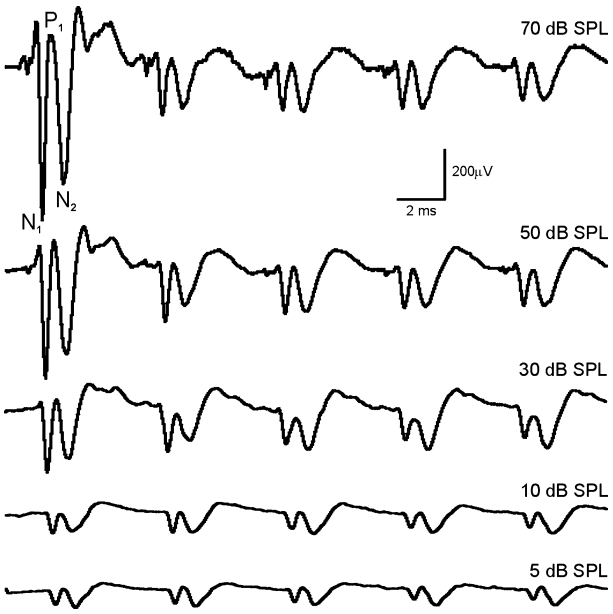

Fig. 1 Typical ventral cochlear nucleus near-field evoked potentials (CNP) elicited by 250-ms trains of repetitive clicks presented at a rate of 200 pps (Rat #6). Only the first 25 ms of the train are shown in order to easily identify the N_1, P_1 and N_2 deflections (negative polarity is downward). Note that the decrease of N_1–P_1 amplitude as a function of time became more obvious at high levels of stimulation. Stimulus intensity is given to the *upper right* of each trace

Results

As shown in Fig. 1, CNP amplitude measured as the voltage difference between the negative peak N_1 and the subsequent positive peak P_1 varied as a function of both intensity of stimulation and position of the stimulating click in the train. In Fig. 1, one of the most obvious effects of an augmentation in stimulus intensity is the increase of the first through-to-peak N_1–P_1 amplitude and the decrease of its latency. Then, it can also be noticed that increasing the intensity of stimulation induced an accentuation of amplitude differences between responses to the first click and the subsequent ones. In other words, these qualitative data show that adaptation was more pronounced when stimulus intensity increased.

Amplitudes of individual CNPs to consecutive clicks in the train were plotted for each rat; one representative animal is depicted in Fig. 2. In general, curves tend to display an exponential decrease of the normalized CNP amplitudes as a function of time (position of the corresponding stimulating click in the train). Most curves exhibit an initial rapid adaptation followed by a slower adaptation and a plateau, except for those obtained at low repetition rates (100 and 200 pps) and low intensities (5–10 dB SPL) where one phase was sometimes missing. In addition, for each rate tested (100–1000 pps), adaptation became more pronounced when intensities were increased from 5 to 70 dB SPL, as represented by a decrease of the plateau level and a shortening of the rapid and short-term adaptive components. This latter assumption was verified by determining the decay time constants of the two

Table 1 Time constants of cochlear nucleus auditory-evoked potentials as a function of stimulus rate and intensity. K_1, rapid, and K_2, short-term adaptation time constants were determined with non-linear regression fitting curves (see Results section). The few curves that were better described by a one-component time-constant equation are not included in this table. Mean values and standard deviations (SD) were calculated from data obtained from five rats

Stimulus rate	Value	Time constant at stimulus intensity									
		5 dB		10 dB		30 dB		50 dB		70 dB	
		K_1	K_2	K_1	K_2	K_1	K_2	K_1	K_2	K_1	K_2
100 pps	Mean	15.5[a]	46.6[a]	11.4	61.2	12.2	49.9	5.3	50.6	2.4	48.1
	SD			3.8	17.1	5.5	12.1	3.4	8.1	3.2	12.6
200 pps	Mean	6.5	74.4	9.7	64.0	4.6	54.8	2.8	41.4	2.4	44.0
	SD	1.5	25.7	4.3	37.1	1.4	16.0	1.2	21.1	1.6	34.1
400 pps	Mean	4.4	64.5	4.6	66.4	2.2	54.6	1.4	36.4	0.5	6.3
	SD	2.3	25.5	1.4	21.2	0.7	15.5	0.5	36.9	0.5	2.7
600 pps	Mean	3.8	52.2	3.1	45.9	1.2	30.2	0.8	46.4	0.2	6.8
	SD	1.2	15.1	1.6	25.4	0.6	23.4	0.2	49.4	0.2	0.9
800 pps	Mean	2.6	100.0	1.6	38.5	0.7	28.6	0.2	28.1	0.1	4.9
	SD	1.4	100.8	1.0	24.9	0.2	21.8	0.2	18.8	0.1	2.7
1000 pps	Mean	1.5	54.5	1.1	49.7	0.3	15.0	0.3	8.8	0.2	5.1
	SD	1.6	62.5	0.8	55.3	0.3	11.8	0.3	5.4	0.1	0.9

[a]Adaptation curve of only one animal fitted by a two-component time-constant equation

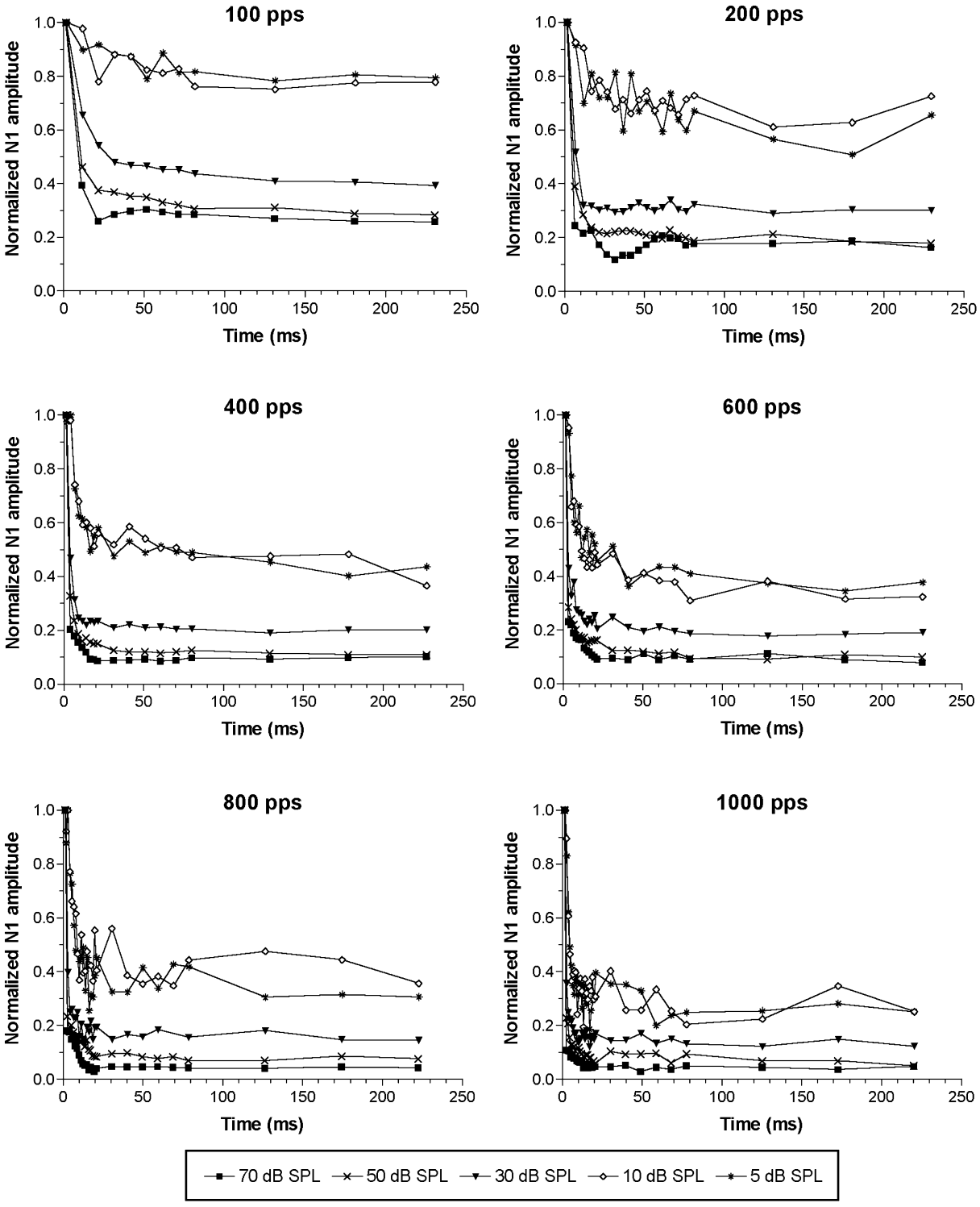

Fig. 2 Normalized amplitudes of ventral cochlear nucleus near-field evoked potentials in Rat #6 displayed as a function of the position of the stimulating clicks in the 250 ms train. Five intensities ranging from 70 to 5 dB SPL are presented for each of the click rates ranging from 100 to 1000 pps

adaptive components using exponential decrease equation fittings that we previously demonstrated to be consistent with adaptation properties of VCN near-field potentials (Loquet and Rouiller 2002). The equation used was:

$$NP(t) = NP_1 e^{-t/\kappa_1} + NP_2 e^{-t/\kappa_2} + Plateau$$

where NP_1, NP_2 are the y-intercepts of the rapid and short-term components respectively; *Plateau* is equal to the

N_1–P_1 amplitudes during the steady state response, and K_1, K_2 are the decay time constants of the two postulated adaptation components. In some instances, in particular at the lowest intensities of stimulation (5–10 dB SPL), data were best fitted with a one-component time constant adaptation equation (NP_2=0). The curve-fitting was run using the Levenberg-Marquardt method with GraphPad Prism v3.02 software and the deviation from the model was assessed by considering the correlation coefficient ($R^2 \geq 0.70$) and by testing the Gaussian distribution of the residuals around the curve ($P>0.1$). Mean values of K_1 and K_2 were calculated from data obtained in five animals; they are summarized in Table 1 and depicted in Fig. 3 (results of fittings using only one-component time constant have not been included in the data presented). The rapid time constants (K_1) exhibited a progressive decrease as intensity of the stimulus increased. A maximum reduction of 13.1 ms (from 15.5 to 2.4 ms) was obtained at 100 pps, and was less pronounced at higher pulse rate (1.3 ms at 1000 pps). The short-term time constants (K_2) appeared to be roughly independent of intensity over an intensity range of 45 dB (from 5 to 50 dB SPL). In contrast, at 70 dB SPL, a marked decrease of K_2 was observed at 400 pps and above. Large inter-individual variabilities were observed at rates of 800 and 1000 pps.

For each rat, the total extent of adaptation was estimated by the ratio of the plateau amplitude to the highest CNP amplitude in the train. The magnitude of the plateau was determined by averaging the CNP amplitude values obtained during the last 150 ms of the train. These data were then averaged across the six rats and plotted in Fig. 4. On the right of the figure, an adaptation indicator has been introduced to underline the fact that the smaller the ratio, the more pronounced the adaptation. The curves, progressively declining from left to right, thus indicate an increase in adaptation for higher levels of stimulation. Indeed, increasing the intensity from 5 to 70 dB SPL led to an augmentation of adaptation of about 50% at 100 pps, and 40% at 200 pps. Interestingly, one can notice that at all higher repetition rates (400 to 1000 pps) this augmentation of adaptation with intensity remained around 30%. This suggests a separation of the data into two groups: at high repetition rates (400, 600, 800, 1000 pps) the change of adaptation with intensity is comparable, whereas at low pulse rates (100, 200 pps), the progressive increase of adaptation with intensity is rate-dependent and, in addition to that, more marked than at high repetition rates.

Discussion

CNP waveforms obtained in the present study in response to click stimuli (Fig. 1) are similar to those elicited by tone bursts that were reported recently (Loquet and Rouiller 2002). The 2.11 ms latency of the N_1 response at 5 dB SPL is consistent with previously observed values for the CN ranging between 2.0 and 3.0 ms (Huang and Buchwald 1980; Møller 1983), as opposed to shorter latency values obtained from the AN ranging between 0.5 and 1.8 ms (Møller 1983). However, as to the exact origin of the N_1 deflection within the CN, latency data do not allow for further conclusions since a large overlap exists between anteroventral, posteroventral and dorsal CN latencies (Godfrey et al. 1975a, 1975b). Nevertheless, under our experimental conditions, the N_1 response most likely reflects synchronized discharges in the VCN for the following reasons. Firstly, the histological verification in the brainstems of all rats (data not shown) demonstrated that the tip of the chronic recording electrode was clearly located in the anteroventral part of the CN. Secondly, the contribution of units located in the dorsal CN (pauser and buildup units) is unlikely, considering their inhibitory response patterns and their low ability to follow repetitive clicks (Rhode and Smith 1986).

The exponential decrease of CNP amplitudes in response to repetitive stimuli shown in Fig. 2 is in

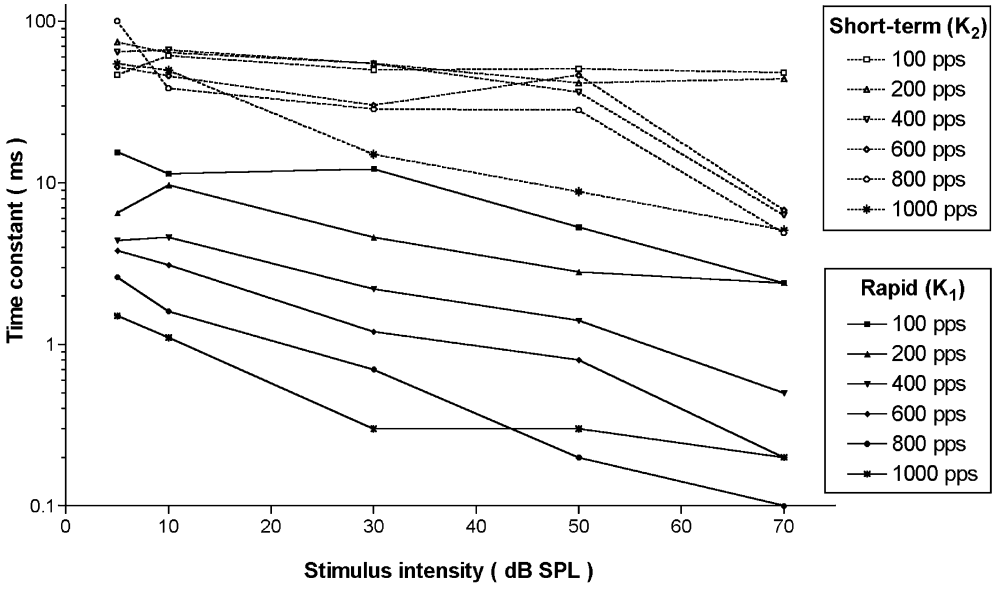

Fig. 3 Mean fitted decay time constants displayed as a function of stimulus rate and intensity. Time constants for rapid (K_1) and short-term (K_2) adaptation components were obtained from five animals by fitting normalized N_1–P_1 amplitude curves (see "Results" section). Standard deviations of data points are omitted for the sake of clarity but can be found in Table 1

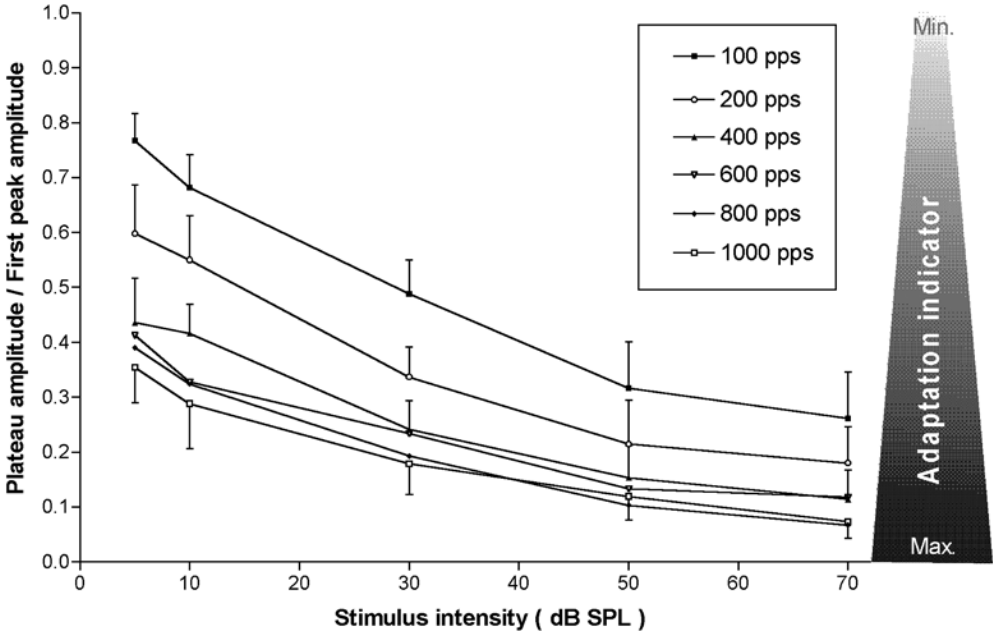

Fig. 4 Amount of adaptation expressed as the ratio of the plateau to the first peak amplitude, as a function of stimulus intensity. Mean values were derived from six animals, the *bars* representing 95% confidence intervals. At two stimulation rates (600 and 800 pps), the bars are omitted for the sake of clarity. An adaptation indicator is depicted on the *right* of the graph

agreement with the data of Huang (1981) and Loquet and Rouiller (2002). Such an adaptation generally follows a two-phase exponential decline (rapid [K_1] and short-term [K_2] adaptive components) to finally reach a plateau. This pattern varies as a function of stimulation rate with a faster (decreasing time constants) and larger (decreasing plateau level) decay as frequency increases. This repetition-rate effect on neural adaptation in the CN is in agreement with our previous report (Loquet and Rouiller 2002) and with data obtained in the AN (Peake et al. 1962a), for which the response amplitude decreased as soon as stimulus rate exceeded 10 pps. Unexpectedly, however, the present study demonstrates that the augmentation of the amount of adaptation as a function of increased stimulus intensity (Fig. 4) does not depend strongly on the repetition rate at 400 pps and above. The reason for such a segregation into two groups (high and low repetition rates) is not known but one may speculate that it is related to the refractory period. At 100, 200 and 300 pps, the unit is not affected by refractory mechanisms, in contrast to high rates (400 pps and above) for which the period between two consecutive pulses falls within the relative refractory period.

Concurrently with the rate effect, the present data indicate that adaptation in VCN depends on the level of stimulation. Indeed, increasing the stimulus intensity from 5 to 70 dB SPL led to a more prominent exponential decrease of CNP amplitudes, irrespective of the rate tested (Fig. 2). As mentioned in earlier studies (Westerman and Smith 1984; Yates et al. 1985), this effect is mainly attributable to the rapid adaptation time constant (K_1), which shows a constant decrease with increasing intensity (Table 1 and Fig. 3). In contrast, the short-term adaptation time constant (K_2) shows little intensity dependence (except for the interval between 50 and 70 dB SPL), an observation in line with data on AN fibers (Smith and Zwislocki 1975; Westerman and Smith 1984). The effects of intensity on VCN adaptation is also well characterized by the level of the plateau (steady-state component), whose decrease was at its most significant between 10 and 30 dB SPL (Figs. 2 and 4). At high stimulus intensities (50–70 dB SPL), average amounts of adaptation were similar to those found in high-spontaneous-rate nerve fibers (Brown 2001). Therefore, in our experimental conditions (awake rats), VCN near-field evoked responses appear to be essentially the same as those recorded in the AN, as far as adaptation is concerned.

Physiological mechanisms

In line with the present study, authors presenting simple short tone bursts, either as described by Blackburn and Sachs (1989) or in the context of a forward-masking paradigm (Boettcher et al. 1990), observed a more pronounced adaptation with increasing intensity in some CN neurons, namely the bushy cells (which produce primary-like and primary-like-with-notch responses) and stellate cells (usually associated with chopper responses), than in cell types generating other response patterns (pauser, buildup, onset). More recently, response decrement differences were found within VCN (Shore 1995), in particular between primary-like, primary-like-with-notch, sustained chopper, transient chopper, low-intensity chopper, onset and on-chopper responses. The author suggested that both adaptation and inhibition were involved in producing these differences. In the present study, it is likely that adaptation recorded in the VCN by using near-field evoked potentials (summation of individual neurons) mainly reflects the adaptive properties of primary-like units, which have themselves properties close to those of AN fibers, in particular comparable adaptive time constants. As far as chopper units are concerned, their contribution seems to be substantially less than that of primary-like units according to Shore (1995) and Burkard

and Palmer (1997). Moreover, it can be noticed that AN and CN adaptations are likely to mirror still more peripheral changes, primarily located at the hair cell-nerve fiber synapse (Norris et al. 1977; Furukawa et al. 1978). At this stage, adaptation was suggested to involve depletion of neurotransmitter in a cascade of reservoirs (Eggermont 1985).

Overall, despite the fact that adaptation is complex and may depend on specific properties of each relay along the auditory pathway, the present study supports the idea of a reconciliation between single unit data and near-field evoked potentials. Indeed, in the same way that adaptation of VCN primary-like units is essentially the same as that of AN fibers, CNP adaptation obtained in VCN was found to be comparable to CAP adaptation obtained in AN. Therefore, it seems reasonable to hypothesize that our CNP data mainly reflect properties of primary-like units in VCN. As a consequence, the present animal model can be used to better understand auditory neural adaptation phenomena and to transpose these features to cochlear implants that aim at restoring, as accurately as possible, normal physiological hearing in profoundly deaf patients. Such studies could lead to direct clinical applications. They could, for example, be used to improve current stimulation paradigms in order to achieve better speech recognition in ambient noise by cochlear implant patients.

Acknowledgements The authors would like to thank B. Aebischer, E. Regli and A. Gaillard for their technical assistance, F. Tinguely for the histology, and J. Corpataux and B. Morandi for taking care of the rats in the animal room. This research project was supported by the Swiss National Science Foundation (Grant no. 32-56352.99; TANDEM) and the National Center for Competence in Research (NCCR) "Neural Plasticity and Repair".

References

Abbas PJ (1984) Recovering from long-term and short-term adaptation of the whole nerve action potential. J Acoust Soc Am 75:1541–1547

Blackburn CC, Sachs MB (1989) Classification of unit types in the anteroventral cochlear nucleus: PST histograms and regularity analysis. J Neurophysiol 62:1303–1329

Boettcher FA, Salvi RJ, Saunders SS (1990) Recovery from short-term adaptation in single neurons in the cochlear nucleus. Hear Res 48:125–144

Brown MC (2001) Response adaptation of medial olivocochlear neurons is minimal. J Neurophysiol 86:2381–2392

Burkard R, Palmer AR (1997) Responses of chopper units in the ventral cochlear nucleus of the anaesthetised guinea pig to clicks-in-noise and click trains. Hear Res 110:234–250

Chimento TC, Schreiner CE (1990) Time course of adaptation and recovery from adaptation in the cat auditory-nerve neurophonic. J Acoust Soc Am 88:857–864

Chimento TC, Shreiner CE (1991) Adaptation and recovery from adaptation in single fiber responses of the cat auditory nerve. J Acoust Soc Am 90:263–273

Chimento TC, Schreiner CE (1992) Adaptation and recovery from adaptation of the auditory nerve neurophonic (ANN) using long duration tones. Hear Res 62:131–141

Eggermont JJ (1985) Peripheral auditory adaptation and fatigue: a model oriented review. Hear Res 18:57–71

Eggermont JJ, Spoor A (1973) Cochlear adaptation in guinea pigs. A quantitative description. Audiology 12:193–220

Evans EF (1975) Cochlear nerve and cochlear nucleus. In: Keidel WD, Neff WD (eds) Auditory system. Handbook of sensory physiology, vol II. Springer-Verlag, Berlin Heidelberg New York, pp 1–108

Furukawa T, Hayashida Y, Matsuura S (1978) Quantal analysis of the size of excitatory post-synaptic potentials at synapses between hair cells and eighth nerve fibers in the goldfish. J Physiol (Lond) 276:211–226

Gelfand SA (1997) Essentials of audiology. Thieme Medical, New York

Godfrey DA, Kiang NYS, Norris BE (1975a) Single unit activity in the posteroventral cochlear nucleus of the cat. J Comp Neurol 162:247–268

Godfrey DA, Kiang NYS, Norris BE (1975b) Single unit activity in the dorsal cochlear nucleus of the cat. J Comp Neurol 162:269–284

Gorga MP, Abbas PJ (1981) AP measurements of short-term adaptation in normal and in acoustically traumatized ears. J Acoust Soc Am 70:1310–1321

Hafter ER, Richards VM (1988) Discrimination of the rate of filtered impulses. Percept Psychophys 43:405–414

Harris DM, Dallos P (1979) Forward masking of auditory-nerve fiber responses. J Neurophysiol 42:1083–1107

Huang CM (1981) Time constants of acoustic adaptation. Electroencephalogr Clin Neurophysiol 52:394–399

Huang CM, Buchwald JS (1980) Changes of acoustic nerve and cochlear nucleus evoked potentials due to repetitive stimulation. Electroencephalogr Clin Neurophysiol 49:15–22

Javel E (1996) Long-term adaptation in cat auditory-nerve fiber responses. J Acoust Soc Am 99:1040–1052

Kiang NYS, Watanabe T, Thomas EC, Clark EF (1965) Discharge patterns of single fibers in the cat auditory nerve. Research Monograph No. 35. MIT Press, Cambridge MA

Loquet G, Rouiller EM (2002) Neural adaptation to pulsatile acoustical stimulation in the cochlear nucleus of the rat. Hear Res 171:72–81

Møller AR (1969) Unit responses in the rat cochlear nucleus to repetitive, transient sounds. Acta Physiol Scand 75:542–551

Møller AR (1983) On the origin of the Compound action potentials (N_1, N_2) of the cochlea of the rat. Exp Neurol 80:633–644

Müller M, Robertson D (1991) Relationship between tone burst discharge pattern and spontaneous firing rate of auditory nerve fibres in the guinea pig. Hear Res 57:63–70

Norris CH, Guth P, Daigneault EA (1977) The site at which peripheral auditory adaptation occurs. Brain Res 123:176–179

Peake WT, Goldstein MH, Kiang NYS (1962a) Responses of the auditory nerve to repetitive acoustic stimuli. J Acoust Soc Am 34:562–570

Peake WT, Kiang NYS, Goldstein MH (1962b) Rate functions for auditory nerve responses to bursts of noise: effect of changes in stimulus parameters. J Acoust Soc Am 34:571–575

Rhode WS, Smith PH (1985) Characteristics of tone-pip response patterns in relationship to spontaneous rate in cat auditory nerve fibers. Hear Res 18:159–168

Rhode WS, Smith PH (1986) Physiological studies on neurons in the dorsal cochlear nucleus of the cat. J Neurophysiol 56:287–307

Shore SE (1995) Recovery of forward-masked responses in ventral cochlear nucleus neurons. Hear Res 82:31–43

Smith RL (1977) Short-term adaptation in single auditory nerve fibers: some poststimulatory effects. J Neurophysiol 40:1098–1112

Smith RL (1979) Adaptation, saturation, and physiological masking in single auditory-nerve fibers. J Acoust Soc Am 65:166–178

Smith RL, Brachman ML (1982) Adaptation in auditory-nerve fibers: a revised model. Biol Cybern 44:107–120

Smith RL, Zwislocki JJ (1975) Short-term adaptation and incremental responses of single auditory-nerve fibers. Biol Cybernetics 17:169–182

Westerman LA, Smith RL (1984) Rapid and short-term adaptation in auditory nerve responses. Hear Res 15:249–260

Wickesberg RE, Stevens HE (1998) Responses of auditory nerve fibers to trains of clicks. J Acoust Soc Am 103:1990–1999

Yates GK, Robertson D, Johnstone BM (1985) Very rapid adaptation in the guinea pig auditory nerve. Hear Res 17:1–12

XII CURRICULUM VITAE

Lebenslauf

Personalien	Name	Meyer
	Vornamen	Kaspar Ueli
	Geburtsdatum	18. Juni 1978
	Geburtsort	Neuchâtel
	Heimatort	Zürich

Schulen	1985 – 1991	Primarschule, Benken ZH
	1991 – 1993	Sekundarschule, Marthalen
	1993 – 1998	Gymnasium Typus C, Kantonsschule Im Lee, Winterthur
	1995 – 1996	High School Senior Year, Mary D. Bradford High School, Kenosha, Wisconsin, USA
	1999 – 2001	Vorklinisches Medizinstudium, Universität Fribourg
	2001 – 2002	Klinisches Medizinstudium, Universität Lausanne
	2002 – 2003	Klinisches Medizinstudium, Universität La Laguna, Teneriffa, Spanien
	2003 – 2004	Wahlstudienjahr mit Praktika in Innerer Medizin, Chirurgie, Pädiatrie und Anästhesie
	2004 – 2005	Klinisches Medizinstudium, Universität Zürich

Diplome	1996	Graduation from Mary D. Bradford High School, Kenosha, Wisconsin, USA
	1998	Matura Typus C, Kantonsschule Im Lee, Winterthur
	2005	Eidgenössisches Staatsexamen, Universität Zürich